New approaches for flavoenzyme applications

Krzek, Marzena

New Approaches for

Flavoenzymes Applications

Cofactor-mediated immobilization & in vitro production of human metabolites

Marzena Krzek

The research described in this thesis was carried out at the University of Groningen, in the Molecular Enzymology Group of the Groningen Biomolecular Sciences and Biotechnology Institute. The financial support was provided by the Netherlands Organisation for Scientific Research (NWO) through an excellence in chemical research (ECHO) grant (project no. 711.012.006)

university of groningen

New approaches for flavoenzymes applications

Cofactor-mediated immobilization & in vitro production of human metabolites

PhD thesis

to obtain the degree of PhD at the
University of Groningen
on the authority of the
Rector Magnificus Prof. E. Sterken
and in accordance with
the decision by the College of Deans.
The thesis will be defended in public on
15 September 2017 at 12:45 hours

by

Marzena Krzek

born on 22 Februari 1987
in Proszowice, Poland

Supervisors
Prof. M.W. Fraaije
Prof. R.P.H. Bischoff

Assessment committee
Prof. W. J. H van Berkel
Prof. D.B. Janssen
Prof. G. Maglia

To explorers

THESIS CONTENT

CHAPTER 1

INTRODUCTION

Marzena Krzek, Marco W. Fraaije

Molecular Enzymology Group, University of Groningen, Nijenborgh 4, 9747AG Groningen, the Netherlands

1 FLAVOENZYMES

1.1 FLAVIN COFACTORS

Flavoenzymes are enzymes that depend on a flavin cofactor for their function. They are expressed in every kind of living organisms. The most common flavin cofactor is flavin adenine dinucleotide (FAD), which typically binds to the target flavoenzyme with very high affinity. FAD contains a ribityl chain to which two phosphate moieties and an adenosine are attached at one side, and at the other side it is linked to the isoalloxazine ring (Figure 1). The typical, tricyclic isoalloxazine ring is responsible for the yellow-orange color of this molecule and determines its redox properties (Kamerbeek, 2004)

In living cells the biosynthesis of FAD-containing flavoenzymes is a three-step process, in which vitamin B2 (riboflavin, Figure 1) is a precursor. Riboflavin is phosphorylated by the riboflavin kinase into flavin mononucleotide (FMN). Subsequently, FMN is adenylated by FAD synthetase and forms FAD. Once the FAD cofactor is present in the cell, its incorporation into the flavoprotein active center is typically spontaneous due to the high affinity towards this ligand.

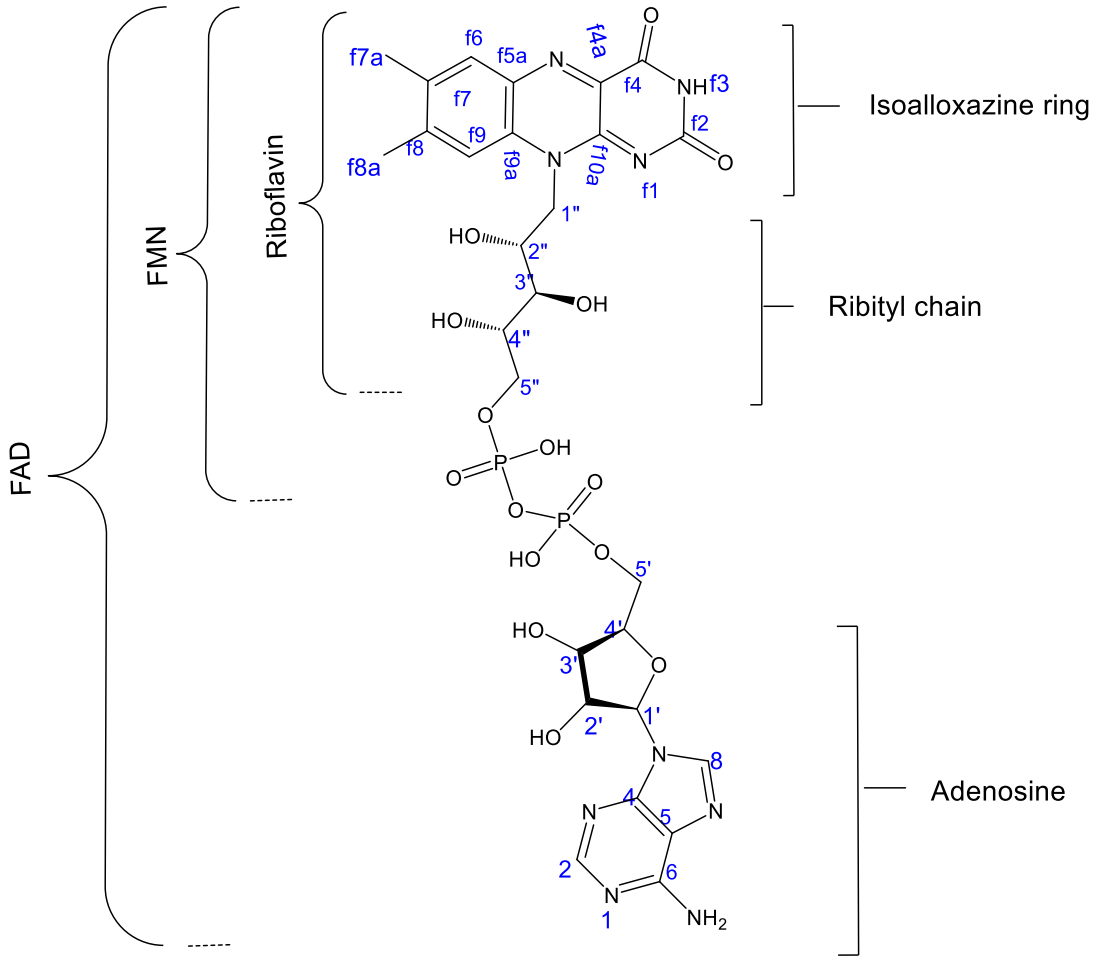

***Figure 1**. Structural formula of FAD with indicated subcomponents and atom numbering.*

The minority (around 10%) of flavoenzymes bind FAD covalently (Macheroux, Kappes and Ealick, 2011). The covalent binding most commonly involves the f8a-methyl or f6 carbon atoms of the isoalloxazine ring (Jin *et al.*, 2008; Heuts *et al.*, 2009) (Figure 1) and alters the redox properties of the molecule (Heuts *et al.*, 2009). For example, it was reported that after removal of the histidyl-FAD bond in vanillyl alcohol oxidase (VAO) from *Penicillium simplicissimum*, the redox potential drops by 0.12 V (Jin *et al.*, 2008).

1.2 Classification of FAD-containing enzymes

Regarding catalytic activity, FAD-containing flavoenzymes can be classified based on their mechanism of action, type of chemical reaction that is catalyzed or the type of reducing/oxidizing substrates used during conversion (Massey, 2000). The most common classification is based on the types of chemical reactions catalyzed. By such discrimination, there are a few classes defined: oxidases, dehydrogenases/reductases, disulfide oxidoreductases, monooxygenases and non-redox flavoenzymes. Such a diverse activity of enzymes is observed due to different microenvironments of their active centers, that are tuned by the amino acid side chains that encompass the isoalloxazine ring of the FAD cofactor. Below, two groups of oxidative flavoenzymes are introduced as they are most relevant to the rest of the thesis: the FAD-containing flavoprotein monooxygenases and oxidases. Both enzyme groups are also intensely studied because of their potential for biotechnological applications.

1.2.1 Flavoprotein monooxygenases

Incorporation of one oxygen atom into organic molecules defines the activity of flavoprotein monooxygenases (Chaiyen, Fraaije and Mattevi, 2012). Catalysis starts with oxygen activation by a reaction of dioxygen with the f4a moiety of a reduced flavin cofactor which results in formation of a flavin peroxide (Figure 2). The peroxyflavin is an intermediate, which in Baeyer-Villiger Monooxygenases (BVMOs) can be stable up to minutes (Torres Pazmiño et al., 2008), and in the so-called flavin-containing monooxygenases (FMOs) can last for hours (Krueger and Williams, 2005). This intermediate performs the direct oxygenation of a substrate molecule in the active center. Upon insertion of one oxygen into substrate, the second oxygen atom is released by formation of water. To perform the next oxygenation, a monooxygenase needs to recharge its flavin cofactor with electrons. The natural electron donors are reduced nicotinamide cofactors: flavoprotein monooxygenases are NAD(P)H-dependent (Torres Pazmiño and Fraaije, 2008). An example of a reaction catalyzed by a FAD-containing and NADPH dependent flavoprotein monooxygenase is shown in Figure 3: the Baeyer-Villiger oxidation of phenylacetone by phenylacetone monooxygenase (PAMO). This flavoenzyme was used as prototype flavoprotein monooxygenase in Chapters 2 and 3 of this thesis.

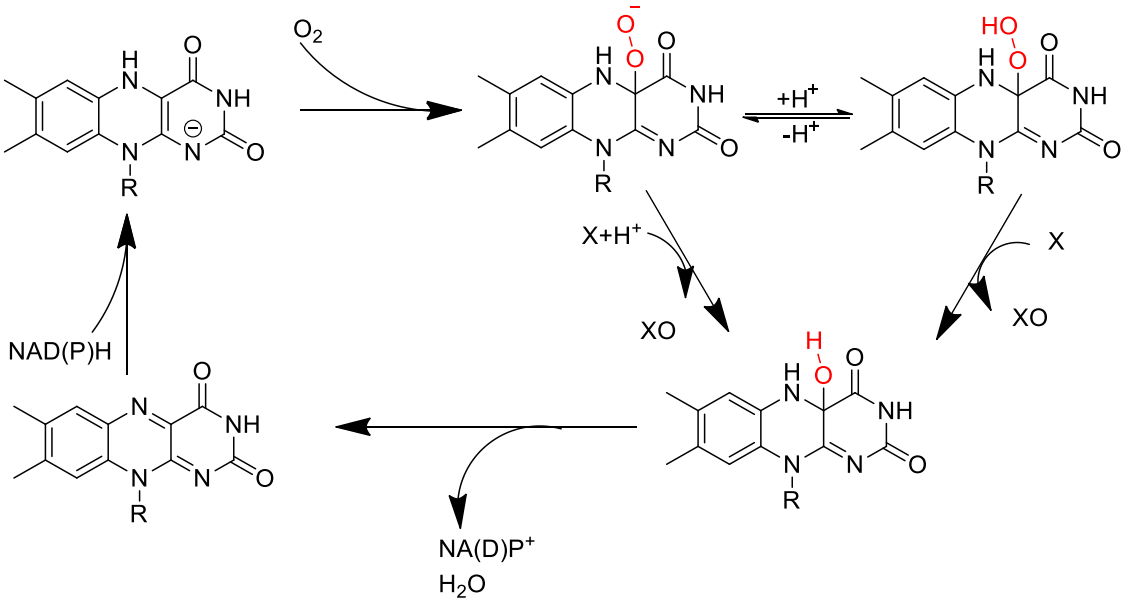

Figure 2. *Catalytic cycle of flavoprotein monooxygenases. The scheme is based on (Torres Pazmiño et al., 2008) and may vary depending on the respective flavoprotein monooxygenase.*

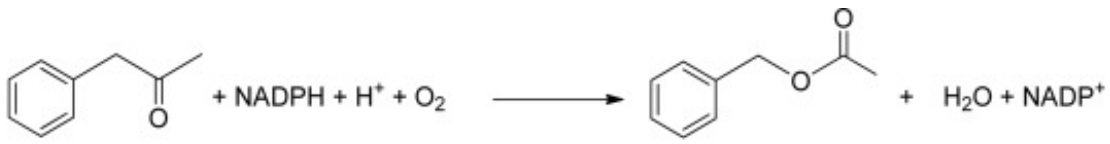

Figure 3*. Schematic representation of the reaction catalyzed by phenylacetone monooxygenase (PAMO): a Baeyer-Villiger oxidation of phenylacetone into benzyl acetate.*

The human proteome contains several flavoprotein monooxygenases. The most intensively studied are the so-called human flavin-containing monooxygenases (hFMOs) due to their considerable contribution to the detoxification of xenobiotics (Motika, Zhang and Cashman, 2007). They catalyze 10% of the oxidative metabolism in liver by oxidation of soft nucleophilic heteroatoms like sulfur or nitrogen (Cashman and Zhang, 2006). They act on drugs like lidocaine, amphetamine and albendazole. Human FMOs are FAD-containing, microsomal flavoenzymes and show some sequence homology with BVMOs such as PAMO. The human proteome contains five FMO isoforms (hFMO1-5), each isoform is encoded by a different gene. Human FMO isoform 3 (hFMO3) is predominantly expressed in human liver and is considered to be the most important hFMO concerning human xenobiotic metabolism (Cashman and Zhang, 2006). Till now, efficient recombinant overexpression of native hFMO3 has not been achieved and isolation of the enzyme or close homologs from mammalian tissue is troublesome, which has hampered detailed studies of this important human enzyme. Chapter 4 provides and overview on the current status on recombinant hFMO3 expression and our attempts to produce the enzyme as fusion enzyme using a bacterial expression host. Chapter 5 offers an alternative

approach for generating hFMO-related metabolites. We demonstrate that microbial sequence-related flavoprotein monooxygenases can be used as mimics of hFMO3 and its isoforms.

1.2.2 FLAVOPROTEIN OXIDASES

Flavoprotein oxidases catalyze the oxidation of various organic compounds. Based on sequence- and structural homology, six different flavoprotein oxidases can be identified (Dijkman *et al.*, 2013). The most common mechanism for oxidizing their substrate involves a direct hydride transfer (Kamerbeek, 2004). After oxidation, the reduced flavin cofactor donates its electrons to molecular oxygen yielding hydrogen peroxide. The largest flavoprotein oxidase family, the GMC family, includes some of the most studied and widely applied oxidases, such as the FAD-containing glucose oxidase and methanol oxidase. Another fairly widely distributed family of flavoprotein oxidases is named after VAO from the fungus *Penicillium simplicissimum*. VAO is able to catalyze the oxidation of various phenolic compounds. The oxidation of vanillyl alcohol leads to the known flavor compound vanillin, which is the main component of the natural vanilla flavor (Figure 4). The VAO family of FAD-containing oxidases is relatively rich in flavoprotein oxidases that carry a covalently attached FAD cofactor. For evaluating the use of the N^6-modified FAD derivative as anchor for enzyme immobilization as described in Chapters 2 and 3, a recently discovered VAO homolog (eugenol oxidase, EUGO) was used.

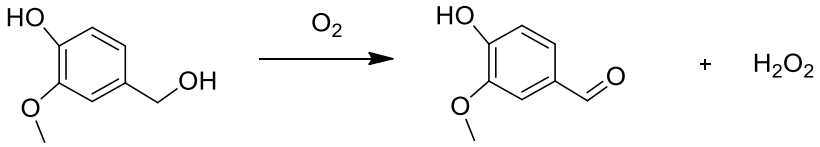

Figure 4. *A typical reaction catalyzed by VAO and EUGO: the oxidation of vanillin alcohol.*

2. APO FLAVOENZYME PRODUCTION

Flavoenzymes typically contain a tightly bound flavin cofactor. For many purposes it can be very useful to have access to a flavoenzyme devoid of its flavin cofactor, in its so-called apo form. Apo flavoenzymes are often prepared with the aim to determine their cofactor affinity. In other experiments apo flavoenzyme have been used for their reconstitution with an artificial cofactor in order to explore new enzymatic properties and applications. Deflavinylation techniques aim to produce the apo form of a flavoprotein which is still in the folded state, competent of binding the cofactor again. Reconstitution of properly prepared apo enzyme should yield a fully active holoenzyme. Most of the described approaches are only applicable to non-covalent FAD- or FMN-dependent flavoenzymes (Hefti,

Vervoort and Van Berkel, 2003). Nevertheless, with some newly developed approaches it is also possible to prepare the apo form for covalent flavoenzymes.

2.1 NON-COVALENT FLAVOENZYMES

For non-covalent flavoenzymes, deflavinylation is typically achieved upon (partial) unfolding enzyme, as it results in release of the flavin cofactor. This process requires mild conditions in order to prevent irreversible deactivation/unfolding (Hefti, Vervoort and Van Berkel, 2003). Usually, the addition of urea, guanidinium hydrochloride, halide ions and/or the use of ammonium sulfate results in deflavinylation. Optimization of the deflavinylation solution usually involves careful balancing the concentration of unfolding agent(s), salt(s) and pH. Glycerol might be added to protect the protein from full denaturation. Reversible immobilization of the target holo protein during the deflavinylation step can assist in this procedure. This has as benefit that the immobilized enzyme tends to be more stable, which is crucial during the application of the deflavinylation buffer, and the immobilized enzyme will not be able to form aggregate with other protein molecules. Furthermore, removal of the flavin cofactor from the immobilized protein can be easily monitored because it can simply be seen whether the yellow cofactor leaves the column. A deflavinylation procedure which involves the use of nickel-Sepharose to bind His-tagged flavoproteins is shown in Figure 5. Despite many trials, some proteins seem to be resilient towards any deflavinylation protocol indicating that preparation of apo flavoproteins can be a challenge (Hefti, Vervoort and Van Berkel, 2003)

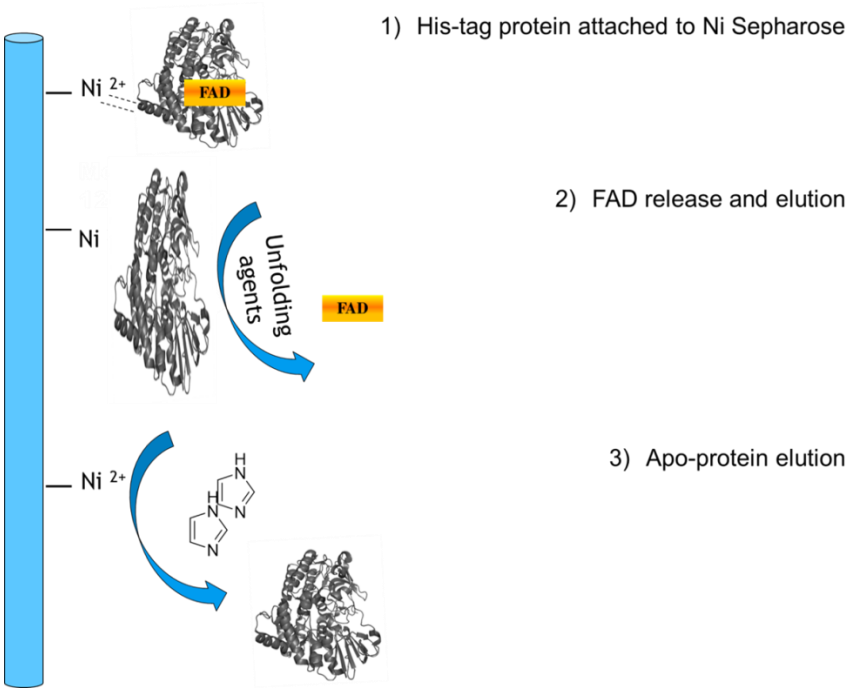

***Figure 5**. Deflavinylation using a nickel-Sepharose column (Hefti, Vervoort and Van Berkel, 2003)*

2.2 COVALENT FLAVOENZYMES

A generic method for deflavinylation has also been developed for the preparation of the apo form of a covalent flavoproteins. For that purpose, riboflavin-auxotrophic yeast and bacterial strains have been employed. By using such strains that are unable to synthesize the mature form of the common flavin cofactors, FMN and FAD, production of apo protein is feasible. For this approach, an effective expression vector is required that can be used in the available riboflavin-auxotrophic strains. The method is rather straightforward and has been successfully demonstrated for several covalent flavoproteins (Hefti, Vervoort and Van Berkel, 2003; Vogl *et al.*, 2007). However, it has as a disadvantage that the amount of produced apo protein is often rather low and often still contains a significant fraction of holo protein.

3. APPROACHES FOR ENZYME IMMOBILIZATION

Protein immobilization techniques have been developed since the 17th century (Cao, 2006). A huge advantage of immobilized proteins is that they can be easily separated from the reaction mixture and reused. Besides that, immobilization yields a high local concentration of enzymes, which is space-efficient. Nevertheless, when the enzymes are densely packed, the protein microenvironment can change, and it may alter enzymes' specificity, stability and kinetic parameters (Brena, González-Pombo and Batista-Viera, 2006). In fact, immobilization usually results in more stable proteins toward elevated temperatures and/or organic solvents. Additionally, immobilized enzymes can be used to perform reactions in atypical media and in a continuous mode, which allows their application in flow systems.

Enzymes can be immobilized by physical non-covalent interactions or in a covalent manner. Besides those two main approaches, there are also cross-linking techniques which result in enzymatic molecules attached one to another or being encapsulated (Brena, González-Pombo and Batista-Viera, 2006).

Covalent immobilization techniques usually employ an activated carrier, which subsequently can be linked to the target enzyme via functional groups localized at the protein surface. The carrier is typically functionalized with amine, carbonyl, hydroxyl or thiol groups or (very rarely) with the prosthetic group of a target enzyme. To create the covalent attachment of an enzyme usually relatively harsh conditions are applied. This often partially or fully inactivates the enzyme of interest. Therefore, optimization of covalent immobilization usually focuses on trying to create conditions that preserve enzyme activity during this process. Covalent immobilization, depending on the orientation of an enzyme molecule towards the carrier, can be divided into two groups: random and oriented.

3.1 RANDOM COVALENT ENZYME IMMOBILIZATION

Random immobilization methods typically exploit the reactivity of amino acids that are on the surface of a protein. Therefore it is applicable for virtually any enzyme. Because the generic nature of the

immobilization method, pure enzyme is required in case contamination with another biocatalysts has to be prevented. While random covalent immobilization is often employed because of its rather facile methodology, it has several disadvantages. The activity of randomly immobilized enzymes often can suffer from steric hindrances, causing limited mass transfer rates and sometimes (partial) loss of enzyme activity due to collapse of the enzyme molecular structure. Moreover, the covalent approach typically results in multiple enzyme layers on the carrier material (Cao, 2006). The latter phenomenon can be beneficial as results in a high enzyme loading. However, at the same time, it is may result in efficient usage of the immobilized enzyme due to limited mass transfer or enzyme deactivation.

Table 1. *Characteristics of standard covalent immobilization techniques (Brena, González-Pombo and Batista-Viera, 2006)*

Covalent immobilization	
Advantages	**Disadvantages**
High rigidity	Decrease in activity
Increased enzyme stability	High purity of enzyme is required during immobilization
High reusability	Change of enzyme characteristics (kinetics, specificity)
Suitable to scale up	Limited mass transfer

3.2. ORIENTED (COVALENT) ENZYME IMMOBILIZATION

Oriented immobilization, in which the site and type of attachment is targeted, usually results in formation of enzyme monolayers on the carrier surface with a tunable spatial distribution (Cao, 2006). This approach has higher chances to preserve full enzymatic activity. It typically depends on the design of a reactive ligand that is recognized by the target enzyme and can form a tight or even covalent complex.

A specific example of the oriented immobilization approach is to employ a cofactor for the attachment of a particular cofactor-binding enzyme to the carrier. This approach has been demonstrated already in 70's. At that time it served also to design affinity chromatography, specific for particular group of enzymes. One example is the immobilization of NAD^+ on reactive Sepharose material for the selective immobilization of the NAD-dependent dehydrogenases (Barry and O'Carra, 1973). Another interesting example was the preparation of Sepharose material functionalized with the cofactor pyridoxal 5'-phosphate. This could be used for successful immobilization of tyrosinase and tryptophanase (Goldstein and Katchalski-Katzir, 1976). The same immobilization approach can be employed to the FAD cofactor (Figure 6). As FAD can selectively bind to apo flavoenzymes with very

high affinity, this procedure does not require a high purity of the protein sample. Immobilization via the FAD cofactor has been demonstrated for a few times in the past few decades (Wingard, 1984). Nevertheless, this approach depends on a flavoenzyme which is able to bind a FAD cofactor to which a linker has been attached. In some cases, protein engineering may be needed to introduce such cofactor binding property. Nowadays, a large number of flavoenzymes have been described in detail, including their molecular structures, and plenty techniques for their engineering are available (van Berkel, Kamerbeek and Fraaije, 2006). Chapter 2 describes the successful FAD-mediated immobilization of PAMO and PAMO fused to phosphite dehydrogenase. We could show that the developed method results in a stable and fully active PAMO.

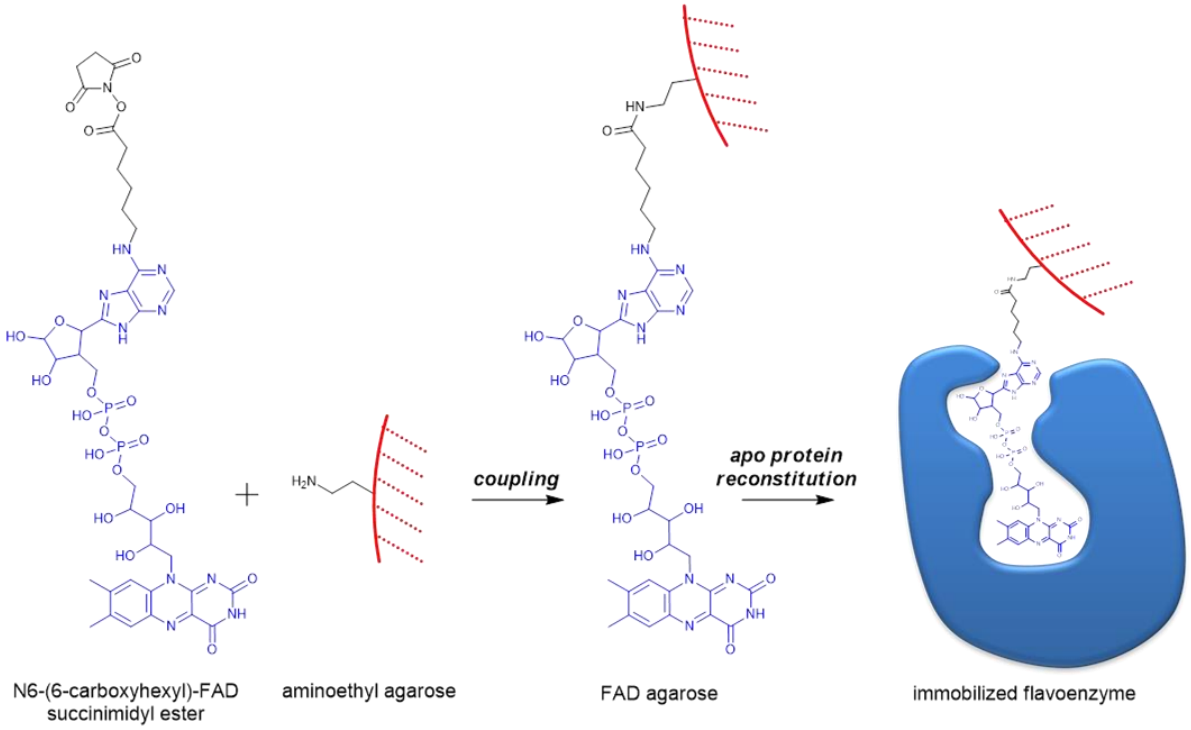

Figure 6. *Example of cofactor-mediated covalent immobilization. The modified FAD cofactor, N^6-(6-carboxyhexyl)-FAD succinimidyl ester, is first covalently immobilized on a carrier and subsequently apo enzyme is reconstituted yielding immobilized holo flavoenzyme.*

3.3 SYNTHESIS OF N^6-SUBSTITUTED FAD ANALOGUES FOR COFACTOR-MEDIATED IMMOBILIZATION

FAD-mediated immobilization requires flavin cofactor derivatives which contain a linker for covalent anchoring to material while it still should bind to the target apo protein. Most commonly it involves incorporation of a primary amine or carboxyl group. Nevertheless, when considering the relatively large and complex FAD molecule (Figure 1), it is clear that a selective derivatization of FAD might be difficult as it contains multiple reactive groups. Besides that, FAD is soluble in aquatic solutions but

poorly soluble in organic solvents and only stable at neutral pH. For these reasons, the scope of chemistry that can be used for modifying FAD is limited and the synthesis of FAD derivatives is very challenging. The most suitable FAD moiety for derivatization is the adenine N^6 as it is usually located close to or at the protein surface (Massey, 2000). This target moiety can be substituted either directly, or first via substitution of the adenine N^1, which subsequently undergoes Dimroth rearrangement into a more stable, N^6-FAD derivative (Bückmann, Wray and Stocker, 1997). FAD analogues synthetized via direct substitution of the adenine N^6 cannot be selectively prepared from the FAD molecule. Therefore, they are synthetized from N^6 functionalized adenosine and FMN, which results in a lengthy multistep and inefficient synthetic pathway (Saleh, Compernolle and Janssen, 1995). Till now, there are only few reports describing methods for chemical FAD derivatization involving a Dimroth rearrangement. In Chapter 3 we describe a new and more efficient pathway for FAD N^6-derivatization.

4. SUMMARY

Flavoenzymes can be used for a wide range of different biocatalytic applications. For their use, efficient immobilization techniques are very valuable. This will allow effective usage of these potent biocatalysts and it may also help in developing new biotechnological tools, such as biosensors in which the flavoenzyme is immobilized on electrodes or efficient flow reactors. By exploiting the tight binding of the flavin cofactor, apo flavoenzymes can be subtly immobilized on any material that has been decorated with FAD. Chapter 2 describes a successful example of such FAD-mediated flavoenzyme immobilization approach. It yielded an immobilized monooxygenase that displayed a higher stability when compared with the enzyme when in solution while it was fully active. As the immobilization is based on binding to the FAD derivatives, the method prevents formation of multilayer of immobilized enzymes. As the newly developed method depends on the availability of reactive and well-designed FAD derivative, effort was put in developing a new synthesis route towards such modified flavin cofactor, derivatized at the adenine N^6. Chapter 3 described such new synthesis protocol which is more efficient when compared with previous reported methods.

A flavoenzyme of significant interest is hFMO3, which catalyzes oxidative metabolism of xenobiotics in human liver. This monooxygenase is of high importance for health-related studies but is very difficult to obtain as isolated enzyme. Chapter 4 describes previous attempts for recombinant expression of this membrane-associated enzyme. Heterologous expression of hFMO3 has been shown to be extremely troublesome. A detailed sequence analysis reveals which parts of the protein may be involved in membrane association and which residues may play a crucial role in catalysis. Furthermore, work is presented on a new attempt of expressing hFMO3: the expression of hFMO3 fused to a coenzyme regenerating enzyme, phosphite dehydrogenase, in *E. coli*. This led to a low level of bacterial expression of active hFMO3. Another and new strategy for generating hFMO-related

metabolites is described in Chapter 5. It is shown that a library of (thermostable) microbial flavoprotein monooxygenases can be used for chemo- and enantioselective oxygenations of known human drugs and metabolites.

REFERENCES

Barry, S. & O'Carra, P., 1973. Affinity chromatography of nicotinamide-adenine dinucleotide-linked dehydrogenases on immobilized derivatives of the dinucleotide. The Biochemical journal, 135(4), pp.595–607.

Brena, B., González-Pombo, P. & Batista-Viera, F., 2006. Immobilization of enzymes: A literature survey. In Immobilization of enzymes and cells. pp. 15–30.

Bückmann, A.F., Wray, V. & Stocker, A., 1997. Synthesis of N6-(2-Aminoethyl)-FAD, N6-(6-carboxyhexyl)-FAD, and related compounds. Methods Enzymol, 280(1991), pp.360–374.

Cao, L., 2006. Carrier-bound immobilized enzymes: principles, application and design, Wiley.

Cashman, J.R. & Zhang, J., 2006. Human flavin-containing monooxygenases. Annual review of pharmacology and toxicology, 46, pp.65–100.

Chaiyen, P., Fraaije, M.W. & Mattevi, A., 2012. The enigmatic reaction of flavins with oxygen. Trends in Biochemical Sciences, 37(9), pp.373–80.

Dijkman, W.P. et al., 2013. Flavoprotein oxidases: classification and applications. Applied Microbiology and Biotechnology, 97(12), pp.5177–5188.

Goldstein, L. & Katchalski-Katzir, E., 1976. Immobilized enzymes principles. Applied Biochemistry and Bioengineering, 1, pp.1–364.

Hefti, M.H., Vervoort, J. & Van Berkel, W.J.H., 2003. Deflavination and reconstitution of flavoproteins: Tackling fold and function. European Journal of Biochemistry, 270(21), pp.4227–4242.

Heuts, D.P.H.M. et al., 2009. What's in a covalent bond?: On the role and formation of covalently bound flavin cofactors. FEBS Journal, 276(13), pp.3405–3427.

Jin, J. et al., 2008. Covalent flavinylation of vanillyl-alcohol oxidase is an autocatalytic process. FEBS Journal, 275(20), pp.5191–5200.

Kamerbeek, N., 2004. Biochemical properties and catalytic scope of a Baeyer-Villiger monooxygenase, thesis, University of Groningen.

Krueger, S.K. & Williams, D.E., 2005. Mammalian flavin-containing monooxygenases: structure/function, genetic polymorphisms and role in drug metabolism. Pharmacology & Therapeutics, 106(3), pp.357–387.

Macheroux, P., Kappes, B. & Ealick, S.E., 2011. Flavogenomics - A genomic and structural view of flavin-dependent proteins. FEBS Journal, 278(15), pp.2625–2634.

Massey, V., 2000. The chemical and biological versatility of riboflavin. Biochemical Society transactions, 28(4), pp.283–96.

Motika, M.S., Zhang, J. & Cashman, J.R., 2007. Flavin-containing monooxygenase 3 and human disease. Expert Opinion on Drug Metabolism & Toxicology, 3(6), pp.831–845.

Saleh, A., Compernolle, F. & Janssen, G., 1995. An improved synthesis of N6-(6-Aminohexyl)FAD. Nucleosides and Nucleotides, 14(3–5), pp.689–692.

Torres Pazmiño, D.E. et al., 2008. Kinetic mechanism of phenylacetone monooxygenase from *Thermobifida fusca*. Biochemistry, 47(13), pp.4082–4093.

Torres Pazmiño, D.E. & Fraaije, M.W., 2008. Discovery, redesign and applications of Baeyer-Villiger monooxygenases. In T. Mastuda, ed. Future directions in biocatalysis. Amsterdam: Elsevier, pp. 107–128.

Vogl, C. et al., 2007. Characterization of riboflavin (vitamin B2) transport proteins from *Bacillus subtilis* and *Corynebacterium glutamicum*. Journal of Bacteriology, 189(20), pp.7367–7375.

Wingard, L.B., 1984. Cofactor modified electrodes. Trends in Analytical Chemistry, 3(9), pp.235–238.

CHAPTER 2

COVALENT IMMOBILIZATION OF A FLAVOPROTEIN MONOOXYGENASE VIA ITS FLAVIN COFACTOR

Marzena Krzek[a], Hugo L. van Beek[a], Hjalmar P. Permentier[b], Rainer Bischoff[b], Marco W. Fraaije[,a]*

[a] Molecular Enzymology Group, University of Groningen, Nijenborgh 4, 9747AG Groningen, the Netherlands

[b] University of Groningen, Department of Pharmacy, Analytical Biochemistry, Antonius-Deusinglaan 1, 9713 AV Groningen, The Netherlands

Published in Enzyme and Microbial Technology. 2016 (82), p. 138-43,
DOI: 10.1016/j.enzmictec.2015.09.006

ABSTRACT

A generic approach for flavoenzyme immobilization was developed in which the flavin cofactor is used for anchoring enzymes onto the carrier. It exploits the tight binding of flavin cofactors to their target apo proteins. The method was tested for phenylacetone monooxygenase (PAMO) which is a well-studied and industrially interesting biocatalyst. Also a fusion protein was tested: PAMO fused to phosphite dehydrogenase (PTDH-PAMO). The employed flavin cofactor derivative, N^6-(6-carboxyhexyl)-FAD succinimidylester (FAD*), was covalently anchored to agarose beads and served for apo enzyme immobilization by their reconstitution into holo enzymes. The thus immobilized enzymes retained their activity and remained active after several rounds of catalysis. For both tested enzymes, the generated agarose beads contained 3 U per g of dry resin. Notably, FAD-immobilized PAMO was found to be more thermostable (40% activity after 1 h at 60 °C) when compared to PAMO in solution (no activity detected after 1 h at 60 °C). The FAD-decorated agarose material could be easily recycled allowing multiple rounds of immobilization. This method allows an efficient and selective immobilization of flavoproteins via the FAD flavin cofactor onto a recyclable carrier.

Keywords: Flavoenzyme, FAD, immobilization, apo enzyme, monooxygenase

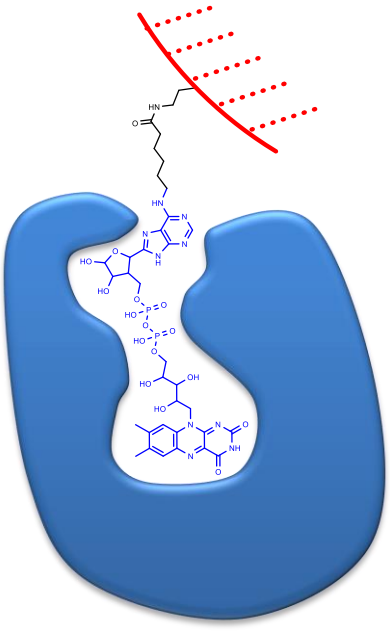

cofactor-mediated flavoenzyme immobiization

1. INTRODUCTION

Enzyme immobilization methods aim at generating a stable and reusable biocatalyst and is driven by diverse enzyme-based applications in industry, analytics and medicine. For detailed information on the various known method of enzyme immobilization, we refer to some recent reviews (Rodríguez *et al.*, 2009; Franssen *et al.*, 2013; Guzik, Hupert-Kocurek and Wojcieszynska, 2014; Barbosa *et al.*, 2015). Typical immobilization methods result in uncontrolled enzyme-carrier orientations which may affect the enzyme performance due to mass transfer obstruction. Apart from that, covalent coupling to the carrier often involves chemicals and conditions that are harmful for the target enzyme, resulting in a decreased activity and/or stability of the biocatalyst (Sheldon, 2007). On the other hand, non-covalent adsorption of enzymes usually involves mild conditions but often results in labile systems (Sheldon, 2007). Moreover, most available methods tend to require either an excess or high purity of the enzyme to be immobilized, which is not favorable for economic purposes. Therefore, it is desirable to develop efficient immobilization methods for creating robust immobilized enzymes with high catalytic performance.

In the field of redox biocatalysis, flavin-containing enzymes are regarded as particularly useful. Flavoprotein reductases, oxidases and monooxygenases convert substrates with high stereo-, enantio- and regioselectivity into valuable products such as functionalized building blocks for further use in polymer, pharmacological, food and fine-chemical industry (van Berkel, Kamerbeek and Fraaije, 2006; Torres Pazmiño, Dudek and Fraaije, 2010; Winter and Fraaije, 2012). In the last decade, the toolbox of flavoenzymes has significantly expanded thanks to enzyme engineering and discovery efforts (Fraaije *et al.*, 2005; Torres Pazmiño, Dudek and Fraaije, 2010; van Beek, Gonzalo and Fraaije, 2012). The majority of flavoenzymes contain a tightly and non-covalently bound FAD cofactor. Various methods have been developed to prepare flavoproteins devoid of their native flavin cofactor (Hefti, Vervoort and Van Berkel, 2003). Once prepared, such apo proteins are typically readily reconstituted with FAD or FAD analogues (Fruk *et al.*, 2009). A large number of synthetic FAD derivatives have been explored before, mostly with the aim to elucidate mechanistic features of FAD-containing enzymes (Massey, 2000). For these studies, the isoalloxazine is typically modified to probe the effects on catalysis. For changing the binding properties of a FAD cofactor without affecting the redox properties, derivatization of the adenine moiety is a better candidate as it is distant from the redox active moiety, the isoalloxazine ring (Figure 2, Chapter 1). In fact, in many flavoproteins the adenine part of FAD is close to the protein surface or even partially exposed to the solvent. Adenine N^6-FAD-derivatives have been shown to be more efficient over adenine N^1-FAD in reconstituting apo forms of flavoprotein oxidases (Zappelli *et al.*, 1978). Using N^6-(2-aminoethyl)-FAD, Willner et al. have shown that it is feasible to anchor glucose oxidase on electrodes (Willner *et al.*, 1996). With this system, a glucose-dependent electric current could be monitored. Moreover, D-amino acid oxidase and

L-aspartate oxidase were shown to bind N^6-adenine modified FAD yielding artificial covalent flavoprotein oxidases (Stocker, Hecht and Bückmann, 1996; Willner *et al.*, 1996). Nevertheless, it resulted in a significant decrease in oxidase activity. In this paper we demonstrate that N^6-hexyl-FAD-decorated agarose beads could be used for efficient immobilization of a flavoprotein monooxygenase.

For this study we have chosen phenylacetone monooxygenase (PAMO) from *Thermobifida fusca* as a model flavoenzyme. It has been demonstrated by several groups that this bacterial monomeric FAD-containing monooxygenase can be used for a number of industrially interesting oxygenation reactions, e.g., enantioselective sulfoxidations and Baeyer–Villiger oxidation (van Berkel, Kamerbeek and Fraaije, 2006; de Gonzalo, Mihovilovic and Fraaije, 2010). In addition, its crystal structure has been solved (Malito *et al.*, 2004), the catalytic performance and substrate scope has been well described, the expression in Escherichia coli is efficient (van Bloois *et al.*, 2012), and the enzyme displays remarkable stability against elevated temperatures and a wide range of organic solvents (Rodríguez *et al.*, 2009; Secundo *et al.*, 2011). This renders it as a convenient model flavoenzyme. PAMO belongs to the class of Baeyer–Villiger monooxygenases (BVMOs) which require the coenzyme NADPH for catalysis (Figure 1). A number of research efforts have been directed toward efficient regeneration of the nicotinamide coenzyme (Wichmann and Vasic-Racki, 2005). One approach for efficient NADPH recycling is represented by the production of Baeyer–Villiger monooxygenases fused to a thermostable phosphite dehydrogenase (PTDH) rendering the monooxygenase a self-sufficient biocatalyst. PTDH is able to regenerate NADPH at the expense of relatively cheap phosphite. The fused PTDH-BVMO biocatalysts were shown to display a high catalytic performance, moreover the expression of BVMOs fused to PTDH was found to boost protein expression (Torres Pazmiño *et al.*, 2009).

In this contribution, we present an approach for immobilizing flavoenzymes via their FAD cofactor which offers a mild and controllable enzyme loading on the target carrier material.

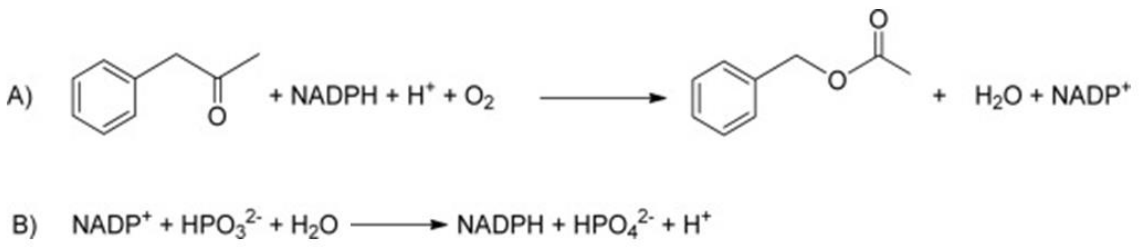

Figure 1. *(A) The Baeyer–Villiger oxidation of phenylacetone into benzyl acetate catalyzed by PAMO. The enzyme uses NADPH as electron donor and molecular oxygen asoxygen donor. (B) Phosphite oxidation catalyzed by PTDH which results in formation of NADPH.*

2. MATERIALS AND METHODS

2.1. MATERIALS

Low density aminoethyl 6 Rapid Run™ agarose beads (spherical beads of 50–150 μm, with 15–25 μmol/mL of gel) were obtained from Agarose Beads Technology. The amino groups have been introduced as described in literature (Fernandez-Lafuente *et al.*, 1993). N^6-(6-carboxyhexyl)-FAD succinimidylester (FAD*) (Figure 6, chapter 1) was synthesized by BioLog. Nickel-Sepharose HP (GE Healthcare) and DG-10 EconoPac desalting columns (BioRad) were used for protein purification and preparation of the apo forms of enzymes. All other chemicals were purchased from Sigma–Aldrich, Merck or ACROS Organics.

2.2. ENZYME EXPRESSION, PURIFICATION, AND ASSAY

His-tagged PAMO (referred to as PAMO) and His-tagged PTDH-PAMO were overexpressed in E. coli TOP10. The enzymes were purified as previously described (Torres Pazmiño *et al.*, 2009; Dudek *et al.*, 2010). The activity was verified by monitoring NADPH absorbance depletion at 340 nm (ε_{340} = 6.22 mM^{-1} cm^{-1} in 50 mM Tris/HCl pH 7.5) with 0.10 mM NADPH and 0.80 mM of phenylacetone as substrate (Torres Pazmiño *et al.*, 2008) while using an atmospheric dioxygen concentration (0.24 mM).

2.3. FAD-CARRIER PREPARATION

FAD-decorated agarose was prepared by incubating FAD* with aminoethyl agarose beads (0.31 μmol FAD* per 0.25 mg of dry beads, which equals 0.09 μmol amine groups, in a total volume of 2.25 mL) in 50 mM phosphate pH 8.0 at room temperature for 3 h (Fig. 1). Subsequently, the resin was transferred to an empty column and washed with 0.5 M NaCl, 50 mM Tris/HCl (pH 7.5) in order to remove non-covalently bound FAD. After this procedure the agarose beads displayed an intense yellow color due to the coupled FAD.

2.4. APO ENZYMES PREPARATION AND RECONSTITUTION

Different combinations of urea and KBr were tested for release of the FAD cofactor from PAMO when bound to the nickel-loaded Sepharose column (10 mg protein per 1 mL of column material). The non-covalently bound FAD was washed from the protein immobilized on the column until the yellow color had disappeared. The retained apo enzyme was subsequently washed with 50 mM Tris/HCl (pH

7.5) and finally released from the column with 200 mM imidazole with 20% glycerol in 50 mM Tris/HCl (pH 7.5). The eluted apo protein solution was immediately applied on the desalting column and desalted using 50 mM Tris/HCl (pH 7.5). The amount of obtained apo enzyme was calculated from the absorbance at 280 nm using the following absorption coefficients: 157 mM^{-1} cm^{-1} and 210 mM^{-1} cm^{-1} for PAMO and PTDH-PAMO, respectively.

To test the reconstitutability of the obtained apo enzymes, 5.0 μM apo protein in 50 mM Tris/HCl (pH 7.5) was incubated with 100 μM FAD at room temperature for 2 h. Activity of the obtained holo enzymes was measured as described in Section 2.2. The apo enzymes were also tested for storage stability by freezing samples at −20 °C. For that, their reconstitutability with FAD has been measured before and after freezing. Additionally, UV–vis spectra of reconstituted protein, after using a desalting column for removing free FAD, were collected. The reconstitution of apo PAMO with FAD* was performed and evaluated as done for FAD. Additionally, ESI–MS and SDS-PAGE analysis for detecting covalent FAD* was performed as described previously (Jin *et al.*, 2007). PyMOL was used for manual docking of FAD* and visualization of the PAMO structure (PDB ID: 1W4X).

2.5. IMMOBILIZATION OF APO ENZYMES ON FAD*-AGAROSE

Typically, FAD-decorated agarose beads (prepared from 8 mg of dry aminoethyl agarose resin) were incubated with 2.5 mg apo enzyme in 8.0 mL 50 mM Tris/HCl (pH 7.5) on a rotating platform at room temperature for 3 h. Subsequently, the resin was washed with 10 times agarose resin volume using the same buffer. As a control experiment, the agarose beads without covalently attached FAD were incubated with apo enzyme using the same conditions. Some apo PTDH-PAMO tended to form protein aggregates upon mixing with agarose beads. Protein aggregates were removed by centrifugation before testing the material.

2.5.1. ENZYME LOADING DETERMINATION

To determine the amount of enzyme immobilized on the agarose, the bound protein was released from the agarose in gravity flow columns using the deflavinylation solution until complete removal of protein (monitored by 280 nm absorbance detection). The amount of retrieved protein was calculated from its absorbance at 280 nm. Enzyme loading was also determined for beads after repetitive use and for beads after high-temperature incubation.

2.5.2. CONVERSIONS USING IMMOBILIZED ENZYME

For conversions, agarose with immobilized enzyme (151 mg dry carrier in 7 mL) was incubated in a reaction mixture containing 8.0 mM phenylacetone, 100 μM NADPH, 16 mM phosphite, 50 mM Tris/Cl (pH 7.5). In case of immobilized PAMO, 1.0 μM PTDH was added to the reaction mixture to

assure regeneration of NADPH. The reaction mixture in a glass vial was placed on a rotating platform. Samples were withdrawn at various time points and extracted with ethyl acetate containing 0.1% mesitylene. The samples were dried over $MgCl_2$ and subsequently analyzed by GC (AT5 column, 30 m × 0.25 mm × 0.25 μm, Grace) using the following temperature program: 2 min at 100 °C, 5 °C/min up to 120 °C, 20 °C/min up to 160 °C. Retention times of phenylacetone and benzyl acetate were 6.96 min and 7.45 min, respectively. Two negative controls were performed: (1) FAD-decorated beads that had not been incubated with the apo enzyme, and (2) aminoethyl agarose beads (without FAD) incubated with the apo enzyme.

2.5.3. Immobilized enzymes reusability

The reusability of the enzymes immobilized on FAD-decorated agarose beads was tested by determining the activity after repeated use for biocatalytic conversions. After each conversion test, the beads were washed three times with 50 mM Tris/HCl (pH 7.5) by subsequent centrifugation and resuspension, and stored at 4 °C before the next conversion.

2.5.4. Thermostability and reusability of immobilized PAMO

To determine thermostability, PAMO immobilized on the FAD-functionalized agarose and PAMO free in solution (both in 50 mM Tris/HCl, pH 7.5) were incubated at room temperature, 50 °C, and 60 °C. Samples were taken at the indicated time intervals, placed on ice, and subsequently tested for monooxygenase activity by measuring time-dependent oxygen consumption using a Firesting O2 Fiber-optic Oxygen Meter (PyroScience). The oxygen sensor was calibrated for 100% oxygen content with room-temperature air-equilibrated Milli-Q. Activity was measured using 50 mM Tris/HCl pH 7.5) with 0.10 mM NADPH and 0.80 mM of phenylacetone as substrates. The linear decrease in oxygen concentration versus time during the first two minutes after substrate addition was used to determine enzymatic activity.

The FAD-agarose with immobilized enzymes was recycled by protein removal using the deflavinylation solution (4.0 M urea and 2.0 M KBr in 50 mM Tris, pH 7.5). The obtained material could be reused for another round of enzyme immobilization.

3. RESULTS AND DISCUSSION

3.1. PREPARATION AND RECONSTITUTION OF APO PAMO AND APO PTDH-PAMO

To date, a variety of methods to prepare apo forms of flavoproteins have been developed (Hefti, Vervoort and Van Berkel, 2003; Fruk *et al.*, 2009). A relatively recent development is the deflavinylation of His-tagged flavoproteins while bound on nickel-charged resin (Hefti, Vervoort and Van Berkel, 2003). Using this approach, we could successfully prepare the apo forms of PAMO and PTDH-PAMO. It was found that a solution of 4.0 M urea and 2.0 M KBr in 50 mM Tris, pH 7.5 (deflavinylation solution) was needed to induce (partial) unfolding which results in release of the FAD from PAMO and PTDH-PAMO when bound to nickel-Sepharose. After eluting the FAD-free proteins from the nickel-Sepharose with imidazole, the colorless protein solution was applied on a desalting column to exchange the buffer into 50 mM Tris/HCl, pH 7.5. The typical yield of apo protein obtained by this procedure was 70–80%. The resulting apo enzyme did not show any activity and did not show absorbance at 450 nm which confirms that the protein is devoid of the flavin cofactor. Moreover, it was found that apo PAMO (50 mM Tris, pH 7.5) could be stored for three weeks at −20 °C without affecting its reconstitution properties. This shows that apo PAMO, even without its prosthetic group, is a rather robust protein. The apo form of PTDH-PAMO was found to be less stable as extensive shaking or centrifugation caused partial enzyme precipitation.

3.2. RECONSTITUTION OF APO PAMO AND APO PAMO-PTDH

Addition of FAD to apo PAMO led to complete incorporation of the flavin cofactor as evidenced by the complete recovery of activity. The same was found for apo PAMO-PTDH. For another verification of formation of holo PAMO, UV/vis absorbance spectra confirmed its binding to the native protein. The spectral features of the flavin absorbance spectrum and the A280/A440 ratio (indicative for the protein/cofactor content) after FAD reconstitution of apo PAMO were the same when compared with the native holo enzyme (Fraaije *et al.*, 2005; Dudek *et al.*, 2011). This confirms that the microenvironment around the flavin in the reconstituted protein is identical to the native holo protein.
Due to the presence of the succinimidyl-ester moiety, binding of FAD* to apo PAMO can potentially lead to covalent coupling of the flavin cofactor to lysine residues. To test whether FAD* is able to bind and perhaps form a covalent protein-bound FAD, the FAD*-reconstituted enzyme was prepared and analyzed by SDS-PAGE and subsequent in-gel flavin fluorescence detection. This revealed that the FAD*-reconstituted protein indeed contained covalently bound FAD as evidenced by flavin fluorescence of the protein in the gel (Fig. S1). Moreover, it was found that the FAD*-reconstituted

enzyme displayed a similar K_M towards phenylacetone ($K_{M,phenylacetone}$ = 69 μM for FAD*-bound PAMO vs. 66 μM for native holo PAMO), while the apparent kcat had been decreased up to 50% of the value of native PAMO. The FAD*-reconstituted enzyme also did not show an increased uncoupling rate when compared with the native enzyme (consumption of NADPH in the absence of NADPH). The minor effects on the kinetic parameters is in line with the fact that the modification on the flavin (located on the adenine part) is far from the redox-active isoalloxazine moiety. The activity decreased when the incubation with FAD* was prolonged. While many covalent flavoprotein oxidases have been reported in literature, this is the first example of a flavoprotein monooxygenase containing a covalently anchored flavin cofactor. Inspection of the crystal structure of PAMO disclosed that there is one plausible candidate for such covalent FAD* tethering: the NH_2 group of Lys398 is only 7.6 Å away from the N^6-adenine of the FAD while all other lysines are at a distance of >10 Å. MS analysis of a tryptic digest of FAD*-bound PAMO did not reveal any FAD-containing peptides, possibly due to FAD-peptides being too large or displaying poor ionization behavior. Yet, comparison of the tryptic digest MS peptide patterns of PAMO reconstituted with FAD or FAD* showed that the peptide containing Lys398 decreased significantly when analyzing FAD*-reconstituted PAMO. ESI–MS analysis of unfolded FAD*-bound PAMO revealed several protein species: a species that corresponds to merely the protein (25% of the total intensity of PAMO peaks), a species with the mass of the protein and an additional mass of an FAD* molecule (40%), a species with the mass of the protein and two attached FAD* molecules (20%) and some other higher mass protein species with multiple FAD* molecules (Fig. S2).

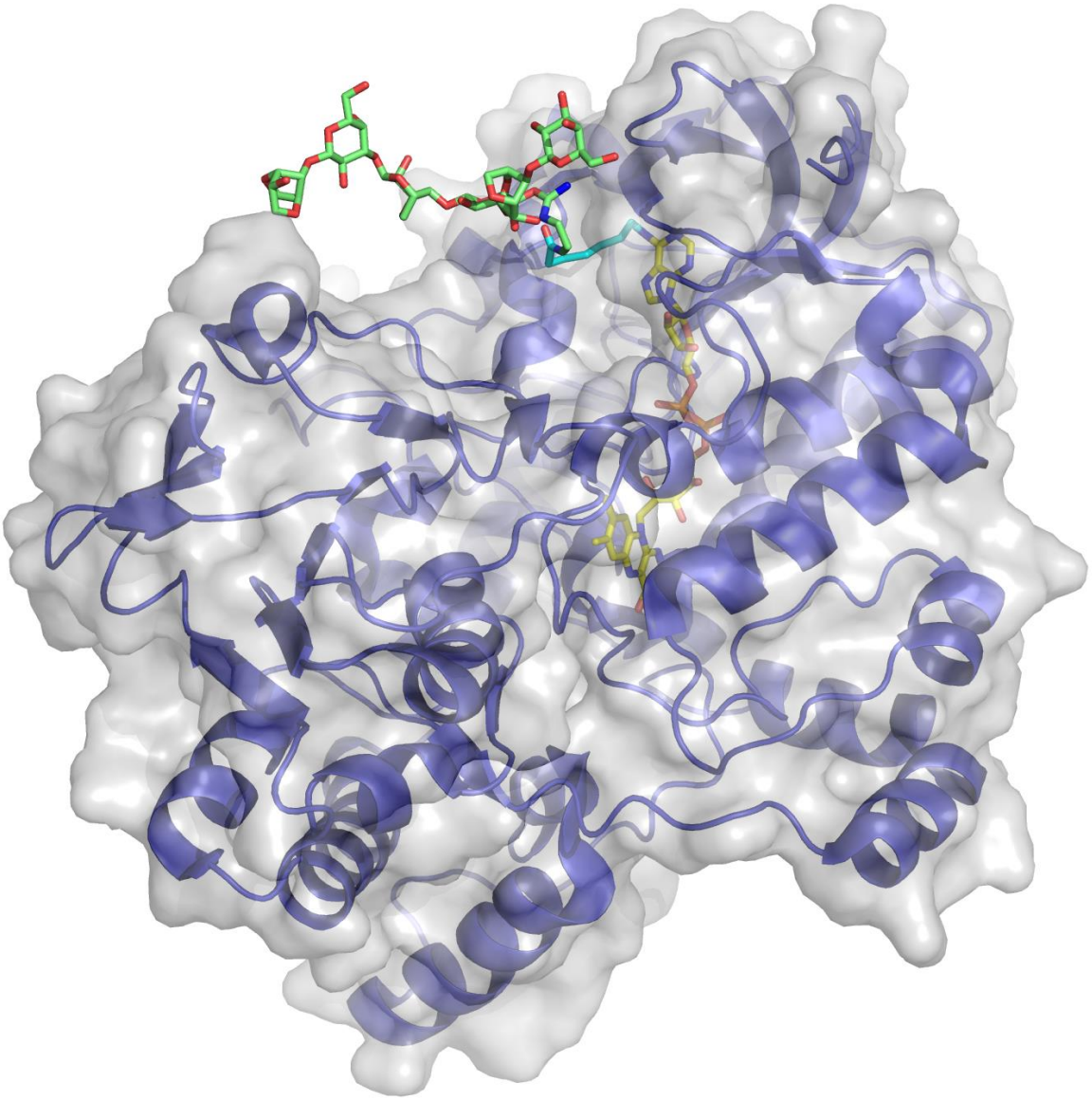

Figure. 2. *PAMO reconstituted with N^6-(6-carboxyhexyl)-FAD succinimidylester on the aminoethyl agarose beads. Binding of FAD* was modeled in the structure of PAMO (PDB ID: 1W4X) by manually adding to the N^6-adenine atom of FAD (FAD carbons in yellow) the hexyl linker part (carbons in cyan) coupled to an ethyl-N-agarose moiety (carbons in green).*

This revealed that except for PAMO with one covalently attached FAD*, some protein does not contain any covalently attached FAD while other protein molecules have two or more covalently attached FAD* molecules. The heterogeneous FAD* binding modes may well explain the lower activity observed for the FAD*-reconstituted PAMO. Overall, the results show that apo PAMO is able to accommodate FAD* in a catalytically competent conformation.

3.3. PREPARATION OF FAD-FUNCTIONALIZED AGAROSE

After having established that PAMO can be reconstituted with a N^6-adenine-FAD derivative into a fully active biocatalyst, we explored the possibility to exploit this promiscuous cofactor binding property to anchor the enzyme to a carrier via its cofactor. For the envisaged method of enzyme immobilization, FAD-functionalized carrier had to be prepared. Binding of apo protein to such material would allow immobilization of any target apo flavoprotein while it would also eliminate the binding of multiple flavin cofactors to single apo protein as observed above. For this, aminoethyl agarose was coupled to the FAD* via the succinimidyl ester moiety (Fig. 6 in Chapter 1). As a result, a stable amide bond was formed between the agarose-based carrier and the flavin derivative resulting in a brightly yellow agarose material. The generated FAD-agarose was stable upon extensive washing with buffer, water and 1.0 M sodium chloride as it retained its yellow color. Moreover, a similar incubation with normal FAD (negative control) yielded colorless beads.

3.3.1. ENZYME IMMOBILIZATION

The FAD-agarose was tested as carrier for enzyme immobilization using two apo flavoproteins, apo PAMO and apo PTDH-PAMO. Inspection of the PAMO crystal structure suggested that the designed FAD*-agarose would allow binding to the apo protein: the hexyl linker between the FAD and agarose carrier seems compatible with the protein structure (Figure. 2). Incubation with both apo proteins resulted in agarose material that indeed displayed monooxygenase activity (Figure. 3, Table S1). The FAD-agarose beads incubated without apo proteins did not show any activity. Enzyme loading on the FAD-agarose was 3.9 mg (0.060 μmol) and 3.5 mg (0.035 μmol) of protein per gram dry beads for PAMO and PTDH-PAMO respectively. The specific activity was 2.9 and 3.0 U per gram of dry beads (Table S1). These results show that the immobilized enzymes display activities that are similar when compared with their free forms. It indicates that the porous beads do not impose diffusion limitations that translate into lower rate of conversion. By varying the concentration of reactive amino groups on the carrier and optimizing the incubation conditions higher enzyme loading may be achieved but such optimization was not pursued in this study. Recently, it was shown that PAMO can also be covalently immobilized on polyphosphazenes yielding 8 U per gram of carrier after multiparametrical optimization (Cuetos *et al.*, 2012). However, in that case, a significant decrease of enzymatic performance was observed upon immobilization.

3.3.2. STABILITY OF PREPARED BIOCATALYSTS AND CARRIER

A study on the reusability of the immobilized enzymes was performed. Figure. 3 summarizes the catalytic performance of PAMO and PTDH-PAMO immobilized on FAD-agarose. Each enzyme

variant was immobilized on agarose beads and the immobilized enzyme was used in three subsequent conversions. The data show that PAMO-containing beads lose 13% of their activity after the first conversion. This may be caused by dissociation of some apo enzyme molecules during recycling of the immobilized biocatalyst. The loss of activity for PTDH-PAMO (44%) is more severe and may be related to higher mechanical stress experienced by the fusion protein and/or by a lower cofactor affinity. Nonetheless, the data show that FAD-immobilized PAMO and PTDH-PAMO can be reused. Furthermore, for PAMO we observed that the immobilized biocatalyst can be stored for over 5 months at 4 °C while retaining 68% of its activity. For generating a more stable immobilized biocatalyst, the use of heterofunctional support could be considered as this would allow, after FAD-mediated immobilization of the enzyme, to strengthen immobilization by a subsequent alternative covalent immobilization approach (Dos Santos *et al.*, 2015). This would prevent enzyme release while it still affords control on how the enzyme is positioned on the support.

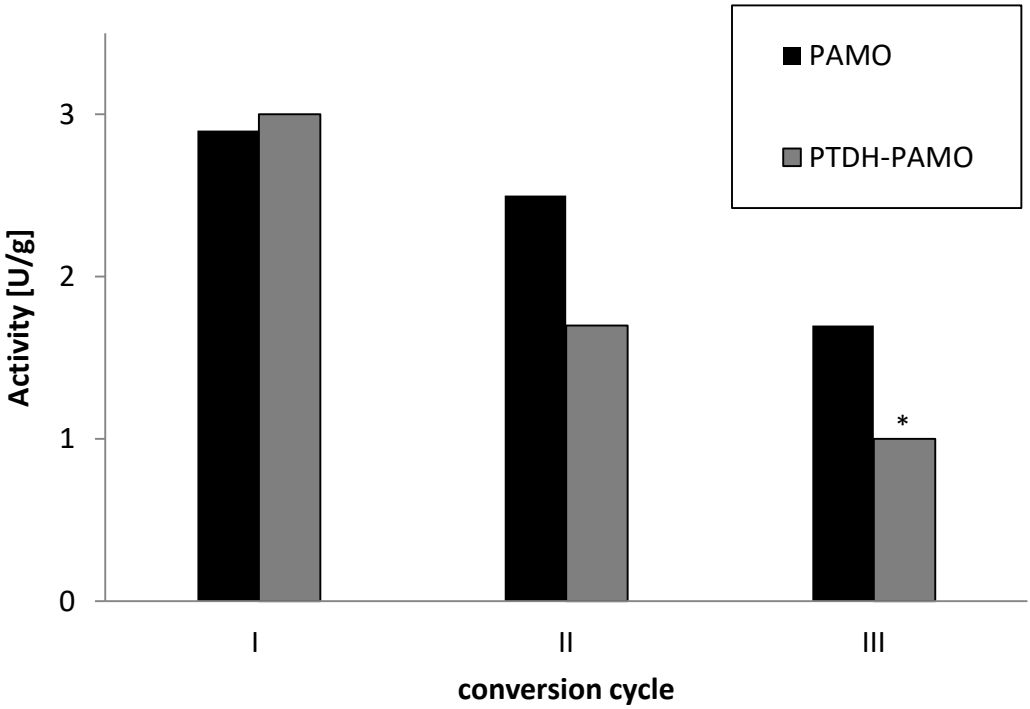

Figure . 3. *Activity of immobilized enzymes after several round of conversion.*

To probe the thermostability of immobilized PAMO, the time dependent inactivation at elevated temperatures (50 and 60 °C) was monitored. This revealed that the immobilization has a beneficial effect on enzyme stability (Figure. 4). After an incubation for 1 h at 60 °C, the agarose beads with immobilized PAMO retained 40% activity, while the free enzyme displayed no significant activity anymore and started to precipitate. The latter is in line with the previously determined apparent melting temperature of native PAMO: T_m = 60 °C (Cuetos *et al.*, 2012). The activity decrease for immobilized enzyme at elevated temperatures was accompanied by release of apo protein from the carrier.

By using the deflavinylation solution, PAMO-agarose could be regenerated into FAD-agarose by stripping of the protein. The resulting FAD-agarose lost all enzyme activity confirming release of the protein. The recycled FAD-agarose was reused for another round of immobilization. The resulting immobilized PAMO again displayed catalytic activity identical to the freshly immobilized enzymes. This shows that the method is flexible in the sense that the generated FAD-agarose can be reused for other flavoprotein immobilizations.

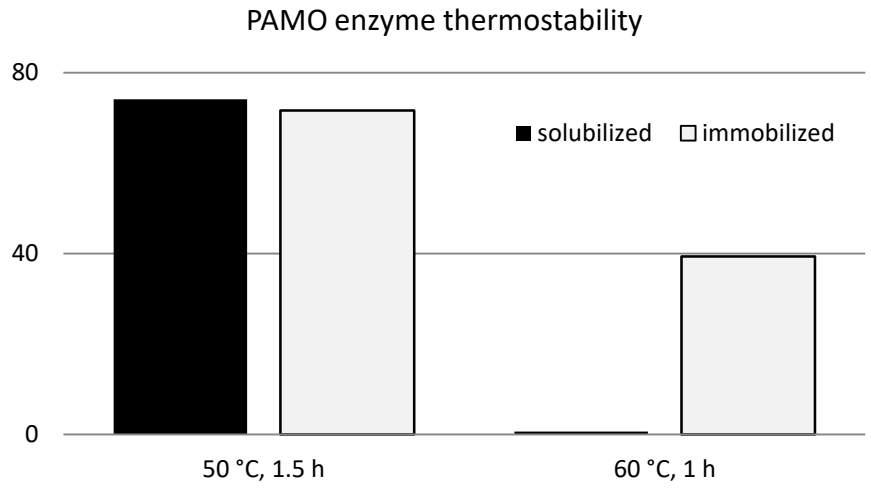

Figure 4. *PAMO activity after incubation for 90 min at 50 °C and 60 min at 60 °C. Enzyme activity was measured by monitoring oxygen depletion.*

4. CONCLUSIONS

We developed a new method for FAD-mediated flavoenzyme immobilization. It yielded fully active and stable immobilized biocatalysts. For this method, agarose was covalently functionalized with a synthetic FAD cofactor which could be used for an efficient and quick reconstitution and immobilization of apo PAMO and apo PTDH-PAMO. The immobilized enzymes restored full activity, could be reused, and displayed a higher thermostability than the enzyme in solution. The FAD-agarose was shown to be a robust carrier, recyclable for multiple immobilizations. The presented method opens up new avenues for the tunable and gentle immobilization of other flavoenzymes.

ACKNOWLEDGEMENTS

We thank Esther van Duijn (University of Utrecht) for performing the ESI–MS experiment. This work is part of the “Electrochemically-assisted redox enzyme reactors by cofactor immobilization” ECHO research project founded by the Netherlands Organization for Scientific Research (NWO).

REFERENCES

Barbosa, O., Ortiz, C., Berenguer-Murcia, Á., Torres, R., Rodrigues, R. C. and Fernandez-Lafuente, R. (2015) "Strategies for the one-step immobilization–purification of enzymes as industrial biocatalysts," Biotechnology Advances, 33(5), pp. 435–456.

van Beek, H. L., Gonzalo, G. de and Fraaije, M. W. (2012) "Blending Baeyer-Villiger monooxygenases: using a robust BVMO as a scaffold for creating chimeric enzymes with novel catalytic properties," Chemical Communications, 48(27), pp. 3288–3290.

van Berkel, W. J. H., Kamerbeek, N. M. and Fraaije, M. W. (2006) "Flavoprotein monooxygenases, a diverse class of oxidative biocatalysts," Journal of Biotechnology, 124(4), pp. 670–689.

van Bloois, E., Dudek, H. M., Duetz, W. a and Fraaije, M. W. (2012) "A stepwise approach for the reproducible optimization of PAMO expression in Escherichia coli for whole-cell biocatalysis," BMC Biotechnology, 12(1), p. 31.

Cuetos, A., Rioz-Martínez, A., Valenzuela, M. L., Lavandera, I., de Gonzalo, G., Carriedo, G. A. and Gotor, V. (2012) "Immobilized redox enzymatic catalysts: Baeyer–Villiger monooxygenases supported on polyphosphazenes," Journal of Molecular Catalysis B: Enzymatic, 74(3), pp. 178–183.

Dudek, H. M., de Gonzalo, G., Torres Pazmiño, D. E., Stepniak, P., Wyrwicz, L. S., Rychlewski, L. and Fraaije, M. W. (2011) "Mapping the Substrate Binding Site of Phenylacetone Monooxygenase from Thermobifida fusca by Mutational Analysis," Applied and Environmental Microbiology, 77(16), pp. 5730–5738.

Dudek, H. M., Torres Pazmiño, D. E., Rodríguez, C., De Gonzalo, G., Gotor, V. and Fraaije, M. W. (2010) "Investigating the coenzyme specificity of phenylacetone monooxygenase from Thermobifida fusca," Applied Microbiology and Biotechnology, 88(5), pp. 1135–1143.

Fernandez-Lafuente, R., Rosell, C. M., Rodriguez, V., Santana, C., Soler, G., Bastida, A. and Guisán, J. M. (1993) "Preparation of activated supports containing low pK amino groups. A new tool for protein immobilization via the carboxyl coupling method," Enzyme and Microbial Technology, 15(7), pp. 546–550.

Fraaije, M. W., Wu, J., Heuts, D. P. H. M., van Hellemond, E. W., Spelberg, J. H. L. and Janssen, D. B. (2005) "Discovery of a thermostable Baeyer–Villiger monooxygenase by genome mining," Applied Microbiology and Biotechnology, 66(4), pp. 393–400.

Franssen, M. C. R., Steunenberg, P., Scott, E. L., Zuilhof, H. and Sanders, J. P. M. (2013) "Immobilised enzymes in biorenewables production.," Chemical Society reviews, 42(15), pp. 6491–533.

Fruk, L., Kuo, C.-H., Torres, E. and Niemeyer, C. M. (2009) "Apoenzyme Reconstitution as a Chemical Tool for Structural Enzymology and Biotechnology," ChemInform, 40(19).

de Gonzalo, G., Mihovilovic, M. D. and Fraaije, M. W. (2010) "Recent Developments in the Application of Baeyer-Villiger Monooxygenases as Biocatalysts," ChemBioChem, 11(16), pp. 2208–2231.

Guzik, U., Hupert-Kocurek, K. and Wojcieszynska, D. (2014) "Immobilization as a strategy for improving enzyme properties- Application to oxidoreductases," Molecules, 19(7), pp. 8995–9018.

Hefti, M. H., Vervoort, J. and Van Berkel, W. J. H. (2003) "Deflavination and reconstitution of flavoproteins: Tackling fold and function," European Journal of Biochemistry, 270(21), pp. 4227–4242.

Jin, J., Mazon, H., Van Den Heuvel, R. H. H., Janssen, D. B. and Fraaije, M. W. (2007) "Discovery of a eugenol oxidase from Rhodococcus sp. strain RHA1," FEBS Journal, 274(9), pp. 2311–2321.

Malito, E., Alfieri, A., Fraaije, M. W. and Mattevi, A. (2004) "Crystal structure of a Baeyer-Villiger monooxygenase," Proceedings of the National Academy of Sciences, 101(36), pp. 13157–13162.

Massey, V. (2000) "The chemical and biological versatility of riboflavin.," Biochemical Society transactions, 28(4), pp. 283–96.

Rodríguez, C., Gonzalo, G. de, Torres Pazmiño, D. E., Fraaije, M. W. and Gotor, V. (2009) "Baeyer-Villiger monooxygenase-catalyzed kinetic resolution of racemic α -alkyl benzyl ketones: enzymatic synthesis of α -alkyl benzylketones and α -alkyl benzylesters," Tetrahedron Asymmetry. Elsevier Ltd, 20(10), pp. 1168–1173.

Dos Santos, J. C. S., Rueda, N., Torres, R., Barbosa, O., Gonçalves, L. R. B. and Fernandez-Lafuente, R. (2015) "Evaluation of divinylsulfone activated agarose to immobilize lipases and to tune their catalytic properties," Process Biochemistry, 50(6), pp. 918–927.

Secundo, F., Fialà, S., Fraaije, M. W., De Gonzalo, G., Meli, M., Zambianchi, F. and Ottolina, G. (2011) "Effects of water miscible organic solvents on the activity and conformation of the baeyer-villiger monooxygenases from Thermobifida fusca and Acinetobacter calcoaceticus: A comparative study," Biotechnology and Bioengineering, 108(3), pp. 491–499.

Sheldon, R. A. (2007) "Enzyme immobilization: The quest for optimum performance," Advanced Synthesis and Catalysis, 349(8–9), pp. 1289–1307.

Stocker, A., Hecht, H. J. and Bückmann, A. F. (1996) "Synthesis, characterization and preliminary crystallographic data of N6-(6-carbamoylhexyl)-FAD-D-amino-acid oxidase from pig kidney, a semi-synthetic oxidase.," The Federation of European Biochemical Societies Journal, 238(2), pp. 519–528.

Torres Pazmiño, D. E., Baas, B. J., Janssen, D. B. and Fraaije, M. W. (2008) "Kinetic mechanism of phenylacetone monooxygenase from Thermobifida fusca," Biochemistry, 47(13), pp. 4082–4093.

Torres Pazmiño, D. E., Dudek, H. M. and Fraaije, M. W. (2010) “Baeyer-Villiger monooxygenases: recent advances and future challenges,” Current Opinion in Chemical Biology, 14(2), pp. 138–144.

Torres Pazmiño, D. E., Riebel, A., de Lange, J., Rudroff, F., Mihovilovic, M. D. and Fraaije, M. W. (2009) “Efficient Biooxidations Catalyzed by a New Generation of Self-Sufficient Baeyer-Villiger Monooxygenases,” ChemBioChem, 10(16), pp. 2595–2598.

Wichmann, R. and Vasic-Racki, D. (2005) “Cofactor regeneration at the lab scale,” Advances in Biochemical Engineering/Biotechnology, pp. 225–260.

Willner, I., Heleg-Shabtai, V., Blonder, R., Katz, E., Tao, G., Bückmann, A. F. and Heller, A. (1996) “Electrical wiring of glucose oxidase by reconstitution of FAD-modified monolayers assembled onto Au-electrodes,” Journal of the American Chemical Society, 118(42), pp. 10321–10322.

Winter, R. T. and Fraaije, M. W. (2012) “Applications of flavoprotein oxidases in organic synthesis - Novel reactivities that go beyond amine and alcohol oxidations,” Current Organic Chemistry, 16(21), pp. 2542–2550.

Zappelli, P., Pappa, R., Rossodivita, A. and Re, L. (1978) “Carboxylic and polyethyleneimine-bound FAD derivatives. Synthesis, coenzymic properties, conformational and enzyme-coenzyme interaction studies.,” European journal of biochemistry / FEBS, 89(2), pp. 491–499.

SUPPLEMENTARY DATA

Appendix A.

Table S1. *Activity and conversion results for immobilized PAMO and PTDH-PAMO in comparison to both enzymes when free in solution.*

	cycle	Enzyme activity based on benzyl acetate formation per mass of dry resin [U/g]	Referred to theoretical activity calculated for amount of enzyme on the agarose [d] [%]
PAMO	I [a]	2.9	72
	II	2.5	
	III [b]	1.7	
PTDH-PAMO	I [c]	3	94
	II	1.7	
	III	1	

a: the enzyme loading of the agarose was 3.8 mg/g dry agarose; b: the protein-stripped FAD-agarose was stored for 23 weeks at 4 °C before reuse; c: the enzyme loading of the agarose was 3.5 mg/g dry agarose; compared with the known k_{cat} values of PAMO and PTDH-PAMO, respectively.

SUPPORTING INFORMATION FIG. S1

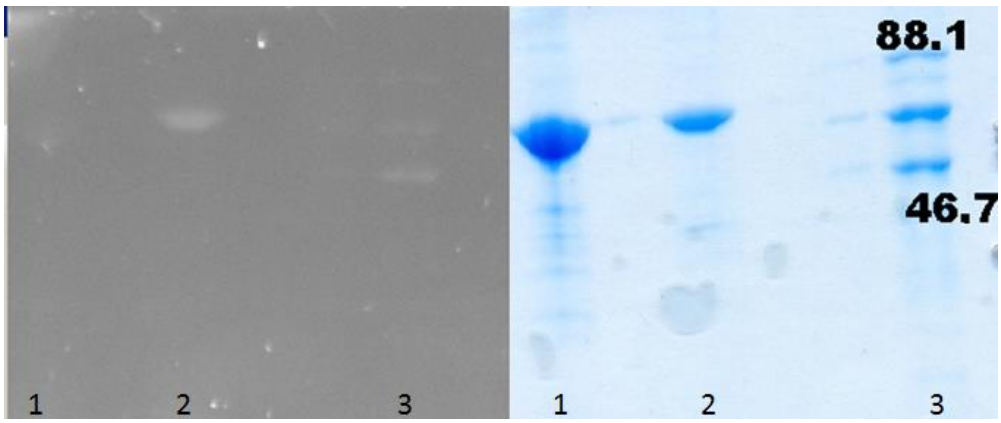

Fig. S1. *SDS PAGE analysis: left, UV-fluorescence for detecting protein-bound flavins in gel; right, Coomassie blue protein staining. Lane 1, protein reconstituted with FAD; lane 2, protein reconstituted with FAD*; lane 3, fluorescent proteins markers.*

SUPPORTING INFORMATION FIG. S2

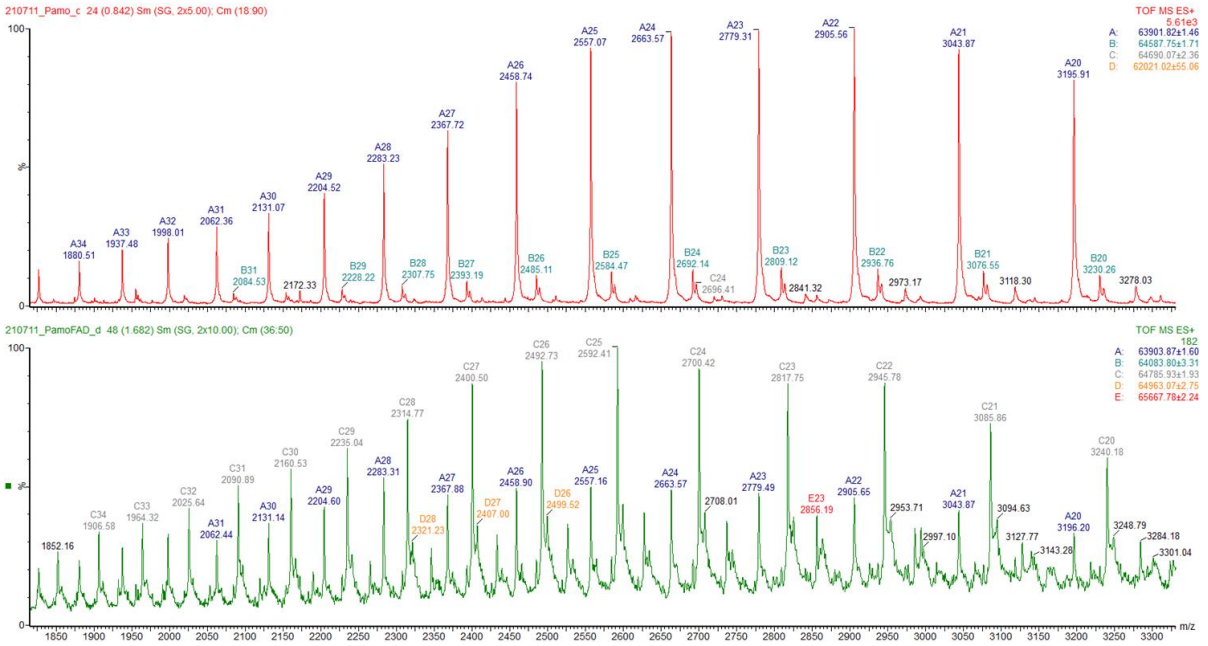

Fig S2. ESI-MS analysis of denatured native PAMO (upper panel) and denatured FAD*-reconstituted PAMO (lower panel). Species A represents the protein without any cofactor bound and is most dominant in native PAMO, while in FAD*-reconstituted sample species C (additional mass of FAD*, ~882 Da) is dominant.

CHAPTER 3

SYNTHESIS OF A NOVEL FLAVIN COFACTOR ANALOGUE, N^6-(BUTYL-2-EN-4-AMINE)-FAD FOR ENZYMES IMMOBILIZATION

Marzena Krzek[a] , Jeffrey Buter[b] , Adriaan J. Minnaard[b] , Marco W. Fraaije[a]

[a] Molecular Enzymology Group, University of Groningen, Nijenborgh 4, 9747 AG Groningen, The Netherlands

[b] Chemical Biology Group, Stratingh Institute for Chemistry, University of Groningen, Nijenborgh 7, 9747AG Groningen, The Netherlands

Abstract

Flavin-containing enzymes can be used in various biotechnological applications. For that, their immobilization is advantageous and often required for a cost-effective process. We have recently shown that flavoenzymes can be immobilized via their flavin adenine dinucleotide (FAD) cofactor. This approach utilizes FAD derivatized at the adenine part with a linker containing a specific functional group, which can form covalent bond with a target material. The FAD-decorated material can serve for cofactor-mediated immobilization of apo flavoenzymes yielding tightly immobilized, stable and active biocatalysts (Krzek *et al.*, 2016). A limitation for this approach is the accessibility of a suitable FAD analogue. Currently known synthesis procedures are laborious, time consuming and inefficient.

In this chapter, a new method for the efficient preparation of a novel FAD analogue substituted at the adenine moiety (N^6-(butyl-2-en-4-amine)-FAD) is described. The FAD analogue contains an aliphatic linker with a terminal primary amine which makes it suitable for cofactor-mediated flavoenzyme immobilization. The FAD analogue was prepared, starting from FAD, with 40% yield. The final structure of the FAD analogue was confirmed using spectroscopic and spectrometric methods (NMR, UV-Vis, MS) and cyclic voltammetry. Furthermore, the compound was successfully applied for FAD-mediated immobilization of the flavoenzyme phenylacetone monooxygenase.

Key words: FAD, immobilization, Dimroth rearrangement, NMR, alkylation

1. INTRODUCTION

Flavin adenine dinucleotide (FAD)-containing enzymes are regarded as particularly useful as oxidative biocatalysts in the pharmaceutical, food and fine-chemical industry (van Berkel et al. 2006) and they can be also exploited for biosensors (Posthuma-Trumpie *et al.*, 2007). To enable such biotechnological applications, an efficient and robust immobilization of a flavoenzyme is often essential. We have recently reported on a new method for the FAD-mediated flavoenzyme attachment to a solid carrier (Krzek *et al.*, 2016). This approach exploits the common characteristics of flavoenzymes that (1) the adenosine part of FAD is close to the protein core surface, while (2) the affinity of this cofactor towards apo flavoenzymes is very high. By using a FAD derivative that has been modified at the adenine moiety, e.g. having a linker with a terminal functional group, covalent attachment of the flavin cofactor to a carrier can be achieved. Subsequently, such a FAD-decorated material can serve for reconstitution of apo flavoenzymes yielding fully active, robustly immobilized holo flavoenzymes (Krzek *et al.*, 2016). Importantly, through the use of different linkers, this approach allows tuning the distance and orientation between the enzyme and surface. The key compound in this approach is an FAD analogue modified at the adenosine moiety (Stocker et al. 1996; Krzek et al. 2016; Hefti et al. 2003)(Hefti, Vervoort and Van Berkel, 2003)(Hefti, Vervoort and Van Berkel, 2003)(Hefti, Vervoort and Van Berkel, 2003). However, such FAD derivatives are not commercially available and their synthesis using previously described protocols is laborious and inefficient.

Several methods to prepare FAD derivatives for covalent coupling to a surface and subsequent enzymatic reconstitution were already described in the 80's (Zappelli *et al.*, 1978; Wingard, 1984). Originally, those cofactor analogues were studied with the FAD-containing glucose oxidase from *Aspergillus niger*. The low yields of reconstitution of this enzyme and difficulties in apo enzyme preparation inhibited further development of flavin-mediated immobilizations and, related to that, synthesis routes for obtaining relevant FAD analogues (Wingard, 1984). FAD modifications can change the functional properties of the cofactor, which would alter flavoenzyme characteristic as well. When derivatized at the isoalloxazine ring, it typically alters the redox potential and the spectral properties (Nishina *et al.*, 2003; Roth *et al.*, 2004). Additionally, this part of FAD is located within the protein core and may prevent apo protein reconstitution or trigger detrimental conformational changes in the protein (Wingard, 1984; Nishina *et al.*, 2003; Roth *et al.*, 2004). In contrast to that, substitution at the adenosine part does not influence the redox properties of the isoalloxazine moiety and is often compatible with apo protein reconstitution because the adenosine moiety is often very close to the protein surface (Stocker, Hecht and Bückmann, 1996). The adenosine part can be alkylated at positions 1 and 6. To obtain N^6-alkylated adenosine, nitrogen at position 6 may first undergo halogenation (Ikehara, Ogiso and Maruyama, 1977). However, such modification typically requires harsh conditions under which the FAD structure will not be preserved. As alternative approach, the 1 position may be targeted, as it is more reactive when compared with N^6. While N^1 analogues have

been reported as relatively unstable (Bückmann, Wray and Stocker, 1997), the analogues alkylated at position 1 can rearrange into N^6 derivatives via a so-called Dimroth rearrangement. Therefore, for obtaining generally applicable FAD analogues with preserved catalytic properties, the most preferable way is to obtain the N^6 analogues via Dimroth rearrangement.

Untill now, not many studies on synthesis of N^6-FAD analogues have been reported. The first published strategy was to substitute the N^6 position of adenosine and subsequently build up the complete FAD molecule by coupling it to the flavin mononucleotide (FMN) (Morris and Buckler, 1983; Stocker, Hecht and Bückmann, 1996). Functionalized N^6 substituted adenosine compounds can be further modified in order to obtain the desired FAD analogue (Stocker, Hecht and Bückmann, 1996). Nevertheless, this synthesis pathway involves multiple steps starting from very costly FMN giving only 17-20% overall yield (Stocker, Hecht and Bückmann, 1996). Another, simpler approach involves only two steps and uses FAD as a starting compound (Scheme1). First, the selective alkylation at the FAD adenosine 1 position is performed. This step is followed by a Dimroth rearrangement into a more stable, adenosine N^6 FAD derivative (van der Plas et al., 1995). The method has been patented in 1995 (Bückmann et al., 1995). Herein, we describe a more efficient approach to prepare a N^6-FAD analogue and compare it with the approach reported by Bückmann.

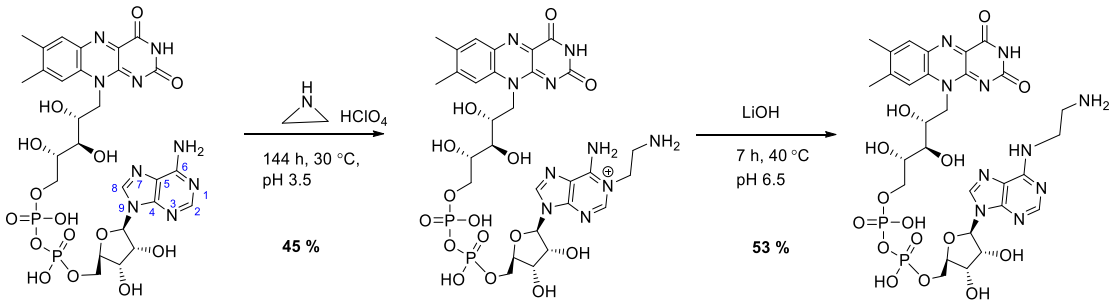

Scheme 1. *Synthesis of N^6-substituted FAD analogue as patented in 1995 by Bückmann. Atom numbering at the adenine moiety is indicated with blue numbers.*

The largest bottleneck of the first step of the published synthesis route is the very low rate of alkylation at position 1 of adenosine. In the published method it takes around 3 days (Bückmann, Wray and Stocker, 1997) (Scheme 1). The second step, rearrangement from position 1 into N^6 in the method described by Bückmann suffers from the formation of significant amounts of side products as a result of reactions of the linker's terminal, reactive group, which may lead *inter alia* to cyclisation into the 1,N^6-ethanoadenosine derivative (van der Plas, Henk C. Bückmann and Wray, 1995). Moreover, purification of the sample after both steps is laborious and harmful for the products. The overall yield after two steps reaches only 24% (Bückmann, Wray and Stocker, 1997). We attempted to improve both steps for the preparation of a N^6-FAD analogue which contains a short linker moiety and

a primary amine: N^6-(butyl-2-en-4-amine)-FAD. The amine can be exploited for selective, covalent coupling of the FAD analogue to a carrier material or other purposes.

We have attempted to optimize the alkylation at the position 1 of adenosine based on the recently published work on adenosine in DMF as a solvent. It was shown that the addition of salts such as KI and $BaCO_3$ during alkylation with alkyl halides increases the efficiency (Oslovskya, Drenicheva. and Mikhailova, 2015). Additionally, the use of allylic halides may be more powerful than the use of saturated alkyl halides, as the double bond increases its reactivity. Furthermore, iodides (that can be obtained via Finkelstein reaction) provide a very good leaving group (Finkelstein, 1910). Importantly, a similar approach has been recently explored for the synthesis of a natural product from *M. tuberculosis*. Alkylation of adenosine was performed at room temperature overnight with NaI in DMF, which resulted in a yield of 76% (Buter *et al.*, 2016). As FAD is a more fragile molecule and does not dissolve in organic solvents, the same conditions cannot be applied. It dissolves well in water but an aqueous environment will slow down the alkylation. Therefore, we used a mixture of solvents (DMSO:DMF:H_2O). For the alkylation reaction, together with the aforementioned salts, we employed an allyl bromide as it is a more reactive electrophile than several other allylic halides. Moreover, the reaction was performed at 50 °C, which in case of the patented approach was not possible due to the low boiling point of the employed alkylating agent. For simplicity of the product identification, preliminary tests were performed on adenosine with 4-(Fmoc-amino)-1-bromobut-2-ene as the alkylating agent.

The Dimroth rearrangement of adenosine alkylated at position 1 into position N^6 is a nucleophile-assisted process, which involves ring opening and dissociation of a proton (van der Plas et al., 1995). The literature reports a high rearrangement yield for the prepared aminoethyl FAD derivative and low efficiency when using a carboxyl analogue (Bückmannn, 1995). It also suggests that the amine moiety can act as an inter- or less probably intramolecular nucleophile, and indicates a strong dependency of the Dimroth rearrangement on the nucleophile assistance. For this step, Bückmann *et al* employed LiOH (Bückmann, Wray and Stocker, 1997), which is strong base, and the hydroxide anion is relatively strong nucleophile. FAD is unstable at extreme pH values due to the labile pyrophosphate moiety which prevents exploiting hydroxides as nucleophiles for the Dimroth rearrangement (Bückmannn, 1995). We employed a compound which is a weak base and strong nucleophile at the same time; diethylamine. Another aspect to be improved compared to described methods is to reduce side product formation, which are mostly related to the terminal primary amine reactivity. For this reason, we blocked the amine with a protecting group cleavable under the Dimroth rearrangement conditions.

The newly developed synthetic procedure has been applied for the preparation of a new FAD derivative: N^6-(butyl-2-en-4-amine)-FAD. Moreover, the utility of this compound for cofactor-mediated immobilization of a flavoenzyme was demonstrated.

2. RESULTS AND DISCUSSION

2.1 TESTING A MODEL REACTION – ALKYLATION OF ADENOSINE

FAD is an expensive and relatively complex molecule. Therefore, for optimization of reaction conditions we first tested alkylation of the adenosine position 1 of the model compound adenosine The alkylation agent 4-(Fmoc-amino)-1-bromobut-2-ene has been synthesized according to Scheme 2 and used for adenosine alkylation (Scheme 3). The preparation details and data are given in the experimental section. The approach taken suffered from a low overall yield (7%). The major limitation was the difficult purification after the second step as the final product was obtained as a dense oil and was hard to purify. Due to that, the planned pathway could still be performed from the very cheap reagents, nonetheless very large scale was needed to obtain efficient amount for alkylation of FAD on a gram scale.

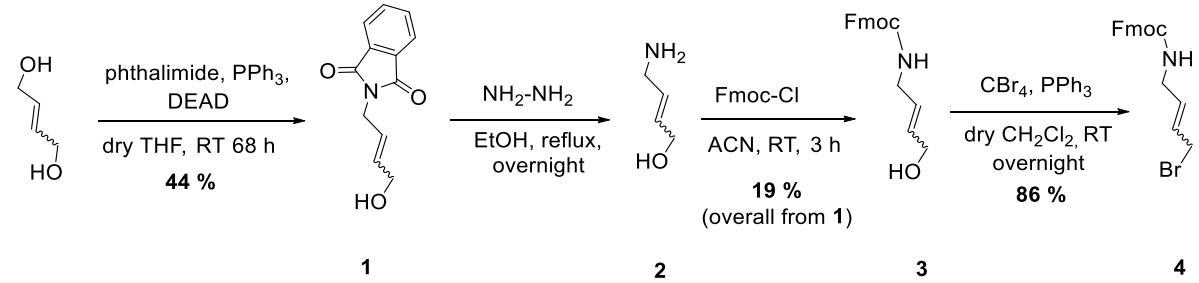

Scheme 2. *Synthesis of the alkylating agent for adenosine derivatization (**4**)*

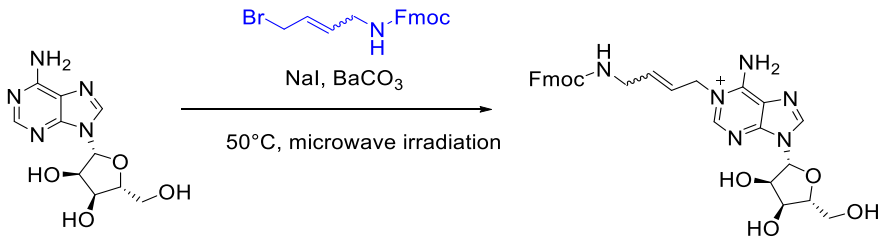

Scheme 3. *Alkylation of adenosine at the position 1 with 4-(Fmoc-amino)-1-bromobut-2-ene was a model reaction for FAD alkylation.*

SYNTHESIS OF N^1 -4-(FMOC-AMINO)-1-BROMOBUT-2-ENE ADENOSINE

The alkylating agent **4** was reacted with adenosine (Scheme 3) in DMF or in the SolventMix (DMSO:DMF:H_2O (2:1:1 v/v/v)). The effect of time and addition of salts ($BaCO_3$, NaI) on the yield was investigated as presented in Table **2**1. All reactions were performed at room temperature or 50 °C using 50 W microwave irradiation. Moreover, the addition of a huge excess of the non-nucleophilic

base 1,8-diazabicycloundec-7-ene (DBU) was tested. The results of the optimization are shown in Table 1 and an example of a ^{1}H NMR spectrum is shown in Figure 1.

Table 1. *Conditions tested for adenosine alkylation optimization. Yields were calculated from ^{1}H NMR spectra based on integrations of signals from the sugar anomeric centre.*

Temperature	Solvent	Time	Molar equivalents of NaI + $BaCO_3$	Yield [%]
room temperature	DMF	20 h	1.2	32
		2 days	1.2	44
	SolventMix	2 days	1.2	42
		4 days	2.4	47
50°C microwave 50W		1 h	1.2	36
		3 h	1.2	45
4 days (RT) +1 h microwave SolventMix			2.4 + 10 DBU	unspecific products

The results show that the both DMF and SolventMix can be used for alkylating adenosine. The yield for all reaction conditions was reasonable, except when DBU was included. The latter base resulted in formation of unspecific products.

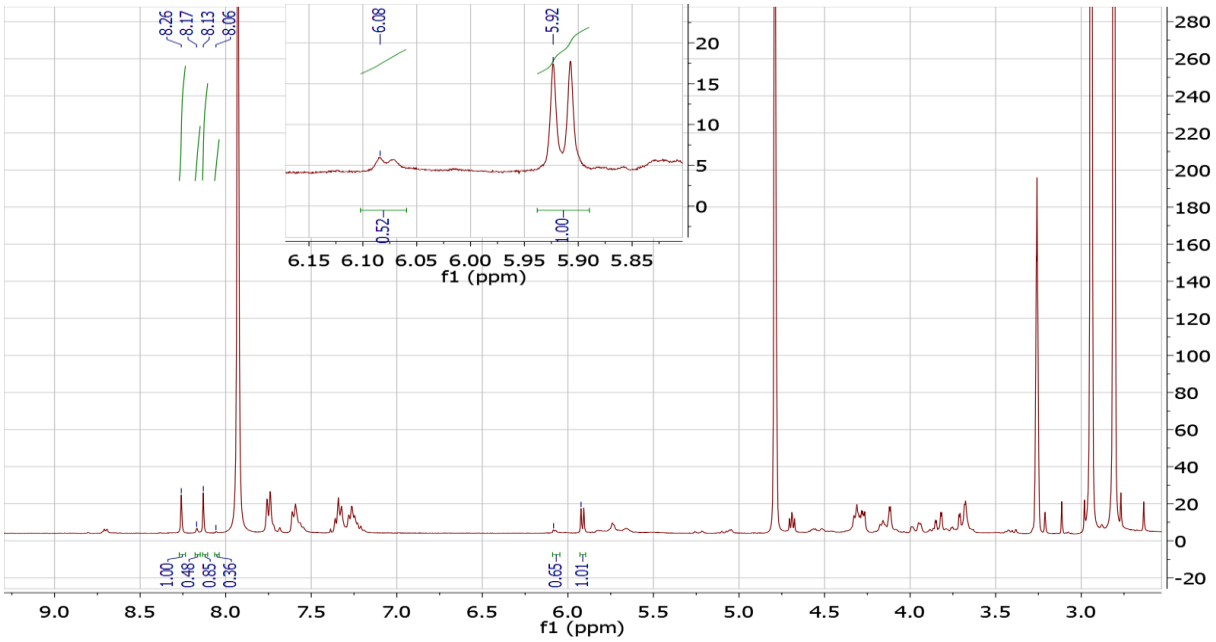

Figure 1 *^{1}H NMR spectrum collected during alkylation of adenosine at position 1 with compound 4. Specific for the substituted product is the downfield shift of the ribose anomeric doublet; 5.92 ppm (unsubstituted adenosine), to 6.08 ppm (product). The spectrum was obtained in deuterated methanol for the sample reacted with alkylating agent over one day at room temperature in SolventMix.*

2.2 EFFECT OF PH ON FAD ^{1}H NMR SPECTRA AND FAD ALKYLATION

Prior to performing actual FAD modifications, the effect of pH on the ^{1}H NMR spectrum of FAD was studied. All ^{1}H NMR spectra were collected in D_2O at ambient temperature. The pD was adjusted with DCl or NaOD. It can be concluded from Figure 2B that chemical shifts from the adenosine part of FAD are not altered in the pH range 4 – 8. Therefore, alkylation at position 1 can be followed using 1D ^{1}H NMR at moderate pH values. Moreover, it was concluded, based on ^{1}H NMR analysis, that FAD does not decompose upon microwave irradiation (50 °C, 50 W). The spectra collected before and after irradiation were virtually identical (data not shown

***Table 2**. Optimisation results for FAD alkylation at position 1 with allyl halide, NaI and $BaCO_3$ in the SolventMix at 50°C upon microwave irradiation*: A decrease in quality of NMR spectrum was observed upon increase of salt concentration.*

Time + time with extra additives [h]	extra reagent	final molarity of the reagents	Yield [%] based on ^{1}H NMR integrations of signals from sugar anomeric center in reaction mix samples
1.5	no	4 (NaI + alkyl halide) + 2 $BaCO_3$	35
5.5	no		46
7	no		48
5.5 + 1.5	NaI + allyl halide	8	57
5.5 + 3	NaI + allyl halide	8	63
5.5 + 1.5	$BaCO_3$	4	48
5.5 + 3	$BaCO_3$	4	60
5.5 + 4.5	$BaCO_3$	4	59
7 + 3	$BaCO_3$ + (NaI + allyl halide)	4 +(8)	Over 60 % (± 10%)*

In order to optimize the nucleophilic substitution at the position 1 in FAD with compound **4**, several conditions were tested. As tested for adenosine, the effect of adding NaI and $BaCO_3$ was investigated. At the same time, the nucleophilic substitution efficiency of allyl halide over alkyl halide was tested. For that, an alkyl bromide *N*-(4-bromobutyl)-phthalimide was used as an analogue of compound **5**.

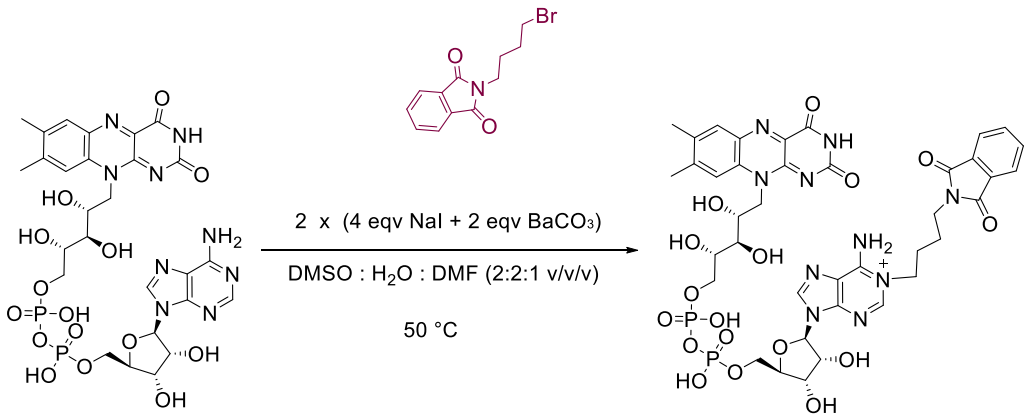

FAD N^1-((4-butyl)-phtalimide)-FAD

***Scheme 4**. The alkylation of FAD with alkyl halide was not detectable after 11 days of stirring at 50 ℃*

^{1}H NMR spectra collected before and after eleven days of stirring did not show any alkylation with the alkyl halide. At the same time, successful alkylation was observed for the allyl halide. Apparently, the lower electrophilicity of the alkyl bromide over the allyl bromide impaired the efficiency of FAD alkylation.

The combined use of NaI and an alkylating agent with stepwise increasing quantities resulted in a dark

red solution with some precipitate and yield improvement (Table 2). Nonetheless, it also triggered difficulties to collect good quality ^{1}H NMR spectra. The highest yield of alkylation reached around 60% (Table 2). Noticeably, similar to results for the adenosine N^6-alkylation, we obtained a higher reaction yield after stepwise addition of salts and the alkylating agent. Based on the obtained results (Table1), the following conditions for the N^6-substitution of FAD were chosen for further experiments: two times addition of reagents: 2 eqv of alkylating agent, 2 eqv of NaI (4 equivalents) and 1 eqv of $BaCO_3$ at 50 °C, 50 W microwave irradiation.

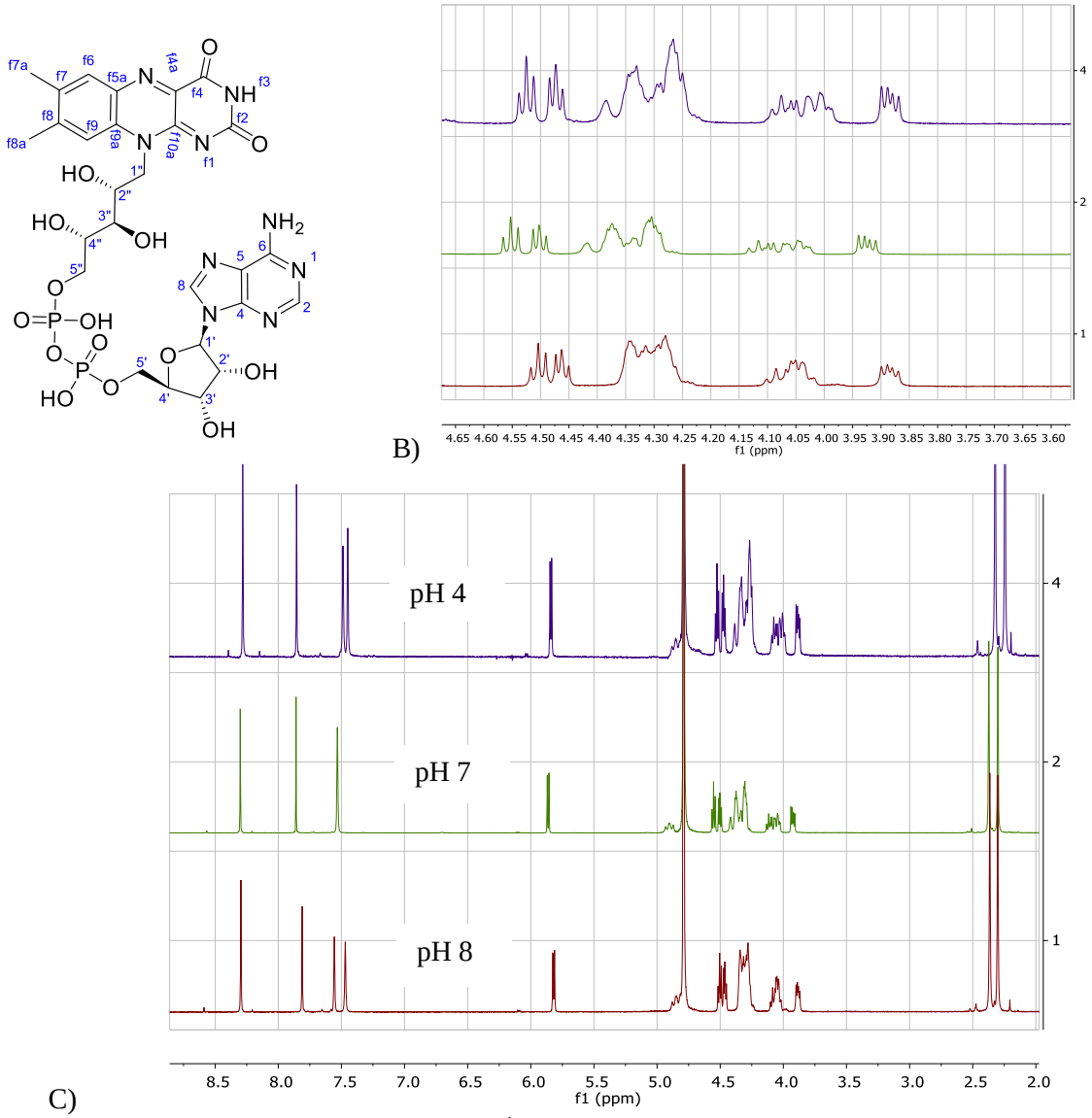

***Figure 2**. (A) FAD atom numbering, and (B,C) ^{1}H NMR spectra of FAD at different pH values.*

2.3 SYNTHESIS OF N^1-[(4-BUTYL-2-EN)-PHTHALIMIDE]-FAD

For the FAD derivatization on preparative scale, a shorter and more efficient synthesis of another alkylating agent, *cis*- and *trans*-*N*-(4-bromobut-2-en-1-yl)phthalimide (**5**), was designed and performed as shown in Scheme 5. The only structural difference versus the previously used alkylating agent **4** is the amine protection group. Compound **4** contains the Fmoc group while compound **5** contains phthalimide. Both groups can be cleaved with 5% diethylamine (Fields, 1995; Sen and Roach, 1995). At the same time, due to its strong nucleophilic character, diethylamine can play an important role to promote the Dimroth rearrangement, the next and very last step of the synthesis (section IV). Preparation of compound **5** is simpler and more efficient than the synthesis of **4** (only 2 steps and 32% overall yield versus 4 steps with 7 % yield). Details for the synthesis of **5** can be found in the experimental section.

FAD was modified using compound **5** as shown in Scheme 5

Formation of the FAD derivative **6** was observed in the reaction mixture by NMR analysis and LC-MS. Based on the first method, conversion was estimated to be around 60% (**Figure 4**), which is in line with the with the preliminary optimization experiments in the section 2.2. For purification of compound **6**, several approaches were tested including precipitation at high pH, silica gel chromatography, and anion exchange chromatography (Q-Sepharose). The latter approach resulted in separation of several major fractions, which indicates that the compound may degrade when in contact with the column material. Moreover, it was found that this FAD derivative is also not stable upon storage at room temperature. Eventually, the reaction mixture was diluted twice in acidified water (final pH 4) and washed twice with CH_2Cl_2. Using this procedure, the (unreacted) alkylating agent was removed, which was confirmed by TLC analysis. It also shows that extraction with CH_2Cl_2 is not harmful for the product.

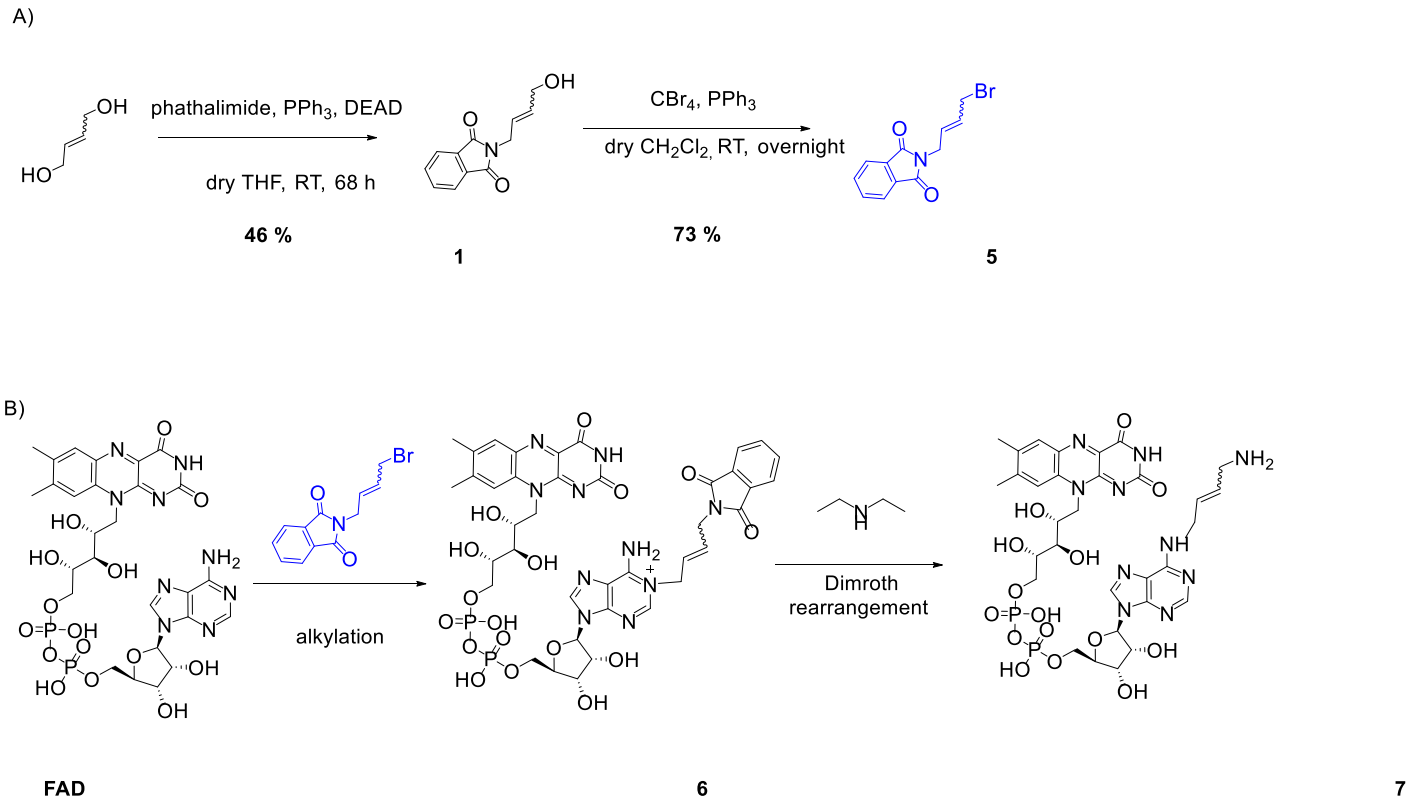

***Scheme** 5. The synthesis pathway of N^6-(butyl-2-en-4-amine)-FAD. A) alkylating agent synthesis, B) modification at the adenosine position 1 and further rearrangement into the N^6 position in combination with phthalimide deprotection.*

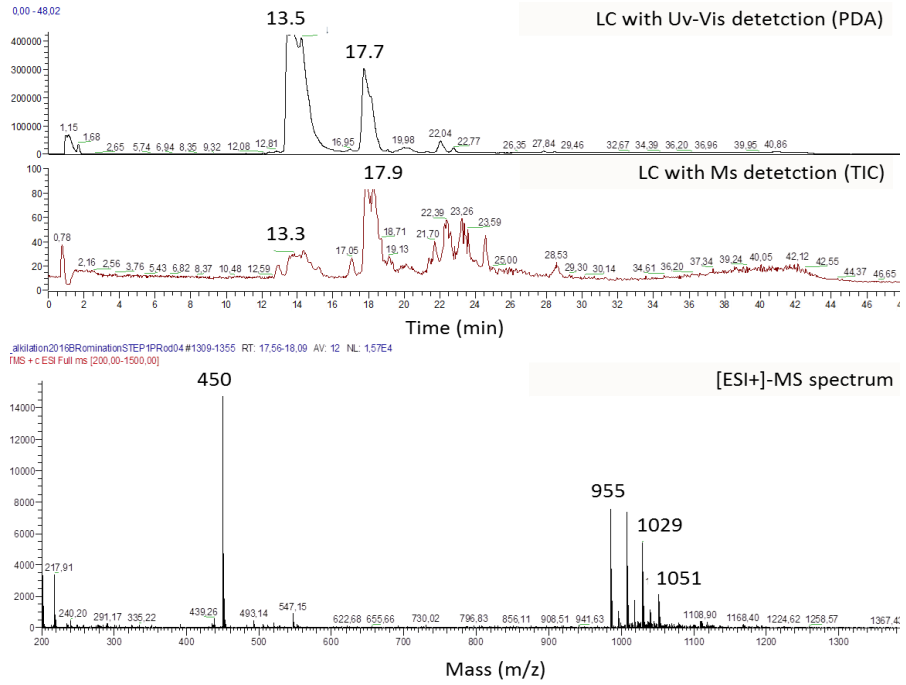

Figure 3*. LC-MS analysis of the reaction mixture of FAD alkylation after two times addition of 4 eq of compound* ***5*** *and NaI, and 2 eq of* $BaCO_3$*. Total microwaving time in 50 °C and 50 W was 12.5 h. The figure shows a peak in the LC chromatogram (retention time 17.7 min, upper panel) that corresponds to compound* ***6*** *(lower panel, double charged: m/2z = 439). The peak with retention time 13.5 min corresponds to FAD*

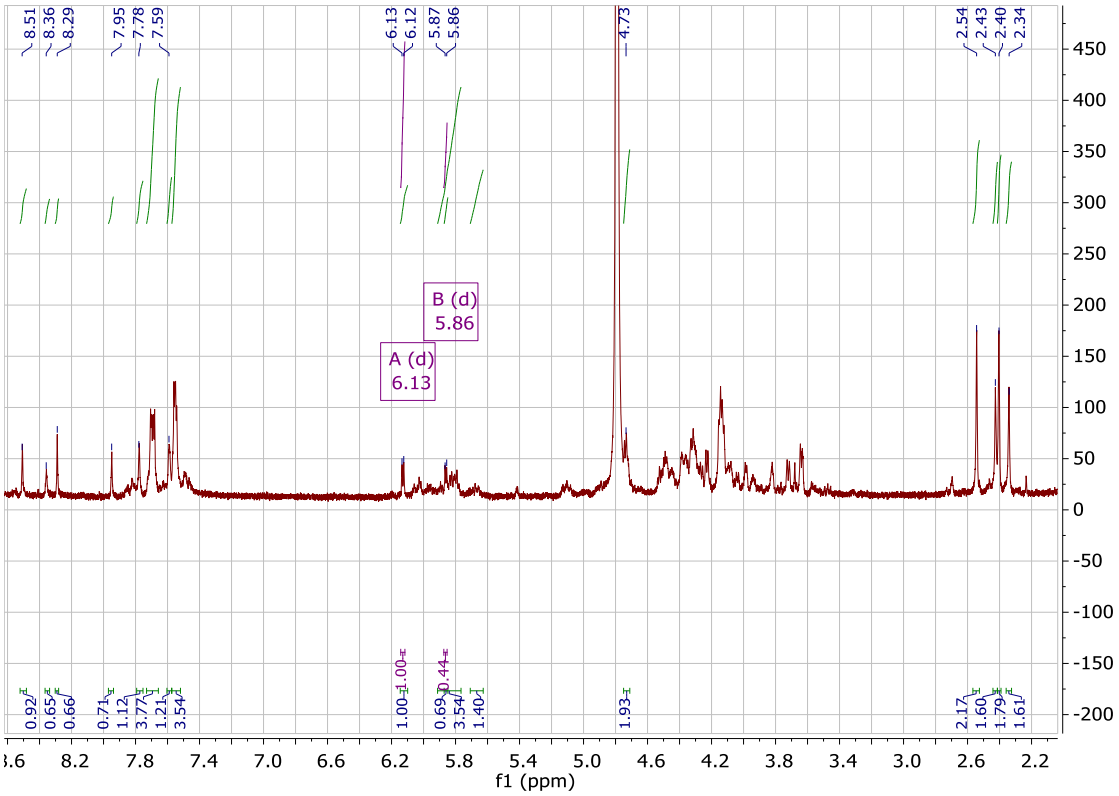

Figure 4. *Spectrum of the aqueous phase of compound* ***6*** *after purification by two times extraction with* CH_2Cl_2*. In blue chemical shifts characteristic for the compound derivatized at position 1 (assigned based on the integration), black – peaks from FAD.*^{1}*H NMR (500 MHz,* D_2O*, pD 4)* δ *8.51, 8.36, 8.29, 7.95, 7.78, 7.59, 6.13 (d, J = 5.6 Hz), 5.86 (d, J = 5.0 Hz), 2.54, 2.43, 2.40, 2.34.*

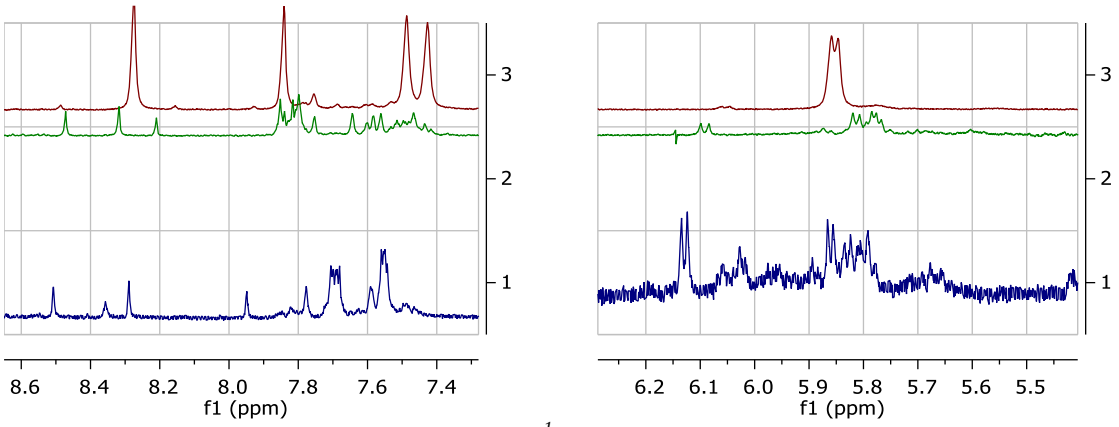

***Figure 5**. FAD alkylation with compound **5**. [1]H NMR spectra were collected at room temperature in D_2O, pD 4. Top: changes in chemical shift of peaks from adenosine C2 and C8 proton singlets); Bottom: doublet from FAD ribose C1' proton upon alkylation at adenosine position 1. Red – starting reaction mix, green – reaction mix after microwaving and extra reagents addition, blue – aqueous, acidified phase after two times extraction with CH_2Cl_2. The alkylating agent is insoluble in water. Therefore, a multiplet around 5.8 (double bond) and 7.5 (phthalimide) ppm correspond to the compound **6**.*

***Table 3.** Chemical shifts for [1]H NMR signals that do change upon alkylation of adenosine. Data were collected for adenosine, alkylated adenosine in CD_3OD and compound **6** in D_2O.*

Compound	**FAD Proton**[a]							
	C8	C2	F9	F6	C'1		F8a	F7a
	shift (ppm)					*J* (Hz)	shift (ppm)	
Adenosine	8.24	8.11	-	-	6.01	6.4	-	-
N^1-(4-Fmoc-but-2-en)-adenosine	8.57	8.46	-	-	6.12	5.1	-	-
Compound **6**[c]	8.51	8.36	7.75	[b]	6.12	5.6	2.54	2.40

[a]: *atom numbers as in Figure 6.*
[b]: *chemical shift was not assigned because of overlap with another signals.*
[c]: *chemical shifts were referred to water peak (4.87 ppm in CD_3OD and 4.90 ppm for D_2O).*

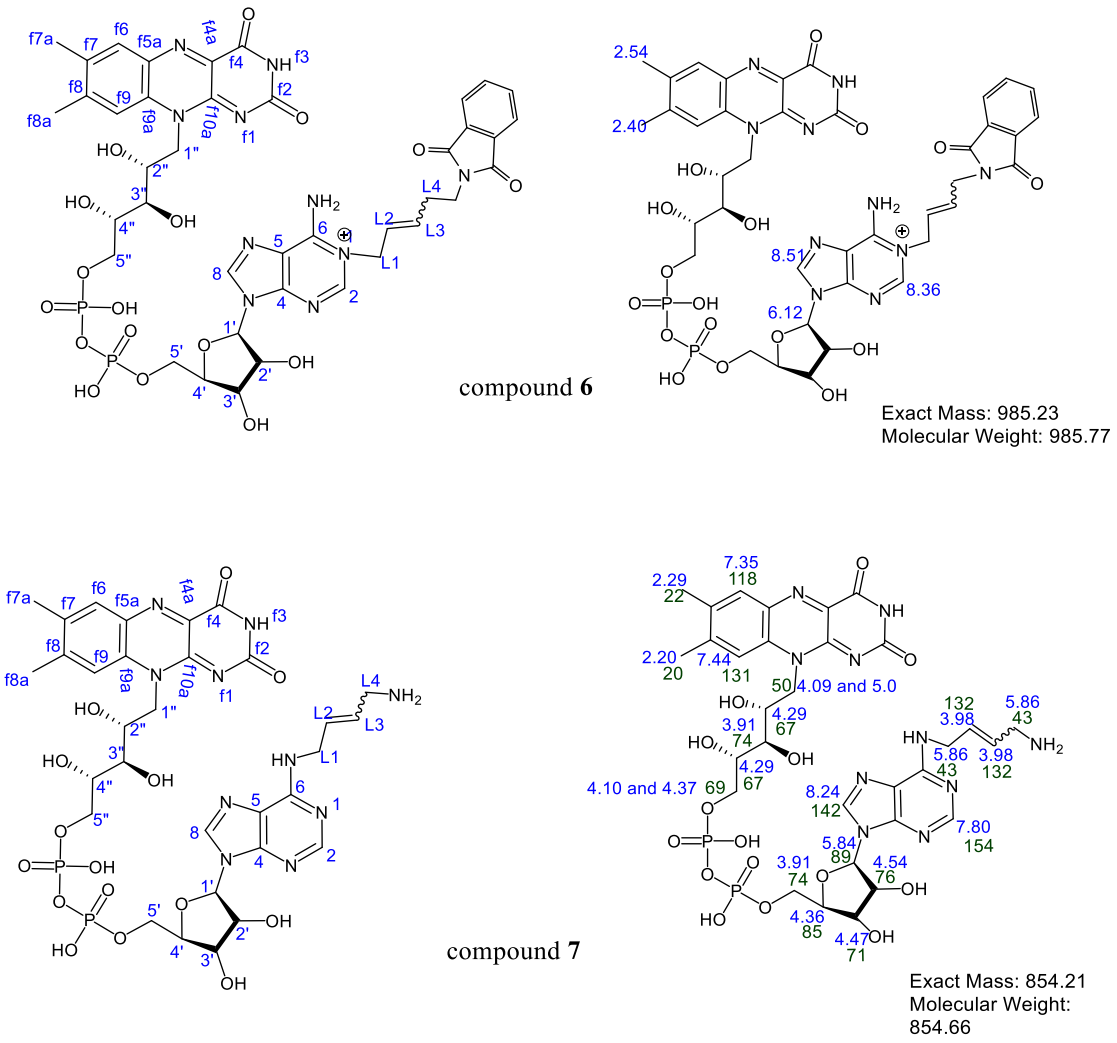

***Figure 6**. Structure of N^1-(butyl-2-en-4-amine)-FAD (compound **6**) and N^6-(butyl-2-en-4-amine)-FAD (compound **7**) with atoms numbering (left) and chemical shifts (right).*

2.4 SYNTHESIS OF N^6-(4-AMINE-BUTYL-2-EN)-FAD: DIMROTH REARRANGEMENT AND DEPROTECTION OF N^1-(4-AMINE-BUTYL-2-EN)-FAD

The final, N^6- substituted FAD analogue **7** is obtained from compound **6** via the Dimroth rearrangement and removal of the protecting group, phthalimide. The efficient removal requires a high amount of diethylamine. On the other hand, the pH should remain mild for preserving the FAD molecule. Therefore, two conditions were tested: phosphate buffer pH 8.5 containing 5% and 0.5% of diethylamine. In both cases, deprotection and subsequent Dimroth rearrangement occurred, which was evidenced by formation of compound **7** (monitored by LC-MS). The conditions resulting in higher conversions contained the highest diethylamine concentration. Therefore, for a larger scale conversion, 0.8 M phosphate buffer (pH 8.5) with 5% diethylamine was employed at 50 °C. As this step is relatively fast (Bückmann, Wray and Stocker, 1997) and diethylamine is a volatile compound with a low boiling point, a microwave irradiation was not used. After a few days, the completion of the Dimroth rearrangement was confirmed by LC-MS analysis (

Figure).

Table 4. *Peaks assignments for N^6-(butyl-2-en-4-amine)-FAD (compound **7**). For atom numbering, see Figure. Assignments are in agreement with literature data* (Halada *et al.*, 2003).

	F7a	F8a	C"3 and C'5	L4	L1	C"5A	C"2B	C"4	C"1A	C'3	C'2	C'4 and C"5B and C"2A	C"1 B	C'1 and L2/L3	F6	F9	C2	C8
H1 [ppm]	**2.2**	**2.29**	**3.91**	**3.98**	**4.09**	**4.1**	**4.25**	**4.29**	**4.82-4.83**	**4.5**	**4.54**	**4.36-4.37**	**5**	**5.82-5.86**	**7.35**	**7.44**	**7.8**	**8.24**
Cross peaks			4.36	5.82-5.85	5.82-5.86	4.29	4.1	3.91	4.36	4.36	5.82	4.5	4.25	4.09				
			4.38				4.36	4.1		4.54	4.5	4.25	4.64-4.68	3.98				
			4				5					4.82		4.54				
			4.29									3.91						
			*		*		*					*						
C13 [ppm]	**20**	**22**	**74, 76**	**43**	**43, 73**	**69**	**67**	**70**	**50**	**71**	**76**	**85, 75, 67**	**50**	**129, 132, 89**	**131**	**118**	**152**	**131**

* Peaks overlap, not well resolved

The final reaction mixture contained only two main compounds with absorbance in the visual range (LC-MS/Vis detection): FAD (RT = 13.03 min, [ESI-] 785.09 m/z), and a compound with a retention time of 13.13 min (Figure). The UV-Vis spectrum of the latter has typical flavin features with maxima at 265 nm, 371 nm and 446 nm. The absence of a broad absorbance peak at around 300 nm suggests that no significant amount of the tricyclic side, products were formed (van der Plas et al., 1995). The most dominant peak in the mass spectrum has a m/z value of 876, which can be assigned as a sodium adduct of **7**. Based on this, no remaining unreacted N^1–alkylated FAD, nor tricyclic side products were present after the Dimroth rearrangement reaction. All in all, it can be concluded that the rearrangement yield is close to quantitative as the peak corresponding to compound **6** disappeared, and there are no other peaks with absorbance in the visual range besides some residual FAD.

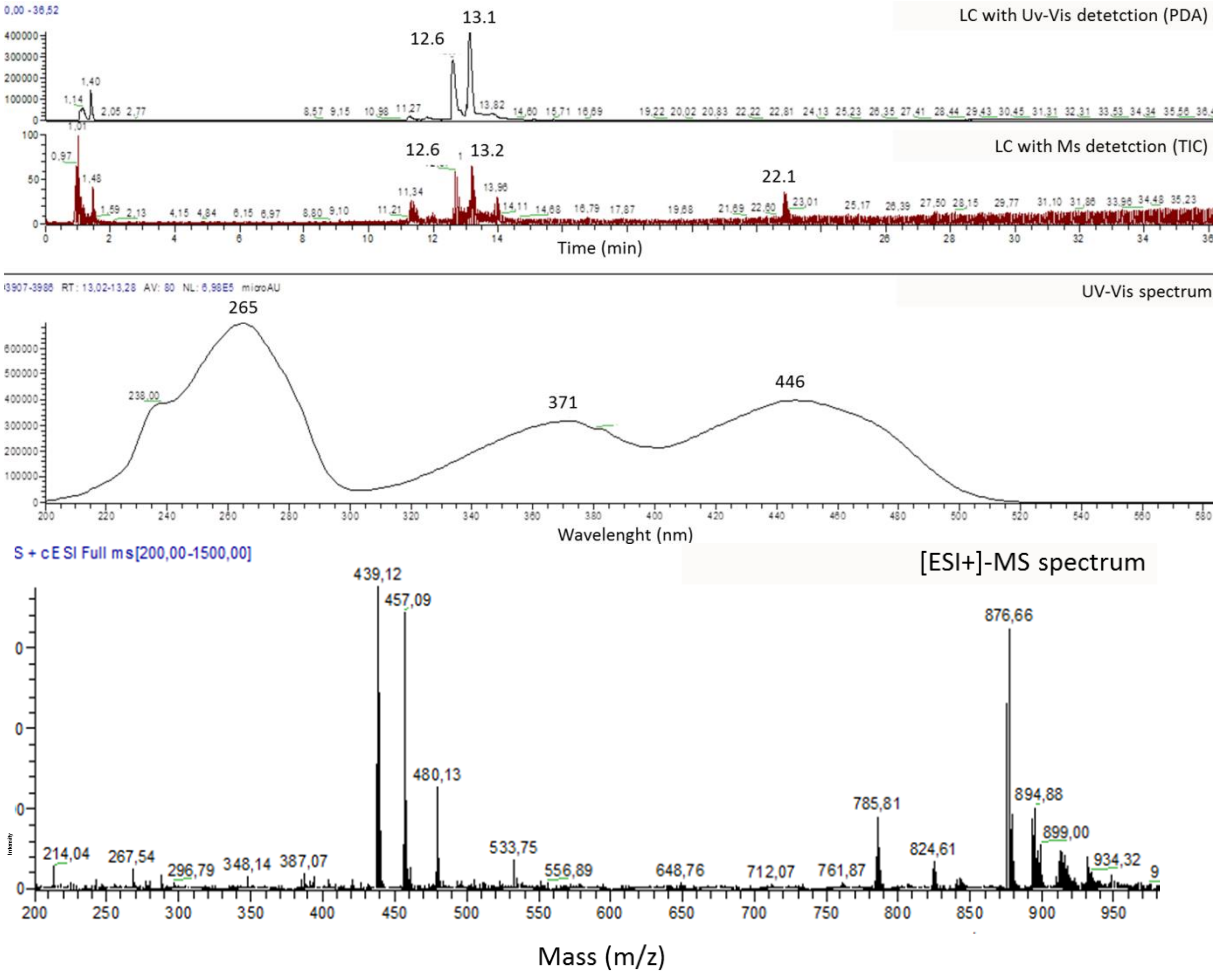

***Figure 7**. LC-MS profile of the final Dimroth rearrangement reaction mixture (top graph). The formation of N^6-FAD is visible at a retention time of 13.13 min: FAD-like spectrum (middle plot), and adduct with sodium ESI + : calculated mass [M + Na^+] = 877.2; found 876.66 m/z (bottom plot.*

2.5 PURIFICATION OF N^6-(BUTYL-2-EN-4-AMINE)-FAD

For the purification of N^6-(butyl-2-en-4-amine)-FAD, several approaches were tested. The use of anion-exchange material (Q-Sepharose) did not give a good separation and unspecific products were formed (LC-MS analysis). Phenyl-Sepharose gave no separation. The best separation with the least amount of side products was obtained using a C18 column. This purification was followed by a desalting column in order to remove salts. After that, the remaining volatile components (diethylamine) were removed using elevated temperatures and a high vacuum. The purified sample was ninhydrin-positive (TLC analysis, Figure 10). As a negative control, FAD incubated with the same concentration of diethylamine did not give a positive response to a ninhydrin test. This confirms the presence of a primary amine in the final compound. The purity of compound **7** is estimated as 80% based on LC-MS profile (Figure 8)**.** After desalting, the expected mass of compound **7** (856 m/z) was observed by LC-MS (Figure 9).

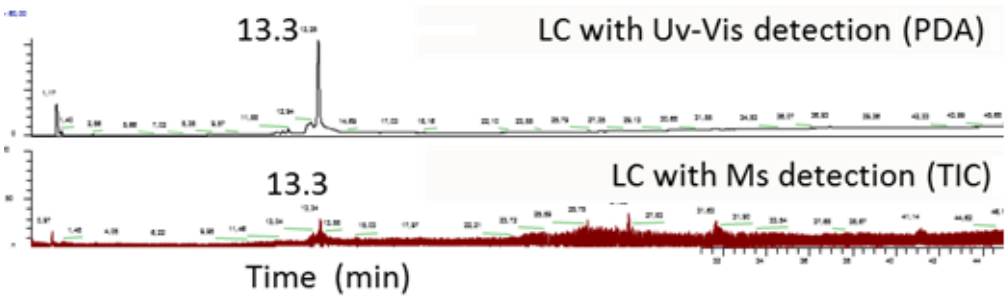

Figure 8. *LC-MS-UV profile of compound **7** after purification using a C18 cartridge (details in experimental section) with retention time 13.28 min. The observed, dominant peak corresponds to the sodium adduct of **7***

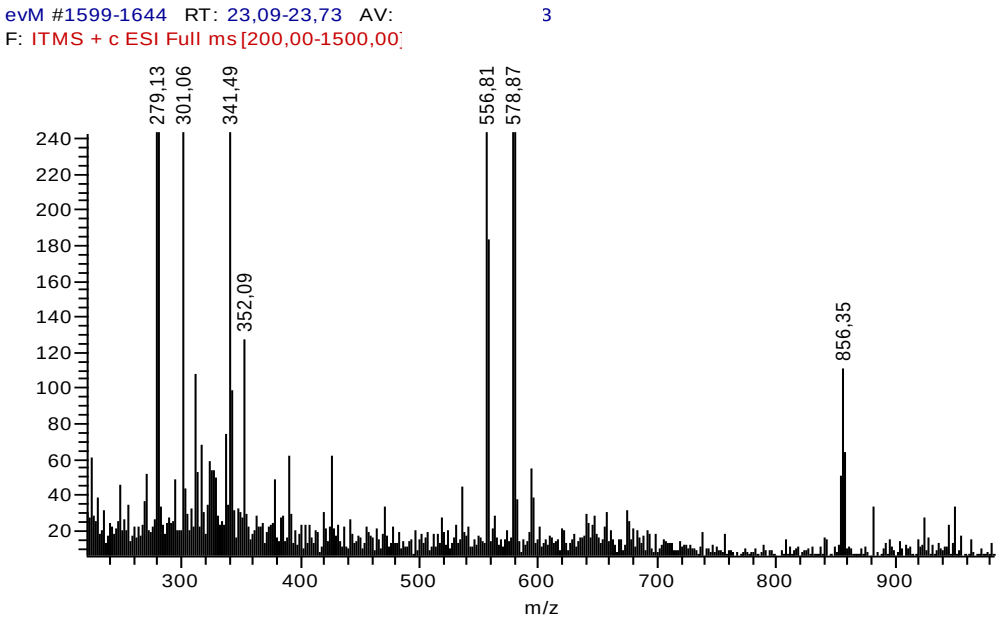

Figure 9. *The mass spectrum in the positive mode. Peak 856 m/z corresponds to a single charged compound **7***

Figure 10. *TLC analysis of reaction mixture containing compound **7** (lane 1) and diethylamine (lane 2) using ninhydrin for detection. As a negative control, FAD incubated with the same concentration of diethylamine did not gave a positive signal(photo not shown).*

2.6 CHARACTERISATION OF N^6-(BUTYL-4-EN-2-AMINE)-FAD

The redox potential of **7** was determined by cyclic voltammetry. The voltamperograms obtained for FAD and **7** are shown in Figure11. Both flavins displayed a similar redox behavior and potential (0.205 V vs Ag/AgCl). This is according to expectations, the FAD derivatization at the adenosine N^6 was not expected to alter the flavin redox properties.

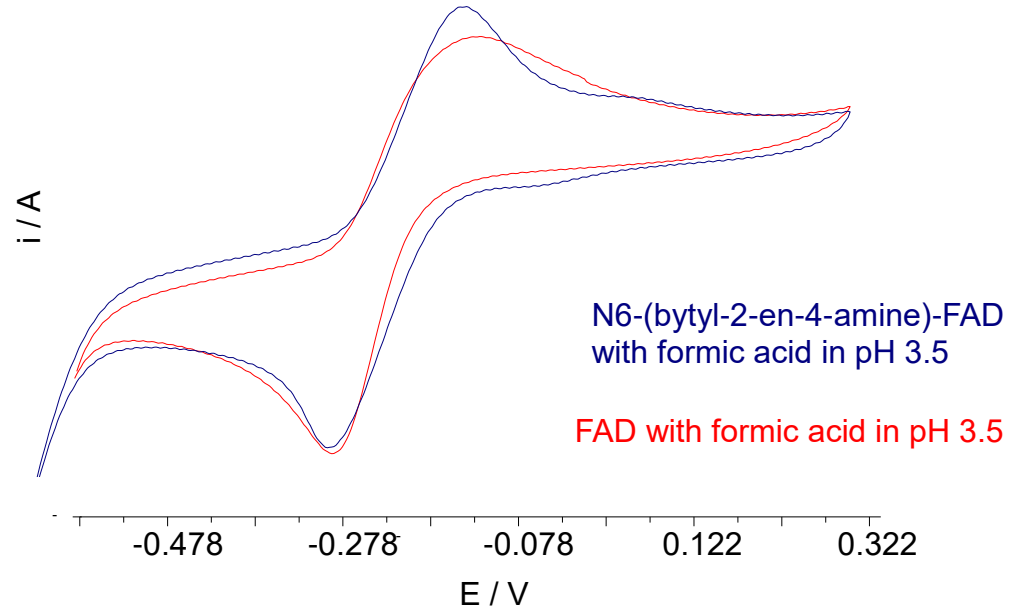

Figure 11. Cyclic voltamperograms measured at room temperature in water with 0.1 NaCl and formic acid, pH 3.5 (red: FAD, blue: **7)** measureds vs AgCl/Cl. Signal from the compound 7 contains small redox-active impurity exchange one electrone (around 0.06V difference between oxidation and reduction), and can be assigned to diethylamine (1.14 vs SCE (Novakova et al., 2014))

For a final check of the prepared material, NMR spectra were obtained. A ^{1}H spectrum of **7** confirmed the presence of an alkene, which was evidenced by a multiplet around 5.87 ppm. This signal overlaps with the doublet from the 1' proton (Figure). It is in line with HSQC analysis (Fig. S10), which revealed two cross-peaks corresponding to ^{13}C NMR shifts: 88 ppm that corresponds to the 1' moiety

and 132 ppm corresponding to L2 and L3 atoms (Figure 6). In addition, separation of ^{1}H NMR peaks around 5.8 ppm region also was obtained using the COSY technique (Fig. S **9**). Considering the fact that the spectra were collected in D_2O and compound **5** is not soluble in water, the observed multiplet most probably comes from the linker part of the substituted, water soluble FAD analogue. The overlap of ^{1}H NMR spectra of FAD and **7** shows extra signals for the latter one, which correspond with a good agreement to expected chemical shifts for the linker part at the L4 and L1 positions (Figure 6 shows atoms) (4 ppm region, Fig. S8). Moreover, the proton spectrum of **7** indicates that the molecule is fully rearranged into the N^6 derivative (Figure 12). This is in line with the absorbance spectrum obtained by LC-MS/UV-Vis analysis, revealing a clear maximum at 267 nm. Moreover, the same peak has a mass corresponding to the adduct with Na^+ (Figure7).

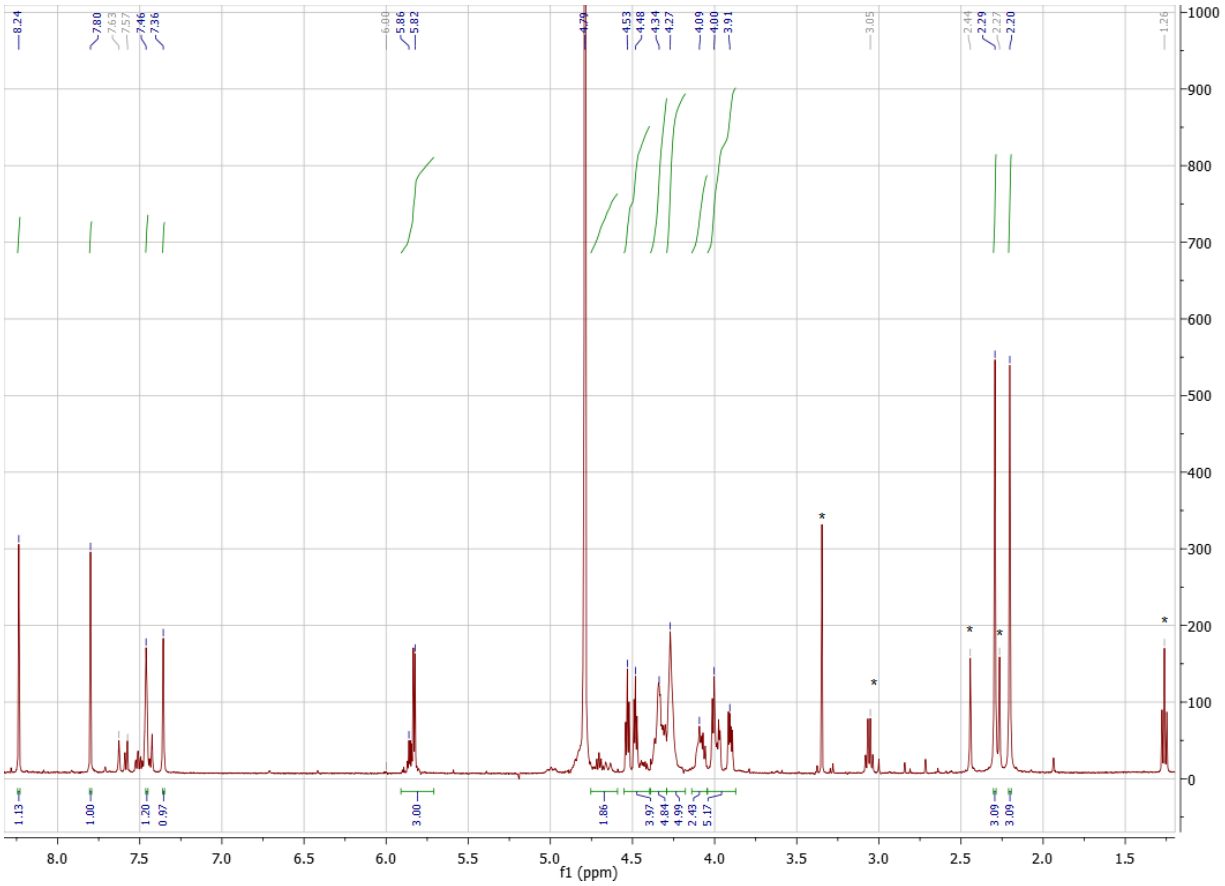

***Figure 12**. Compound **7** after purification with C18 column. The sample still contains some impurities (grey chemical shifts): diethylamine (peaks 1.26 and 3.05 ppm), compound **6** (multiplet around 7.57 and doublet at 6 ppm). Diastereomeric mixture*

The aromatic region of the ^{1}H NMR spectrum (Figure 2) has a weak, characteristic multiplet signal originating from the phthalimide, which is also visible in the HSQC spectrum (Fig. S10). Nevertheless, when normalized for the single proton peak from compound **7**, the integration is 0.61 which corresponds to around 15% of a phthalimide-protected FAD compound (or less likely: some free phthalimide) left in the sample. It suggests that the deprotection is slower than the Dimroth rearrangement. Difficult to interpret is the 0.30 integration for two singlets, shifted downfield versus the methyl groups of **7** (Figure 3). As in the aromatic region no atypical shifts were detected, and there are no unspecified absorptions in the UV-Vis absorbance spectrum, this might come from unspecific molecules coordinated with diethylamine. Yet, also other FAD modifications may have occurred.

Infrared spectra of N^6-(butyl-2-en-4-amine)-FAD and FAD (Fig. S11) indicate the presence of a primary amine. Although most prominent signals from amine N-H stretches (3200 – 3400 cm^{-1}) are covered by a broad peak from hydroxyl groups (Fig. S113I), there are specific signals from other spectral regions. A shift in absorption for the N-H bending vibration from 1608 towards smaller wave numbers suggests that the nature of the primary amine has changed (Fig S11 II), possibly due to substitution of the aromatic adenosine N^6. Diethylamine was excluded to have such an effect on the spectrum by comparison of the FAD IR-spectrum with the IR-spectrum of FAD incubated with

diethylamine. Furthermore, in the 820 cm^{-1} region an extra broad band for compound **7** is observed (Fig S11 III) that can be assigned to N-H wag vibration characteristic for primary amines. Secondary amines have this band at lower frequencies with significantly decreased intensity. Moreover, around 3150 cm^{-1} the relative intensity is slightly increased, which also belongs to the characteristic of primary amines. Barely observable is the higher intensity of a peak at 808 cm^{-1}, which is described as more intense in aliphatic amines (Fig S11III).

Importantly, it was observed that the ^{1}H NMR spectrum of N^{6}-(butyl-4-en-2-amine)-FAD has changed upon two weeks storage in the dark in water at 4 °C. A new doublet with a chemical shift above 6 ppm and three peaks around 6.60-6.70 ppm appeared, moreover the aromatic region had altered (Figure 3). Literature suggests that, in contrast to the derivatives at adenosine position 1, FAD-N^{6} analogues do not require special storage conditions (Bückmann, Wray and Stocker, 1997; El Ashry *et al.*, 2010). Possibly some impurities present in the sample are detrimental for the prepared FAD analogue. Nonetheless, compound **7** in a freeze-dried form and stored in darkness is full preserved for at least three weeks.

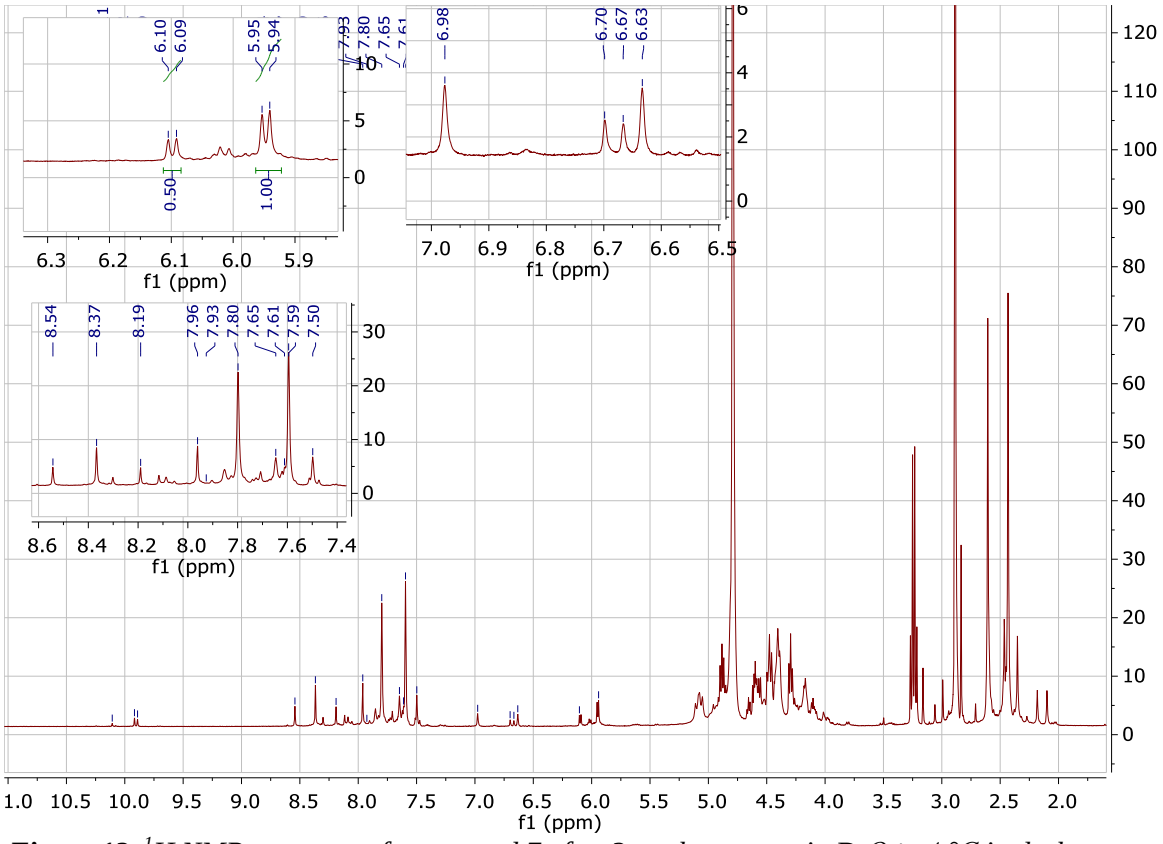

Figure 13. *^{1}H NMR spectrum of compound **7** after 2 weeks storage in D_2O in 4 °C in darkness.*

2.7 APPLICATION OF N^6-(BUTYL-2-EN-4-AMINE)-FAD FOR THE COFACTOR-MEDIATED IMMOBILIZATION

COVALENT IMMOBILIZATION OF N^6-(BUTYL-2-EN-4-AMINE)-FAD ON SEPHAROSE MATERIAL

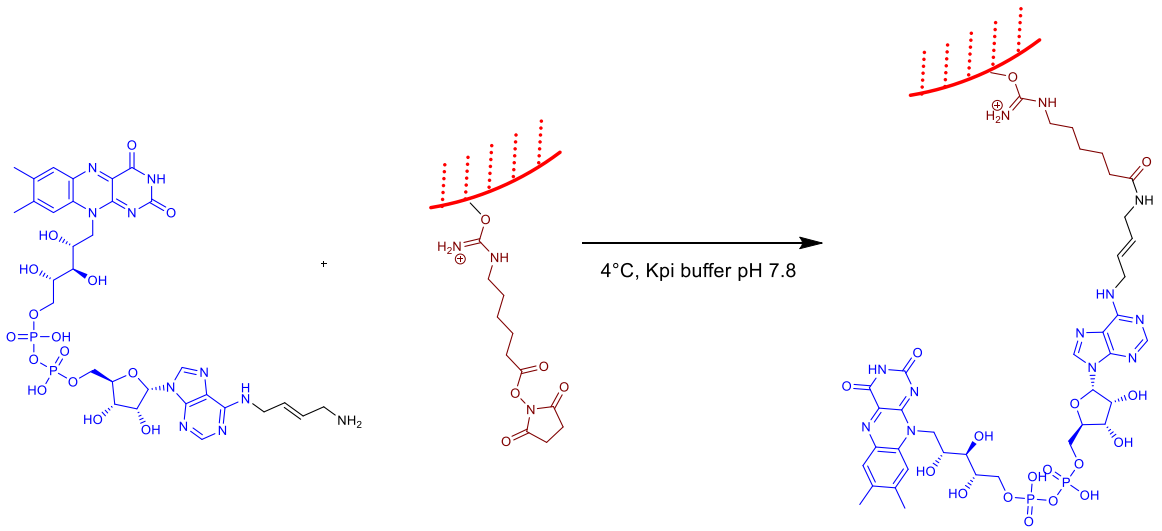

***Scheme 6**. Covalent immobilization of N^6-(butyl-4-en-2-amine)-FAD on N-hydroxysuccinimidyl-Sepharose® via nucleophilic substitution at the terminal primary amine with reactive succinimidyl ester group at the resin. Blue color highlights the natural FAD cofactor moiety. Brown color represents the reactive groups on the commercial resin.*

The NHS Sepharose turned yellow after incubation with both N^6-(butyl-4-en-2-amine)-FAD and FAD. The color remained for both materials after extensive washing with water, a saline solution (2 M NaCl) or with the organic solvents acetonitrile and ethyl acetate. Eventually, 5% diethylamine buffered with saturated KPi buffer pH 8.5 resulted in loss of the yellow color in case of the material incubated with FAD, while the NHS Sepharose incubated with compound 7 remained yellow. It shows that the natural cofactor binds to the NHS Sepharose in a very tight manner and only a combination of highly concentrated salt and a strong amine can cause its release. At the same time, this outcome confirms the robust binding of compound **7** to the Sepharose material (Scheme 6).

COFACTOR-MEDIATED RECONSTITUTION OF PAMO ENZYME ON FAD-SEPHAROSE

The Sepharose material with **7** after incubation with the apo PAMO yielded functional enzyme. This was verified by monitoring the conversion of phenylacetone with GC-MS. In the conversion mixture, accumulation of the enzymatic product (benzyl acetate) was detected only for the material containing N^6-(butyl-4-en-2-amine)-FAD. The immobilized enzyme was used for two consecutive conversions which revealed that the enzyme retained full activity after repeated usage. Based on the conversion experiment, the calculated active enzyme loading on the Sepharose was very low, around 0.1 mg/mL.

This shows that there is room for improving the immobilization procedure. Nonetheless, the reconstitution of an apo flavoenzyme on the N^6-(butyl-4-en-2-amine)-FAD functionalized material was demonstrated (Figure 14).

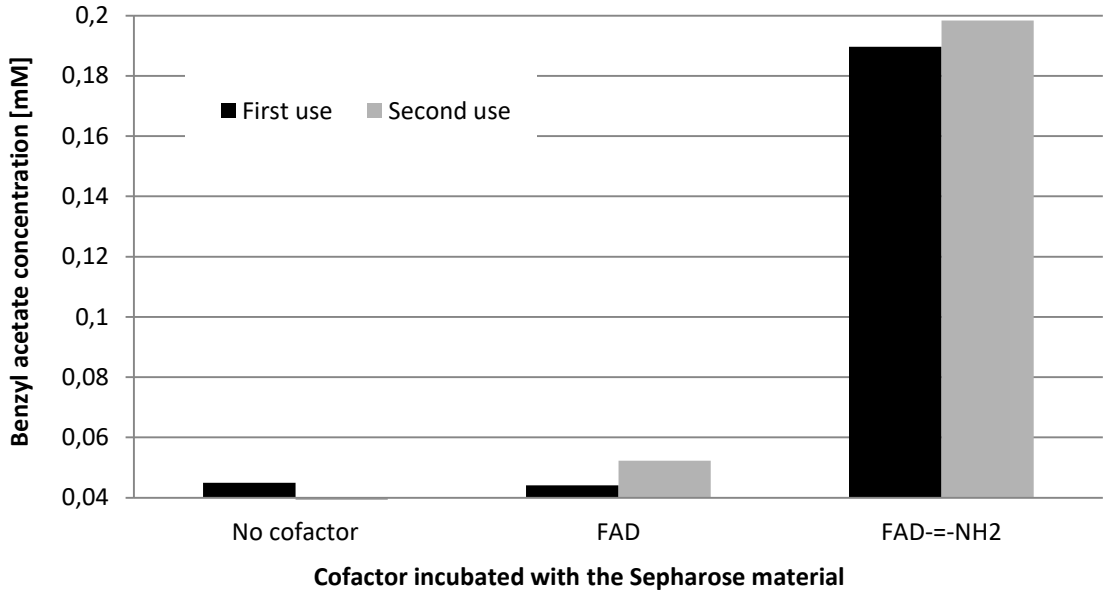

Figure 14 *Enzymatic activity of Sepharose containing flavin cofactors after apo-PAMO enzyme reconstitution. It has been tested for the Baeyer-Villiger oxidation of phenylacetone by product detection (GC-MS). A basal amount of benzyl acetate was present in the starting material. FAD-=-NH_2 represents N^6-(butyl-4-en-2-amine)-FAD.*

4. CONCLUSIONS

A novel FAD analogue, N^6-(butyl-4-en-2-amine)-FAD has been synthesized starting from FAD. The yield of 40% was obtained with around 80% purity. In the first step of the synthetic route, satisfying alkylation at position 1 was achieved within 12.5 h while using microwave irradiation and a strong electrophile, an allyl halide. The second step, which involved a Dimroth rearrangement, gave close to quantitative yield by using a relatively high concentration of a strong nucleophile, diethylamine. Regarding future applications, one drawback of the presented approach is the difficulty of complete removal of diethylamine from the sample. Nonetheless, the developed synthetic procedure is more effective and less laborious than alternative methods published in the patent and scientific literature (Bückmann, Wray and Stocker, 1997).

Additionally, a simple and straightforward synthesis of the alkylating agent (N^1-(butyl-2-en-4-amine)-FAD), which is commercially not available, has been developed (43% yield). It involves only two steps and uses low-cost and accessible chemicals.

The novel FAD analogue could be safely stored in freeze-dried form and it displays identical redox properties when compared with FAD. What is essential, its utility towards the cofactor-mediated

enzyme immobilization has been proven. Furthermore, the newly developed approach towards synthesis of N^6-derivatized FAD may also be employed for synthesis of other, similar FAD analogues. The developed method enables synthesis valuable, key chemicals for cofactor-mediated immobilization of flavoenzymes.

5. EXPERIMENTAL SECTION

GENERAL REMARKS

All chemicals and solvents were purchased from Sigma Aldrich or TCI and were used without extra purification step. Work that involved FAD or FAD analogues was performed without direct exposure to light: all the vessels were wrapped in aluminum foil and stored in complete darkness in order to prevent unspecific light-triggered reactions. All NMR spectra of FAD and its derivatives were collected in D_2O.

For thin layer chromatography (TLC) Merck silica gel 60/Kieselguhr F254 0.25 mm was used. Compounds were visualized using a 365 nm lamp or elemental iodine. Flush chromatography was performed with SiliCycle silica gel type SiliaFlush P60 (230-400 mesh).

MATERIALS

All the chemicals for the synthesis were purchased from Sigma Aldrich or TCI and were used without extra purification. For the immobilization, N-hydroxysuccinimidyl-Sepharose® 4 Fast Flow from Sigma Aldrich was used.

ANALYTICAL METHODS

NMR spectra were recorded on a Varian AMX400 (^{1}H: 400 MHz, ^{13}C: 100 MHz) or a Varian Unity Plus (^{1}H: 500 MHz, ^{13}C: 125 MHz) spectrometer. Chemical shifts are denoted in δ-units (ppm) relative to the residual solvent peak unless another reference is indicated ($CDCl_3$: ^{1}H δ =7.26, ^{13}C δ = 77.0; D_2O ^{1}H δ =4.79). The splitting parameters are named as follows: s = singlet, d = doublet, t = triplet, m = multiplet, dd = doublet of doublets.

LC-MS was performed using LCQ Fleet Ion Trap LC-MS form Thermo Scientific (Finnigan Surveyor with PDA Plus detector connected to the mass spectrometer with ESI ionisation) with C18 3 μm particles with 100 x 2.1 mm diameters column from GRACE. For the separation solvents A: 0.2 % formic acid in H_2O, and B: 0.08 % formic acid in acetonitrile were employed with the following programme with the flow rate 0.3 mL/min : 2 min 100 % A, 30 min up to 20 % A, 7 min 20 % A, 1 min up to 100 % A, 12 min 100 % A

Final product purification was run on a Åkta purifier from Amersham Pharma Biotech using a 40 g Grace™ Reveleris™ SRC C18 Cartridge. Solvents were employed as follow: A) Phosphate buffer pH 4, B) MeOH. 100% A for 12 min, up to 30% A for 5 min, 30% A for 10 min, up to 50 % A for 5 min, 50 % A

FT-IR spectra were recorded on a Perkin Elmer FT-IR spectrometer. For the CV, a μAutolab III potentiostat was used and equipped with a gold disc electrode (working electrode), Ag/AgCl electrode (reference electrode) and a platinum wire (counter electrode).

GC-MS detection of enzymatic conversion of phenylacetone into benzyl acetate was performed on a GC-MS-QP 2010 Ultra from Shimazu with helium as a carrier gas. The instrument was equipped with a non-chiral dimethylsiloxane (100%) column from Agilent (30 mx, 0.25 mm, 0.25 μm). Samples for the GC-MS detection of phenylacetone conversion were prepared by the extraction of the enzymatic conversion mixture solution with two times higher volumes of organic solvent (ethyl acetate). Injection to GC-MS was performed at 250 °C, the linear flow was 21.7 mL/min and pressure was 34.3 Pa. The column temperature program was as follow: 5 min at 110 °C, ramp up to 180 °C (5 degree per minute) and hold at 180 °C for 4 min. The retention times were 3.78 min for phenylacetone and 4.4 min for benzyl acetate.

5.1 Syntheses

2-(4-hydroxybut-2-en-1-yl)phtalamide-1,3-dione (1)

Compound **1** was obtained using a published procedure (Al-Shuhaib *et al.*, 2013). Briefly, a Mitsunobu reaction was performed in 400 mL of dry THF under oxygen free conditions. To the flask on the ice bath, 15 g isomeric mixture of 1,4-butene-diol (170 mmol), an equimolar amount of phthalimide (25 g), and 1.2 molar equivalents (53 g, 204 mmol) of PPh_3 were added. Cold 40% DEAD in toluene and 4 mL of dry THF was added in 1.1 molar equivalent (74 g, 187 mmol) dropwise within 15 min. After that, the ice bath was removed and the reaction was continued at room temperature over 3 days. Progress of the reaction was followed on TCL using a EtOAc : pentane (7 : 3 v/v) mixture (R_f^{trans} = 0.35; R_f^{cis} = 0.27). Purification was performed on a silica column with the same combination of solvents. The desired product 1 was obtained in 46% yield as a white solid. *Cis* and *trans* isomers were mixed and used for further reactions.

Below are NMR spectra of the isolated *trans* isomer with detectable signals from the *cis* isomer. For that reason the integration of alkene's protons has slightly decreased accuracy.

^{1}H NMR (400 MHz, cdcl3) δ 7.85 (s,), 7.72, , 5.84 (m, 2H) 4.39 (d, *J* = 4 Hz, 2H), 4.30 (d, *J* = 4 Hz 2H),

1.55 (s, OH).

^{13}C NMR (100 MHz, cdcl3) δ 163.0, 134.0, 133.0, 131.9, 124.7, 123.2, 62.4, 39.3

The analytical data are in agreement with a previous study (Al-Shuhaib *et al.*, 2013).

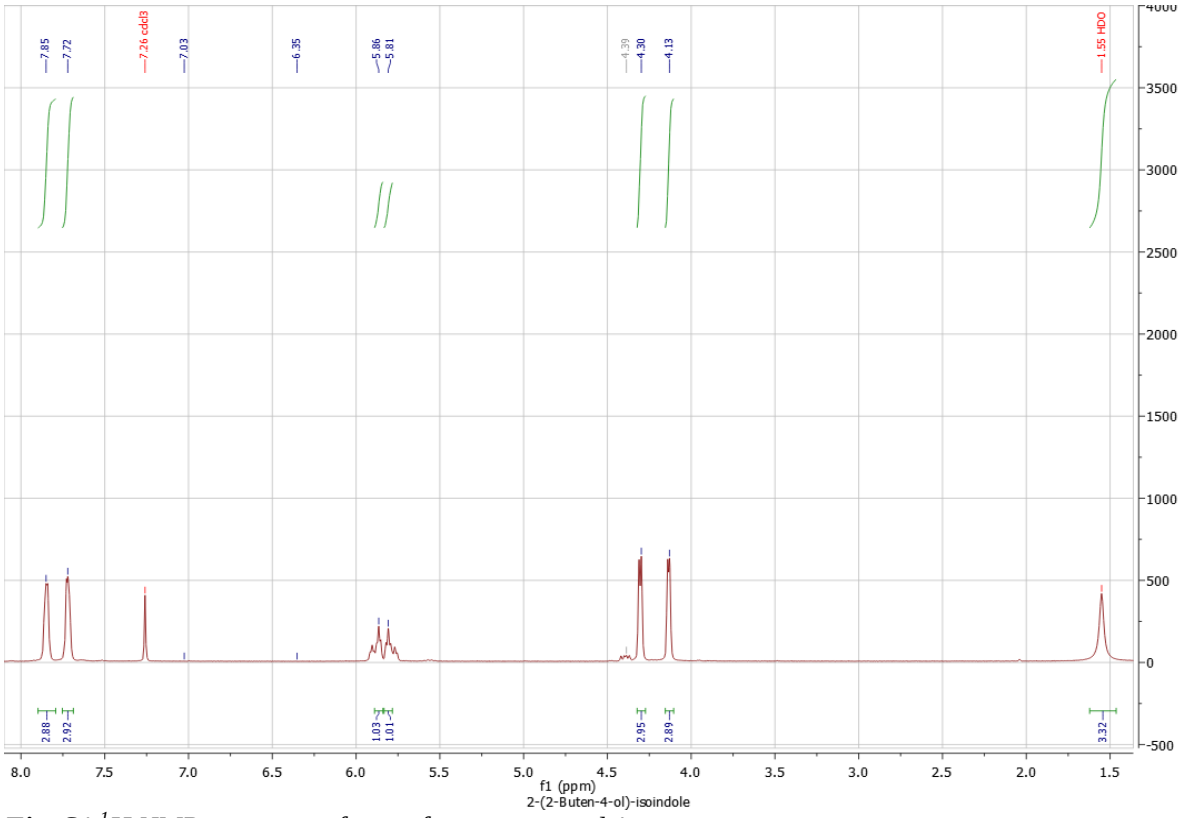

Fig. S1 *^{1}H NMR spectrum of trans form compound* ***1***

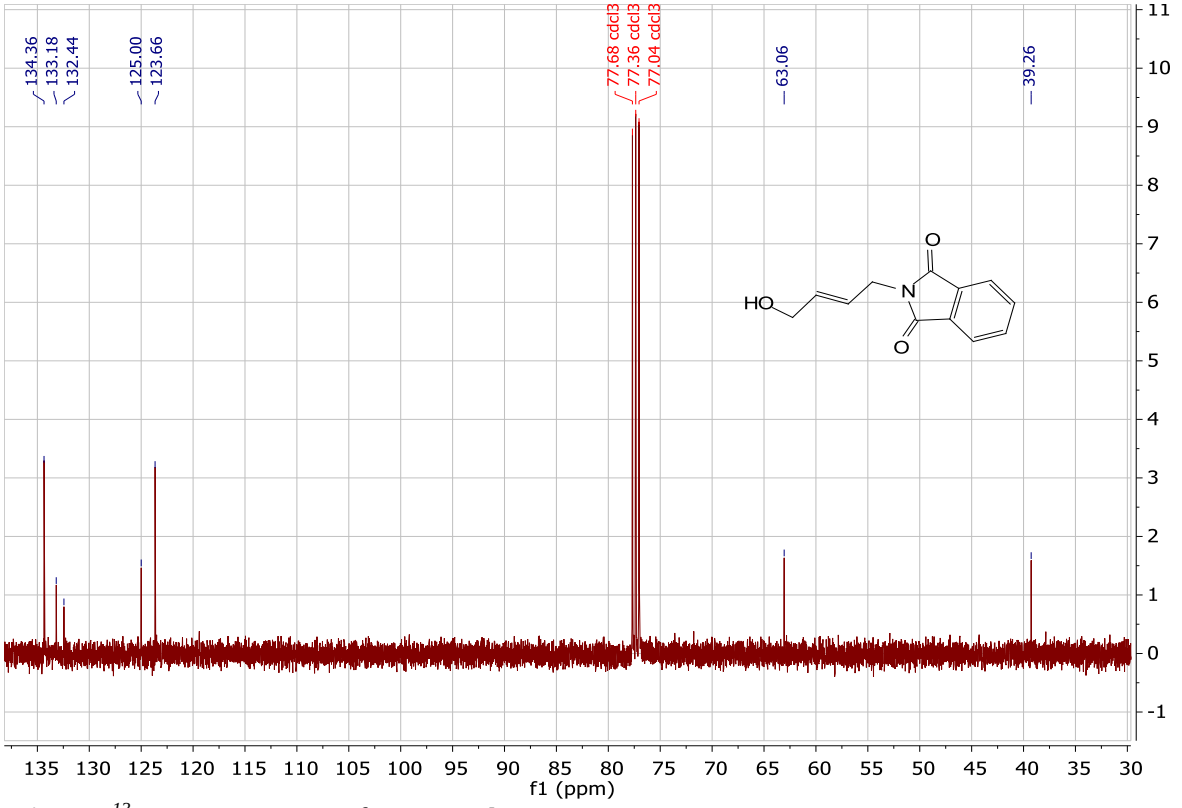

Fig. S2*. ^{13}C NMR spectrum of compound 1*

4-AMINOBUT-2-ENE-1-OL (2) AND 4-(FMOC-AMINO)-1-BUT-2-ENE-OL (3)

Compound **1** (15 g, 69 mmol) was deprotected from phthalimide using 1.1 equivalent of hydrazine hydrate (2.43 g, 76 mmol) dissolved in ethanol overnight at reflux. The reaction was monitored by TLC using EtOAc : pentane 1:1 (v/v) as a solvent mix. The reaction mixture was filtered over a glass filter with cold ethanol three times in order to remove side products. Ethanol was evaporated on a rotary evaporator and white crystalline material has been obtained. It was reacted with Fmoc-Cl as previously reported (Marsault *et al.*, 2006). Briefly, 34.5 mmol of **2** (2.15 g) together with 1.1 equivalent of Fmoc-Cl (7 g, 38.0 mmol) were stirred in 150 mL acetonitrile for 3 hours at room temperature. The TLC with pentane and EtOAc 4:1 (v/v) analysis confirmed completion of the reaction. Acetonitrile was evaporated and the sample was purified with flash chromatography using the same solvent mix. After evaporation, a white solid was obtained with 19% yield after two steps.

^{1}H NMR (400 MHz, $cdcl_3$) δ 7.74 (d, J = 7.5 Hz, 2H), 7.56 (d, J = 7.3 Hz, 2H), 7.42 – 7.24 (m, 4H), 5.75-5.72 (m, 1.5 H), 4.95 (s, broad OH), 4.55 (d, 2H), 4.40 (d, J = 7.0 Hz, 2H), 4.20 (d, J = 6.8 Hz, 1H), 4.12 (s, 1.5 H), 3.81 (s, 1.5 H), 2 (s, broad)

^{13}C NMR (101 MHz, $cdcl_3$) δ 156.68, 144.13, 141.53, 131.35, 127.93, 127.29, 125.23, 120.22, 66.87, 62.83, 47.46, 42.56.

The analytical data are in agreement with Marsault et al. (2006). The 1.5 H integrations can be the result of having two forms, cis and trans, for which those shifts are different. The dominant isomer is cis (> 75%).

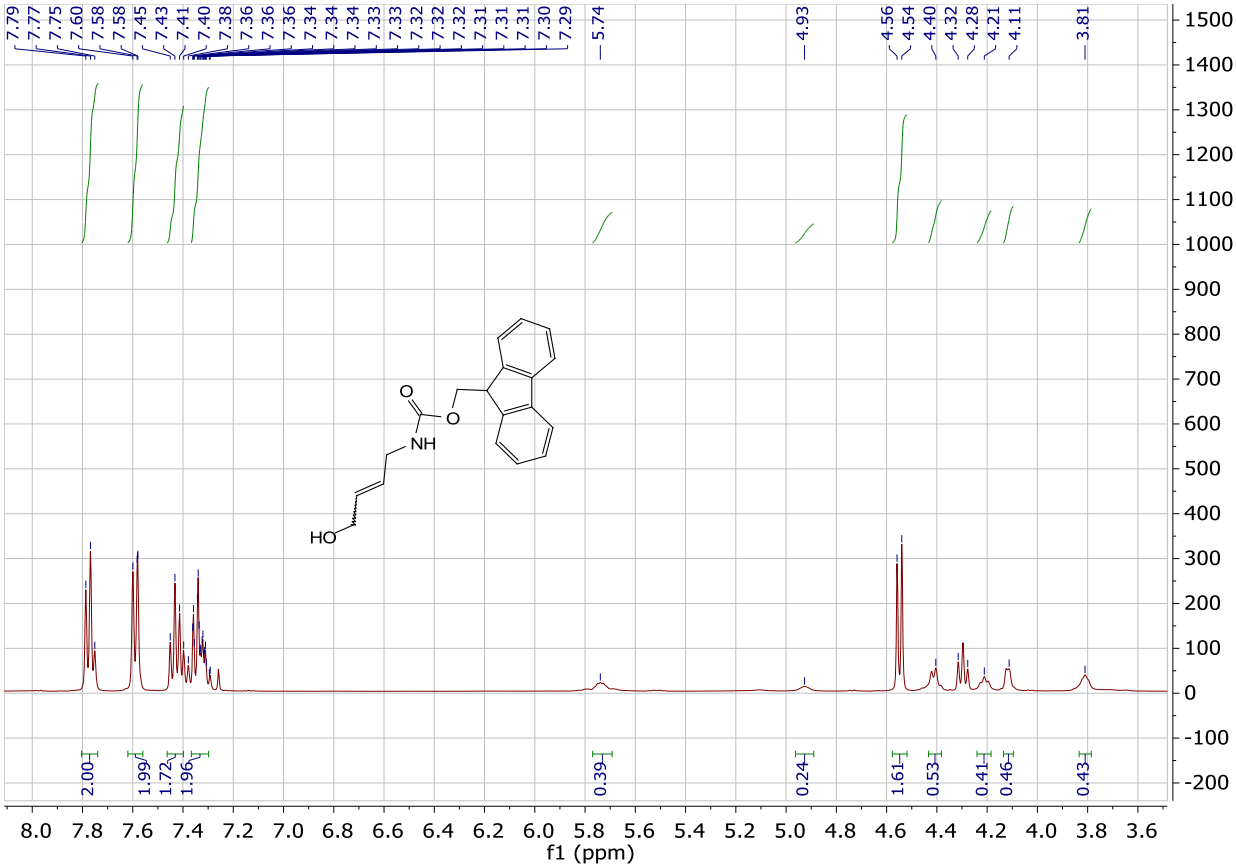

Fig. S3. *^{1}H NMR spectrum of compound* **3**

4-(FMOC-AMINO)-BUT-2-ENE-1-BROMIDE (4)

Compound **3** was brominated as described before (Corey and Kim, 1972). In a Schlenk flask on ice 0.53 g (1.8 mmol) of compound **3** was mixed in 100 mL of dry dichloromethane with PPh_3 (0.52 g, 2.01 mmol, 1.12 eq). Subsequently, 2 mL of cool dry dichloromethane with CBr_4 (0.66 g, 2.01 mmol) solution was added dropwise under inert conditions. A milky solution turned into clear lemon coloured liquid. After addition, the ice bath was removed and the reaction was stirred overnight. TLC with EtOAc and pentane 7:3 (v/v) confirmed that the reaction was complete (R_f = 0.85; R_f = 0.80 for *cis* and *trans*). The material was filtered over a glass filter and purified on a silica gel column. After solvent evaporation te product was obtained as a white crystalline solid with 86% yield.

^{1}H NMR (400 MHz, cdcl$_3$) δ 7.74 (d, *J* = 7.6 Hz, 2H), 7.56 (d, *J* = 7.5 Hz, 2H), 7.34 (m, *J* = 34.8, 7.5 Hz, 4H), 5.74-5.78 (m, 1.2 H*), 4.80 (m, 0.8H*), 4.42 (d, *J* = 7.0 Hz, 2H) 4.19 (s, 1H), 3.91 (d, *J* = 5.9 Hz, 2H), 3.81 (s, 2H), *non-integer integration due to the diastereomeric mixture

^{13}C NMR (101 MHz, cdcl$_3$) δ 156.45, 144.13, 141.60, 131.77, 127.98, 127.32, 125.25, 120.27, 66.95, 47.53, 42.22, 32.12.

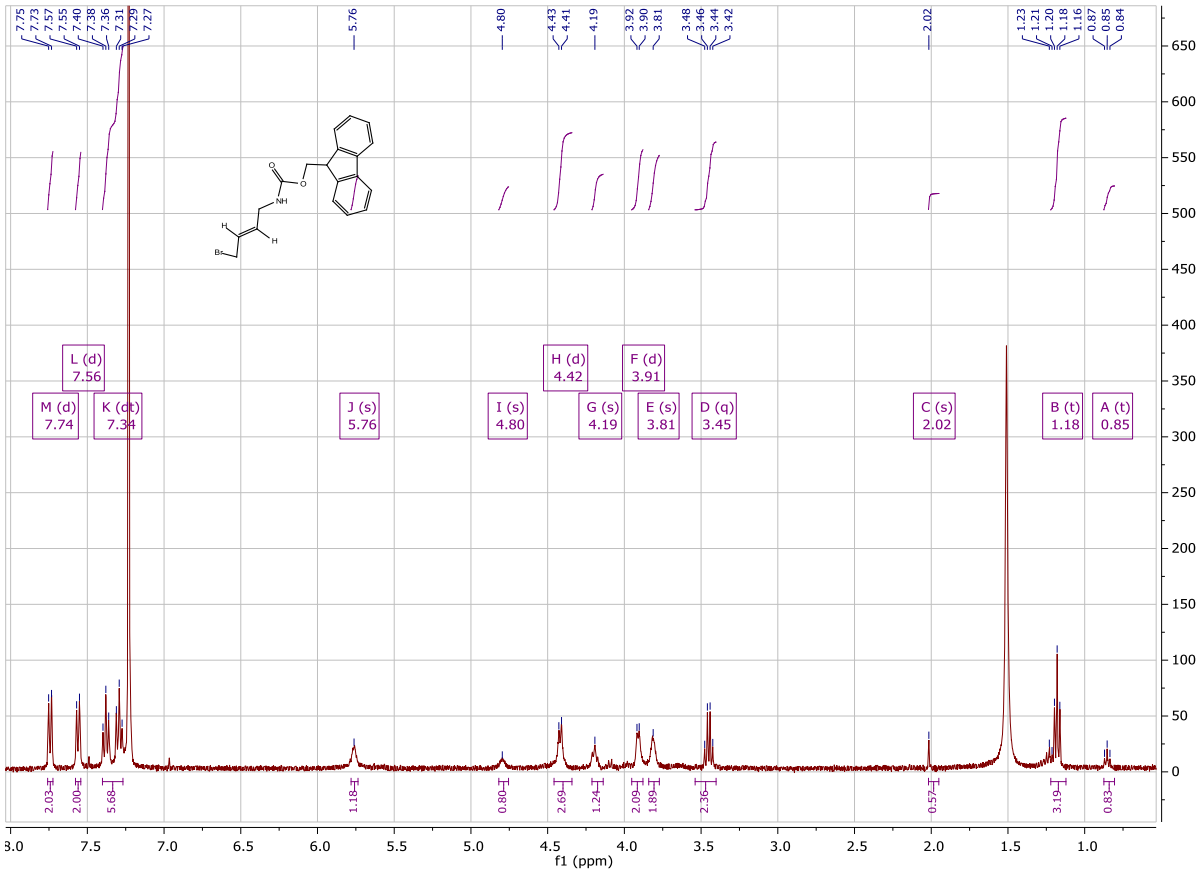

Fig. S4. *[1]H NMR spectrum of compound* **4**

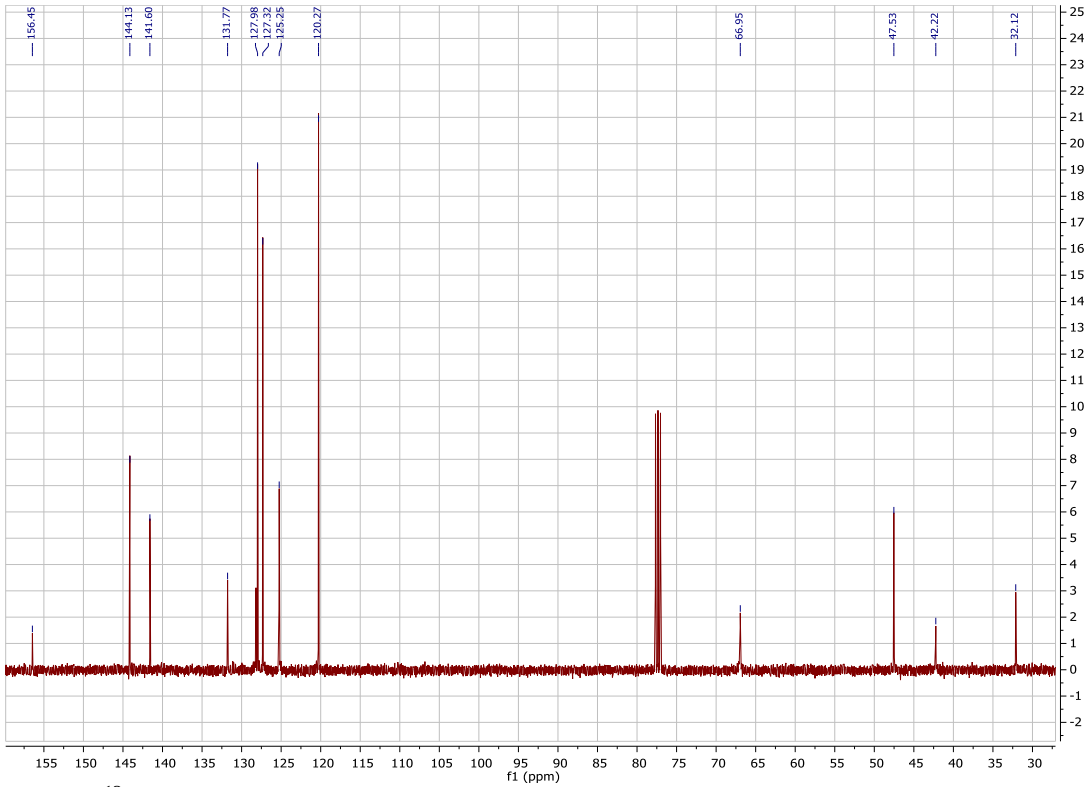

Fig. S5 [13] C NMR spectrum of compound 4

The confirmation that bromination occurred comes from inspecting the ^{13}C NMR spectra that reveals a significant upfield chemical shift for the carbon directly attached to bromide from 62.83 ppm into 32.12 ppm

N-(4-BROMOBUT-2-EN-1-YL)PHTHALIMIDE (5)

Compound **5** was prepared in the same way as compound **4**, only solvent for TLC (R_f = 0.78) and flash chromatography was different, using dichloromethane. Bromination was again confirmed with ^{13}C NMR (Fig. S7). Fig. S6 shows the NMR spectrum of both combined isomers (*cis*:*trans* ratio 1:2.5).
CIS: ^{1}H NMR (400 MHz, cdcl3) δ 7.76 – 7.61 (m, 4H), 5.96 – 5.73 (m, 2H), 4.33 – 4.24 (dd, 1H), 3.85 (dd, 1H). **TRANS** ^{1}H NMR (400 MHz, cdcl3) δ 7.78 – 7.60 (m, 4H), 5.66 – 5.52 (m, 2H), 4.28 (dd, *J* = 4.9, 3.6 Hz, 2H), 4.12 (dd, *J* = 8.2, 3.8 Hz, 2H).
^{13}C NMR (101 MHz, cdcl3) δ 156.7, 134.55, 130.43, 128.81, 123.86, 120.35, 39.08, 31.72

N^1-(BUTYL-2-EN-4-AMINE)-FAD (6)

FAD (0.56 g, 0.71 mmol) was dissolved in water and 4 molar eq (2.87 mmol) of each: 5 (0.8 g), NaI (0.42 g), $BaCO_3$ (0.51 g) was dissolved in DMF and DMSO. Solutions were combined so that the final composition of a solvent gave DMSO : DMF : H_2O (2:1:1 v/v/v). The reaction mixture was stirred at 50 °C, and another 4 molar equivalents of alkylating reagents was added. After a total microwaving time equal to 12.5 h (50 °C, 50 W) the reaction mixture was diluted 2 times with acidified water (final pH 4) and subsequently twice extracted with CH_2Cl_2. Subsequently, evaporation was performed using a rotary evaporator under reduced pressure in order to remove trace amounts of organic solvents. After these procedures, the compound **5** was not detectable by TLC analysis (TLC was performed using MeOH:acetone:ethyl ether, 4:1:1 v/v/v). Compound **6** was obtained in the reaction mixture as measured by 1H NMR the most important peaks could be assigned (4).

N^6-(BUTYL-2-EN-4-AMINE)-FAD (7)

An aquatic solution from the previous step was appropriately diluted with a stock potassium phosphate buffer solution and subsequently with diethylamine. The final solution had a pH of 8.5, contained 0.4 M phosphate and 5 % of diethylamine. The reaction was stirred at 50 °C on an oil bath until the complete rearrangement of **6** into **7** (monitored by LC-MS).
^{1}H NMR (500 MHz, D_2O) δ 8.24 (s, 1H), 7.80 (s, 1H), 7.46 (s, 1H), 7.36 (s, 1H), 5.87 – 5.84 (m, 2H), 5.83 (d, *J* = 5.2 Hz, 1H), 4.78 – 4.61 (m, 1H), 4.51 (dt, *J* = 24.2, 4.9 Hz, 2H), 4.39 – 4.27 (m, 7H), 4.08-3.95 (m, 5H), 3.92-3.87 (m, 1H), 2.29 (s, 3H), 2.20 (s, 3H)
HRMS ESI + : calculated mass [M + H+] = 854,22; found 854,22

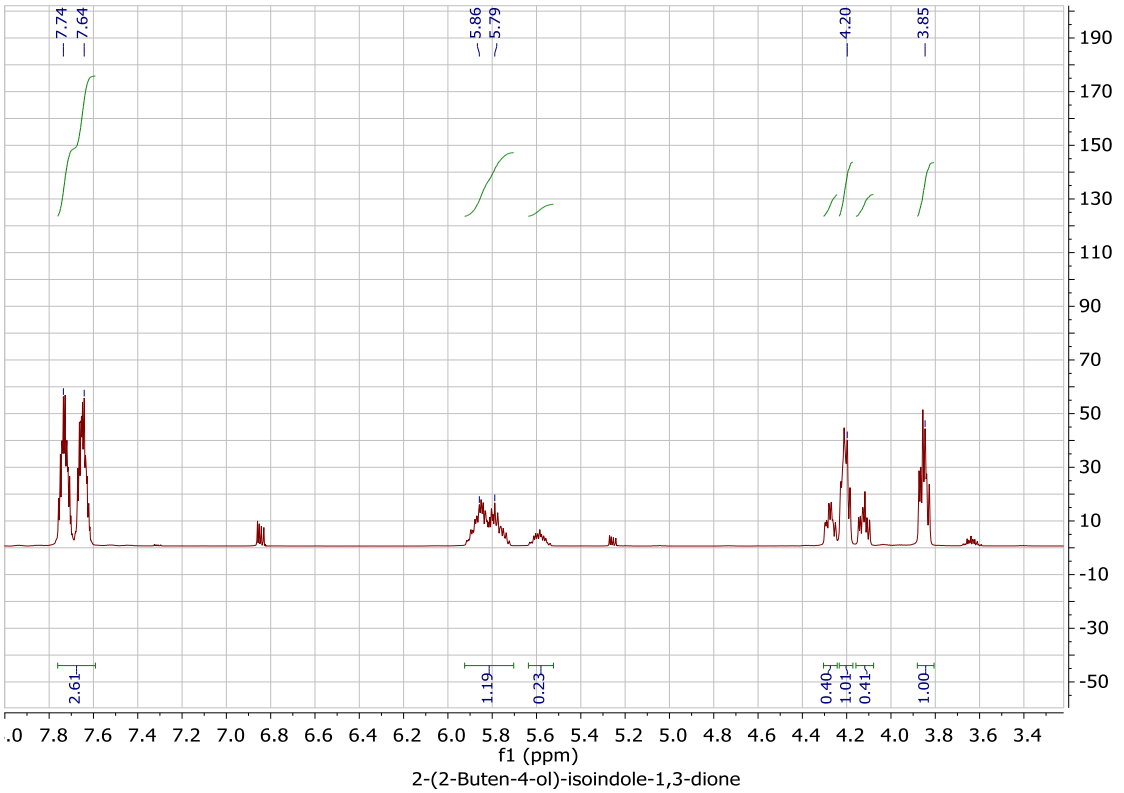

Fig. S6 ^{1}H NMR spectrum of compound 5

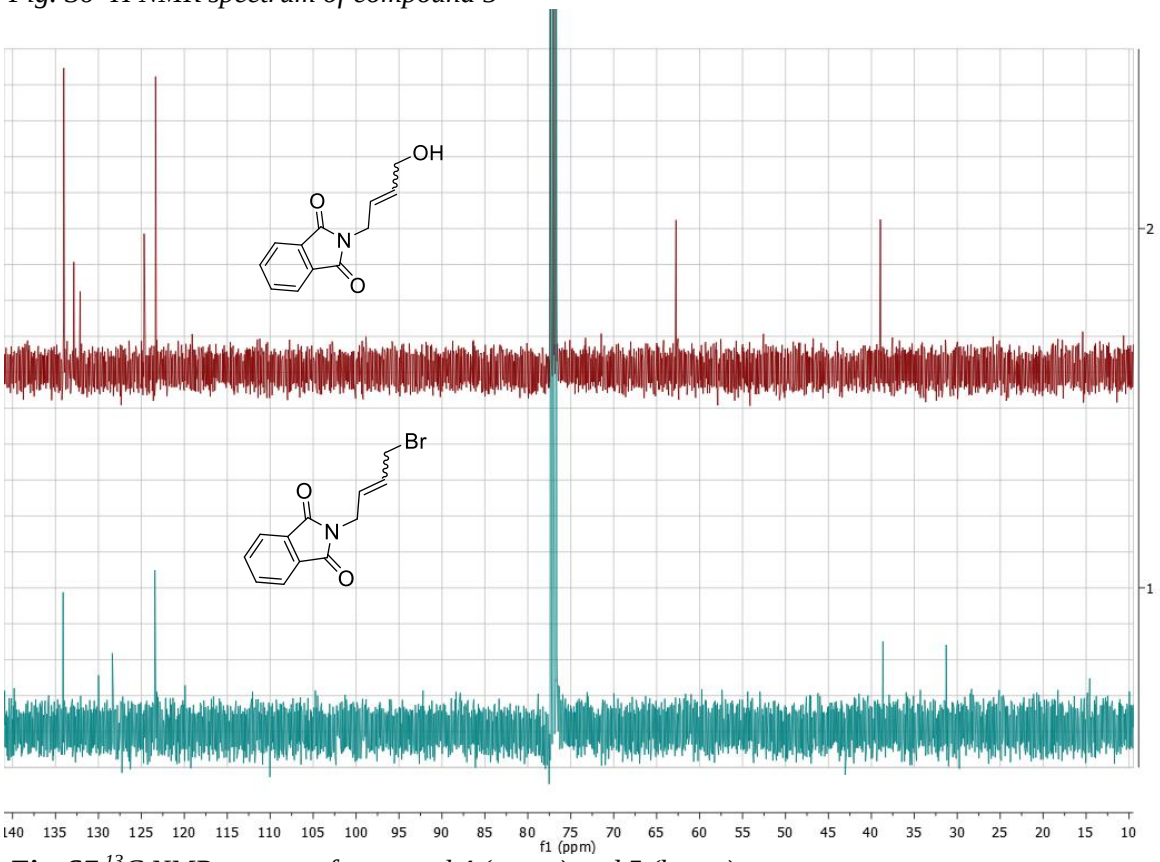

Fig. S7 *^{13}C NMR spectra of compond **4** (upper) and **5** (lower)*

*A comparison of ^{1}H NMR spectra of FAD and **7** collected in the same pD (6.5) is shown in Fig. S8.*

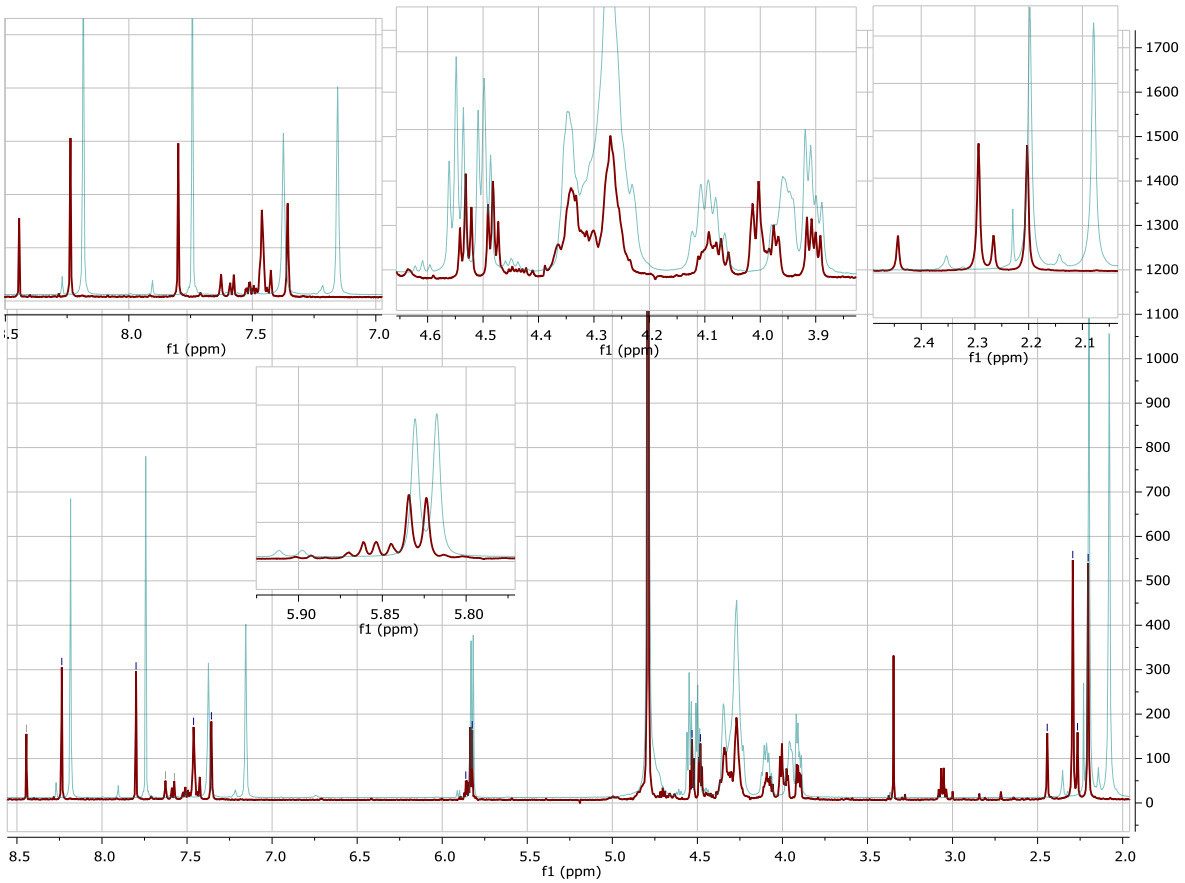

Fig. S8 Comparison of 1H NMR spectra of FAD (green) and N^6-(butyl-2-en-4-amine)-FAD, compound **7** (red). Both were collected in D_2O, pD 6.5.

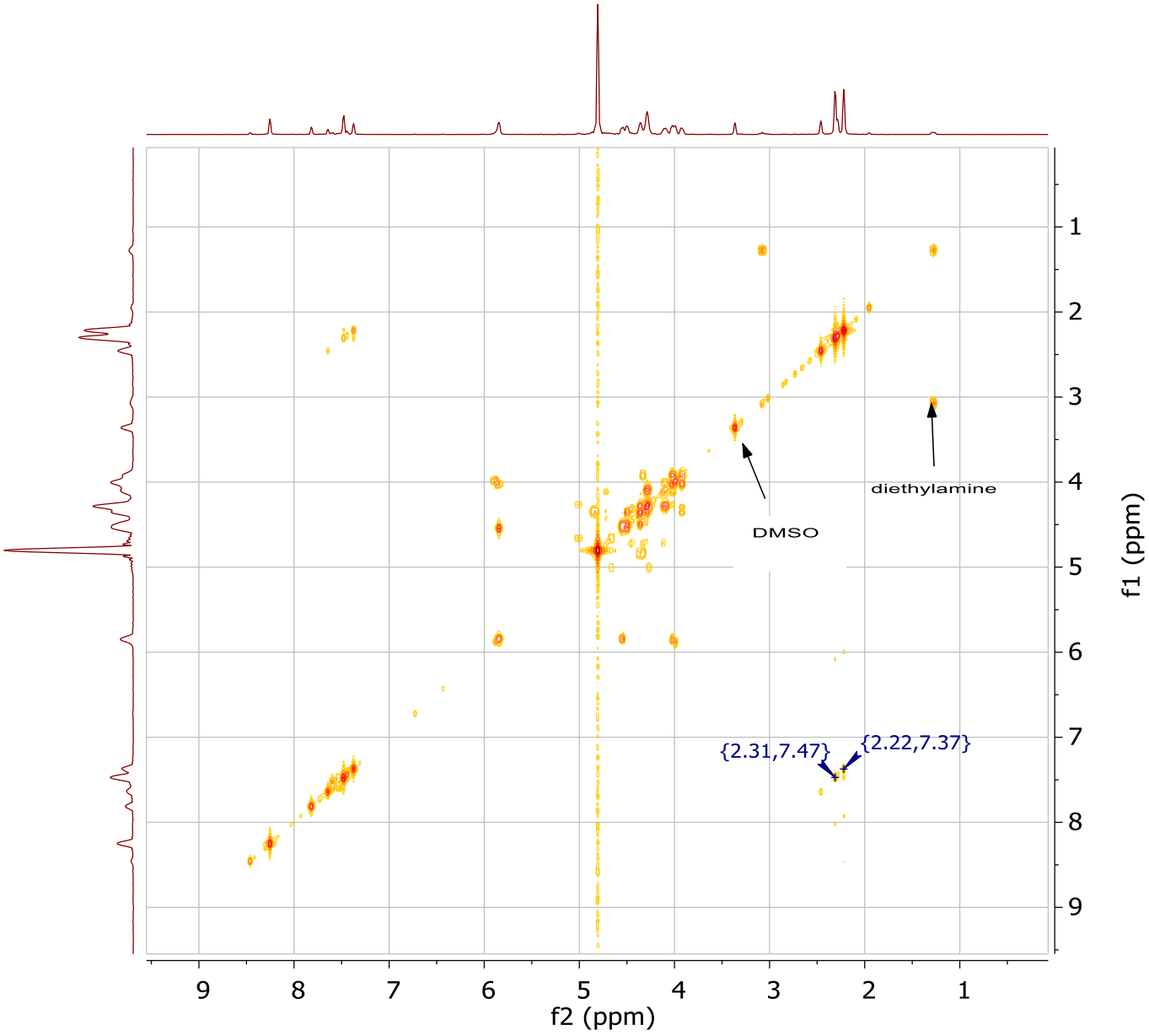

A)

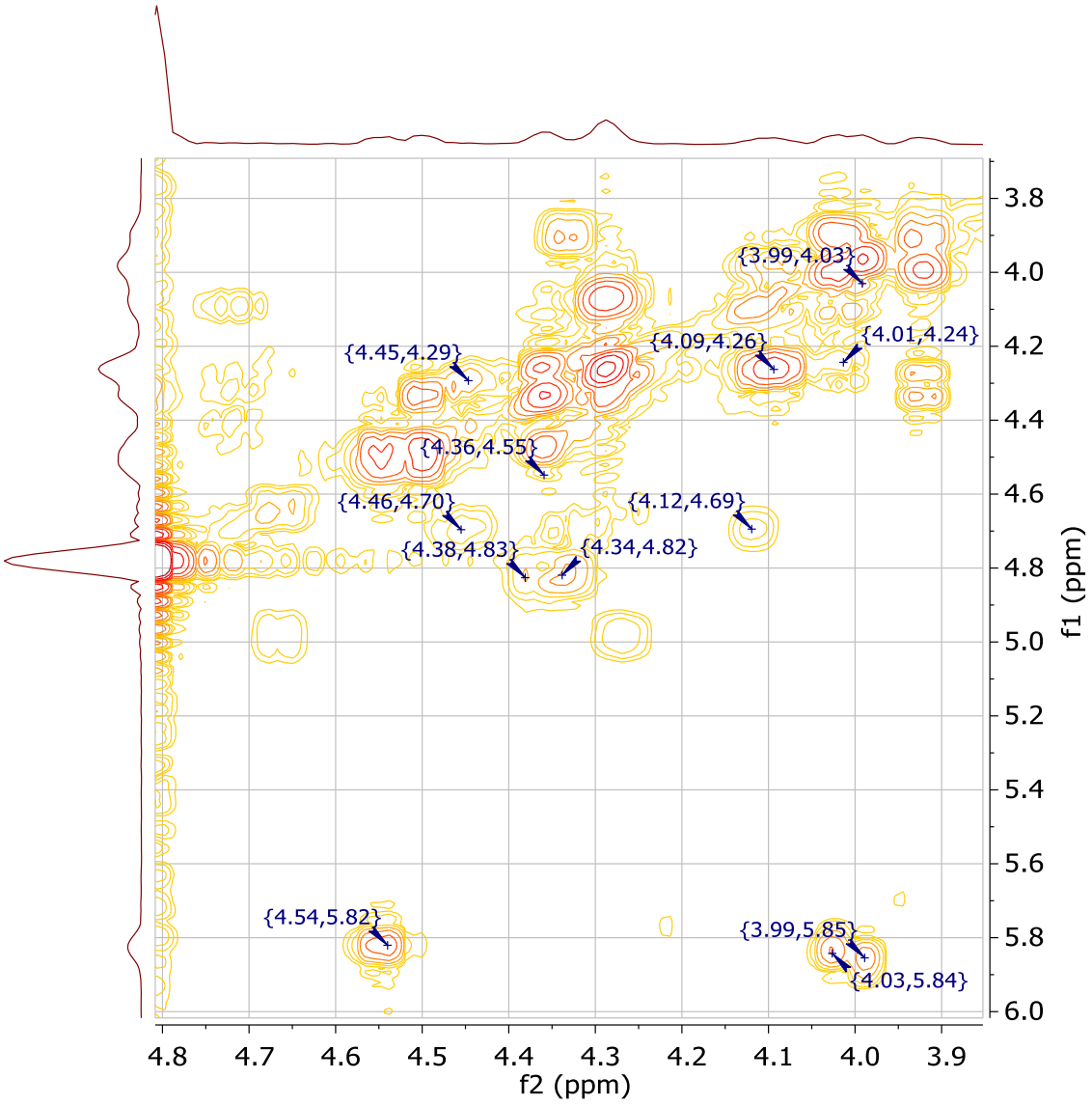

B)

Fig. S 9*. COSY spectrum of compound 7: A- full spectrum, B-magnification*

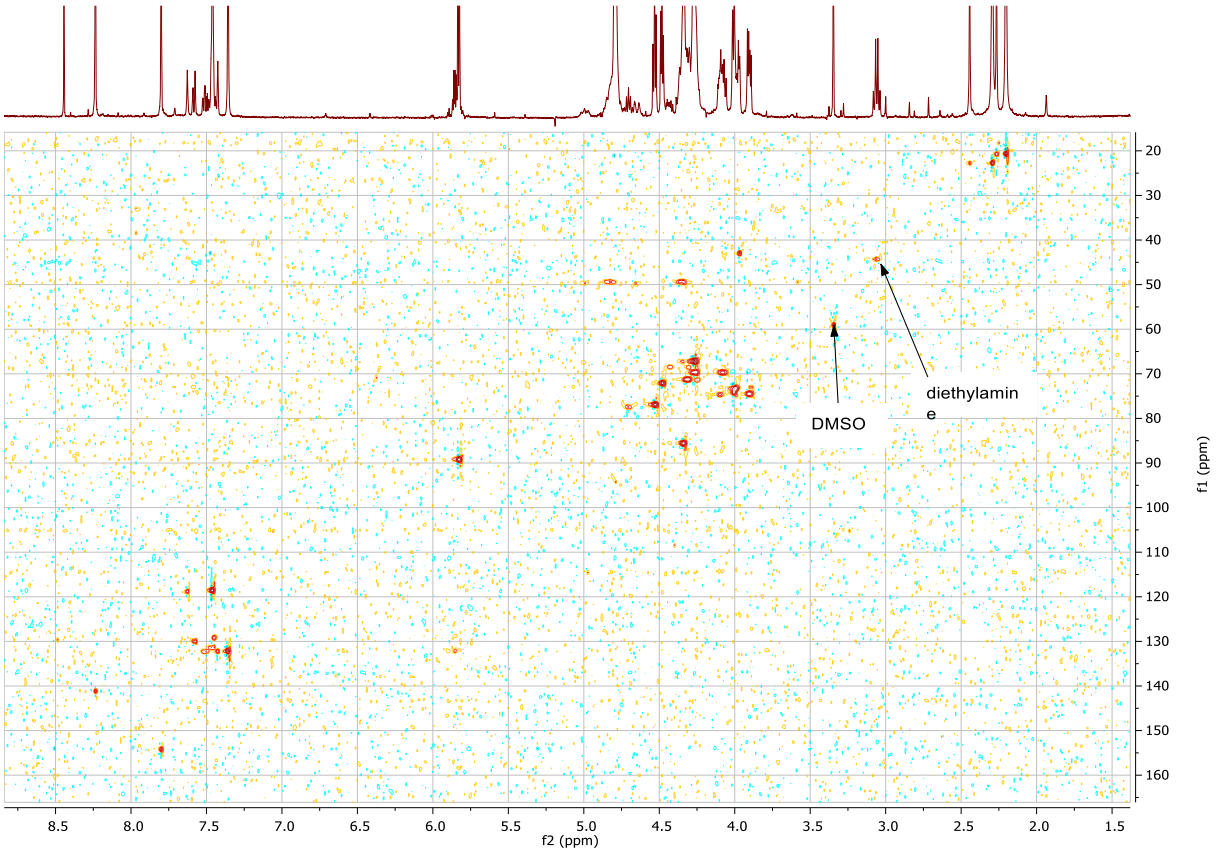
DMSO
diethylamin
e
f2 (ppm)
f1 (ppm)

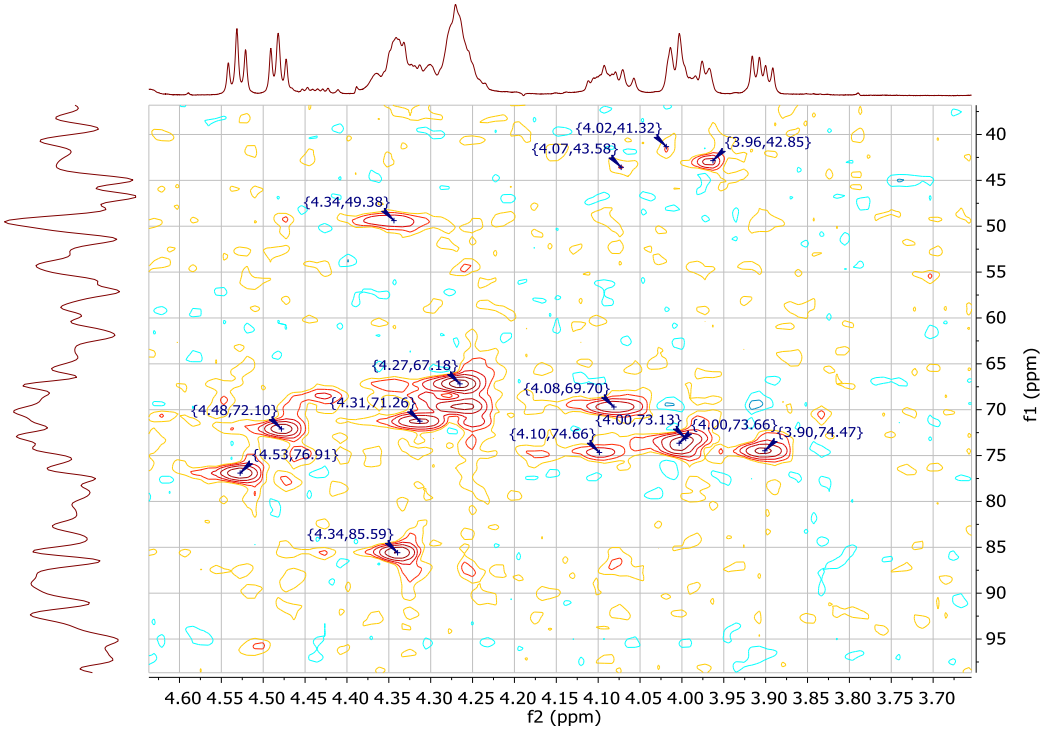
{4.02,41.32}
{4.07,43.58}
{3.96,42.85}
{4.34,49.38}
{4.27,67.18}
{4.08,69.70}
{4.31,71.26}
{4.48,72.10}
{4.00,73.13}
{4.00,73.66}
{3.90,74.47}
{4.10,74.66}
{4.53,76.91}
{4.34,85.59}
f2 (ppm)
f1 (ppm)

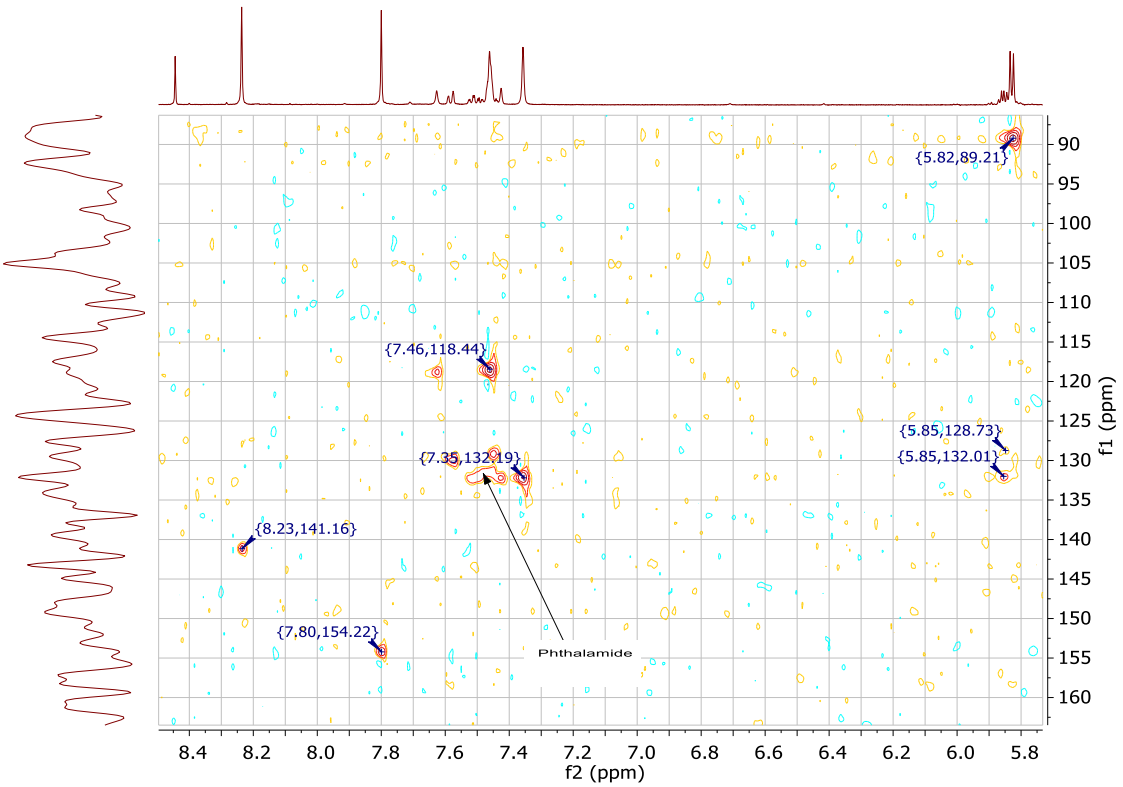

Fig. S10 HSQC spectrum of compound 7

IR spectra

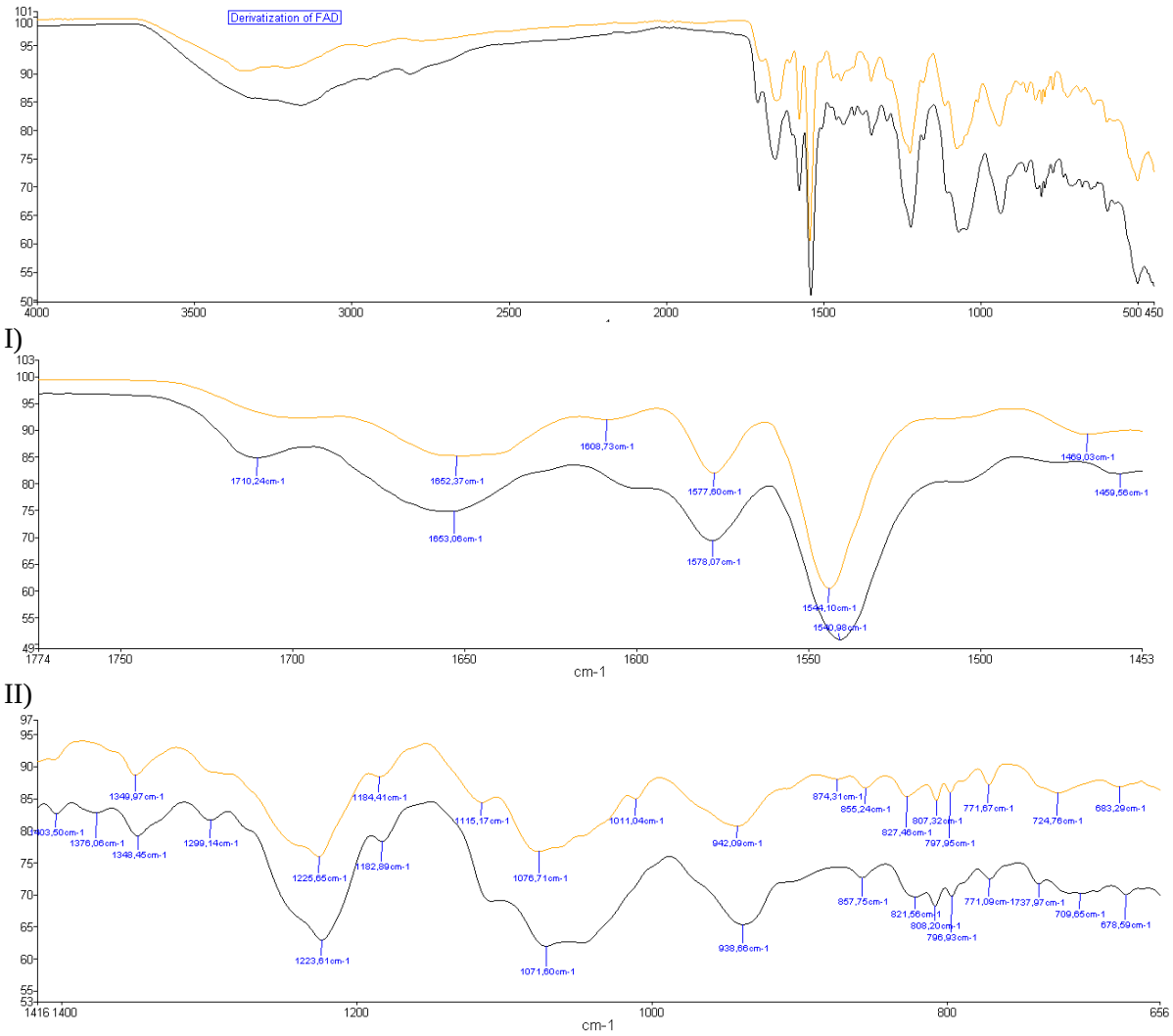

Fig. S11*. IR spectra of solid compounds. Yellow – FAD, Black – compound* ***3****. Spectra I show full range comparison. Spectra II and III are zoomed for primary amine specific regions.*

5.2 Analytical data collected during optimization of adenosine alkylation

Adenosine N^1 substitution detection with NMR

All the spectra were collected in MeOD. Chemical shifts were adjusted to the water peak (4.78 in methanol) as it had very high intensity in each sample. The coupling constants *J*(1'-2') for analyzed doublets assigned to position 1 and N^6 analogues are in agreement with the literature data (van der Plas, Henk C. Bückmann and Wray, 1995).

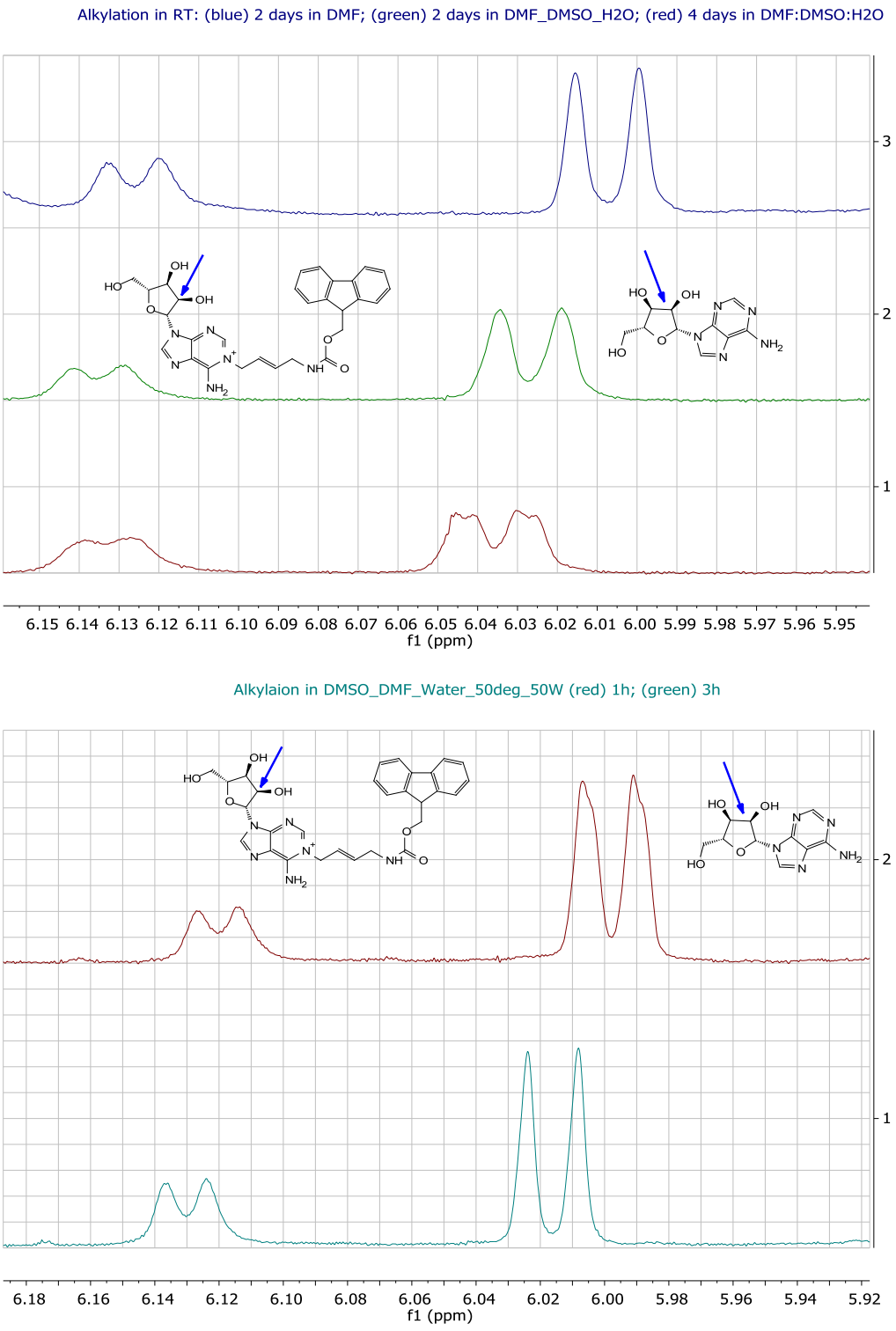

Fig. S12. *^{1}H NMR (400 MHz, spectrum was collected in methanol-d_4 (reaction in DMF), or D_2O. The typical J values for peak around 6.1 ppm was 5 Hz, and for peak 6.0 ppm 6 Hz.Upper spectra show alkylation at room temperature, lower spectrum shows alkylation upon microwave irradiation (50 W)*

5.3 Preparation of FAD-functionalized Sepharose and immobilization of phenylacetone monooxygenase (PAMO)

Aliquots of 60 µl of Sepharose were washed three times with distilled water and incubated with 2 mL of around 10 mM of compound **7**, FAD or MQ water at 4°C, overnight. All but the latter sample turned yellow and retained this color upon washing with ethyl acetate, saturated NaCl solution and aquatic solutions at pH 7, 4 and 8. Subsequently, 5% diethylamine in 1.5 M KPi buffer pH 8 was used for the final wash and blocking of remaining active groups at the agarose. In contrast to sample incubated with **7**, the material incubated with FAD, almost completely lost its yellow color after the final wash with diethylamine. Subsequently, the materials were equilibrated with 50 mM Tris pH 8 and incubated with apo PAMO prepared as reported previously (Krzek *et al.*, 2016). To remove remaining apo PAMO, material was washed with buffer three times by spinning down and resuspension. To test enzyme activity, the resulting material was incubated with phenylacetone as it has been described before (Krzek *et al.*, 2016). Two time point samples were analyzed by GC-MS, after 7 hours of conversion.

References

Al-Shuhaib, Z. et al., 2013. Intramolecular palladium mediated π-allyl cyclisation of bis-Cbz- and bis-Boc-protected guanidines. Tetrahedron Letters, 54(49), pp.6716–6718.

El Ashry, E.S.H. et al., 2010. Chapter 5 - Recent advances in the Dimroth rearrangement: a valuable tool for the synthesis of heterocycles. In Advances in Heterocyclic Chemistry. pp. 161–228.

van Berkel, W.J.H., Kamerbeek, N.M. & Fraaije, M.W., 2006. Flavoprotein monooxygenases, a diverse class of oxidative biocatalysts. Journal of Biotechnology, 124(4), pp.670–689.

Bückmann, A.F., 1995. Method for preparing N6 -substituted NAD, NADP or FAD.

Bückmann, A.F., Wray, V. & Stocker, A., 1997. Synthesis of N6-(2-aminoethyl)-FAD, N6-(6-carboxyhexyl)-FAD, and related compounds. Methods Enzymol, 280(1991), pp.360–374.

Buter, J. et al., 2016. Stereoselective synthesis of 1-tuberculosinyl adenosine; a virulence factor of *Mycobacterium tuberculosis*. The Journal of Organic Chemistry, 81(15), pp.6686–6696.

Corey, E.J.. & Kim, C.U.., 1972. A method for selective conversion of allylic and benzylic alcohols to halides under neutral conditions. Tetrahedron Letters, 13(42), pp.4339–4342.

Fields, G.B., 1995. Methods for removing the Fmoc group. In M. W. Pennington & B. M. Dunn, eds. Peptide Synthesis Protocols. Totowa, NJ: Humana Press, pp. 17–27.

Halada, P. et al., 2003. Identification of the covalent flavin adenine dinucleotide-binding region in pyranose 2-oxidase from *Trametes multicolor*. Analytical Biochemistry, 314(2), pp.235–242.

Hefti, M.H., Vervoort, J. & Van Berkel, W.J.H., 2003. Deflavination and reconstitution of flavoproteins: Tackling fold and function. European Journal of Biochemistry, 270(21), pp.4227–4242.

Krzek, M. et al., 2016. Covalent immobilization of a flavoprotein monooxygenase via its flavin cofactor. Enzyme and Microbial Technology, 82, pp.138–143.

Marsault, E. et al., 2006. Discovery of a new class of macrocyclic antagonists to the human motilin receptor. Journal of Medicinal Chemistry, 49(24), pp.7190–7197.

Morris, D.L. & Buckler, R.T., 1983. Colorimetric immunoassays using flavin adenine dinucleotide as label. Methods in enzymology, 92(1976), pp.413–25.

Nishina, Y. et al., 2003. Molecular mechanism of the drop in the pKa of a substrate analog bound to medium-chain acyl-CoA dehydrogenase: implications for substrate activation. Journal of Biochemistry, 134(6), pp.835–842.

Oslovskya, V.E.., Drenicheva., M.S. & Mikhailova, S.N., 2015. Regioselective 1-N-Alkylation and Rearrangement of Adenosine Derivatives. Nucleosides, Nucleotides and Nucleic Acids, 34(7), pp.475–499.

van der Plas, Henk C. Bückmann, A.F. & Wray, V., 1995. Simultaneous conversion of N-(1)-(2-aminoethyl)-adenosine to N6-(2-aminoethyl)-adenosine and tricyclic 1,N6-ethanoadenosine under mild aqueous conditions. Heterocycles, 41, pp.1399–1419.

Posthuma-Trumpie, G.A. et al., 2007. Reconstitution of apoglucose oxidase with FAD conjugates for biosensoring of progesterone. Biochimica et Biophysica Acta - Proteins and Proteomics, 1774(7), pp.803–812.

Riklin, A. et al., 1995. Improving enzyme-electrode contacts by redox modification of cofactors. Nature, 376(6542), pp.672–675.

Roth, J.P. et al., 2004. Oxygen isotope effects on electron transfer to O_2 probed using chemically modified flavins bound to glucose oxidase. Journal of the American Chemical Society, 126, pp.15120–15131.

Sen, S.E. & Roach, S.L., 1995. A convenient two-step procedure for the synthesis of substituted allylic amines from allylic alcohols. Synthesis, 7, pp.756–758.

Stocker, A., Hecht, H.J. & Bückmann, A.F., 1996. Synthesis, characterization and preliminary crystallographic data of N6-(6-carbamoylhexyl)-FAD-D-amino-acid oxidase from pig kidney, a semi-synthetic oxidase. The FEBS Journal, 238(2), pp.519–528.

Torres Pazmiño, D.E., Dudek, H.M. & Fraaije, M.W., 2010. Baeyer-Villiger monooxygenases: recent advances and future challenges. Current Opinion in Chemical Biology, 14(2), pp.138–144.

Wingard, L.B., 1984. Cofactor modified electrodes. Trends in Analytical Chemistry, 3(9), pp.235–238.

Zappelli, P. et al., 1978. Carboxylic and polyethyleneimine-bound FAD derivatives. Synthesis, coenzymic properties, conformational and enzyme-coenzyme interaction studies. FEBS Journal, 89(2), pp.491–499.

CHAPTER 4

REVIEW ON HUMAN FMO3: TOPOLOGY AND RECOMBINANT PRODUCTION IN *ESCHERICHIA COLI*

Marzena Krzek, Marco W. Fraaije

Molecular Enzymology Group, University of Groningen, Nijenborgh 4, 9747 AG Groningen, The Netherlands

ABSTRACT

Human flavin-containing monooxygenase isoform 3 (hFMO3) is a microsomal enzyme that plays an important role in human oxidative metabolism. It converts xenobiotics containing heteroatoms (e.g. S or N atoms) into easy to secrete oxides. The efficient production of the human enzyme in a recombinant manner is desirable as it could be used for the preparation of hFMO3-related metabolites. It would also enable in-depth biochemical studies, contributing to improved insights into human metabolism and diseases related to malfunctioning of hFMO3. Nevertheless, it has been proven to be extremely difficult to produce and isolate recombinantly expressed hFMO3. As a result, many molecular aspects concerning hFMO3, such as its structure, remain unknown.

This chapter reviews previous studies that focused on obtaining soluble expression of functionally active hFMO3 in *Escherichia coli*. Also the current status of knowledge about the sequence and structural properties of hFMO3 is discussed. Our bioinformatic analysis has revealed two new sequence features. Multiple sequence alignment analysis and inspection of structures of sequence related enzymes suggest that a specific region in hFMO3 (residues 232-250) may form an additional membrane association region besides the hydrophobic C-terminus. Also a new FMO-specific sequence fingerprint was identified: (A/F)a(I/V)Gxxb (a: hydrophobic; b: charged). The respective residues are predicted to be crucial for interactions with the FAD and NADPH cofactors.

The experimental part of this chapter presents the work performed on trying to express hFMO3 as a C-terminally truncated form and/or fused to phosphite dehydrogenase (PTDH). The tested expression conditions did not result in successful overexpression and isolation of soluble hFMO3 variants, again confirming the resilience of this human enzymes towards heterologous expression and subsequent purification. A previously reported approach of functional overexpression of soluble hFMO3 by a specific C-terminal truncation could not be reproduced. Nevertheless, we could show that PTDH-hFMO3 can be expressed in a functional form in a bacterial host.

1. INTRODUCTION

Human flavin-containing monooxygenases (hFMOs, EC 1.14.13.8) are membrane-associated, O_2 and NADPH-dependent, and FAD-containing enzymes encoded by five different genes (Cashman and Zhang 2006). Each of these genes encodes a different FMO isoform, and they share 52-58 % sequence identity between each other (Table 1) (Cashman *et al.*, 1995). Human FMOs are responsible for 10 % of the oxidative, phase I metabolism. The remaining 90 % is catalysed by so-called P450 monooxygenases, which are heme-containing enzymes (Krueger and Williams, 2005). While both monooxygenase families share some catalytic properties (e.g. dependence on NAD[P]H), hFMOs differ from P450 monooxygenases in many ways. For example, they employ a different catalytic

mechanism, can catalyse different reactions, show no significant sequence homology and use different prosthetic groups. Human FMOs catalyse substrate oxygenations via formation of a stable peroxyflavin intermediate, ready to react with a suitable substrate as soon as it enters the active site. The reactive peroxyflavin enzyme intermediate is formed before any substrate is bound to the enzyme. Therefore, formation of this enzyme intermediate seems unregulated and therefore FMOs are often described as "loaded guns" (Eswaramoorthy *et al.*, 2006; Orru *et al.*, 2010). This catalytic strategy has been observed for mammalian FMOs, microbial FMOs, and other sequence-related flavoprotein monooxygenases. The activities of the human FMO and P450 monooxygenase families are usually described as complementary. Human P450 monooxygenases typically perform hydroxylations, demethylations and aminations which supplements the catalytic repertoire of hFMOs. Yet, there is also a large degree of catalytic overlap as various compounds have been found to be targeted by both P450 monooxygenases and hFMOs (Cashman *et al.*, 1995; Krueger and Williams, 2005).

Metabolites generated by hFMOs have significantly increased polarity versus the original drugs, which allows for their rapid excretion from the human body. Most of the research efforts related to hFMOs have focussed on the isoform 3 (hFMO3), which is predominantly expressed in human liver (Cashman and Zhang, 2006). hFMO3 is active toward drugs of huge medical importance. Examples are albendazole (anti-parasite agent), cimetidine (anti-ulcer agent) or recently developed anticancer drugs with a kinase inhibition activity (Ballard, Prueksaritanont and Tang, 2007). Mutations in the hFMO3-encoding gene that lead to inactive or poorly active enzyme result in trimethylaminuria, also called "fish odor syndrome" (Yamazaki *et al.*, 2007). There are numerous mutations known that cause this metabolic disorder which result in the accumulation of trimethylamine leading to a strong and unpleasant body odor. Human FMO3 has been described as a labile enzyme, with relatively low activity (Krueger and Williams, 2005). Even though the monooxygenase is rather inefficient as isolated enzyme, its high regio-, chemo- and enantioselectivity is difficult to be replaced with chemical synthesis. In fact, it is a challenge to generate hFMO3-related metabolites using alternative (bio)catalysts (Gul *et al.*, 2016). Up to now, several systems for generating hFMO3-dependent metabolites have been used. One way is the use of liver tissue or isolated microsomal fractions (Störmer, Roots and Brockmöller, 2000). This approach is rather expensive, due to limited accessibility of the material, its high lability and low activity. Additionally, hFMO3-catalyzed metabolism with such preparations requires inhibition of alternative metabolic enzymes, such as P450 monooxygenases. Alternatively, one can use recombinantly produced hFMO3. It has been shown that hFMO3 can be produced by exploiting the Baculovirus expression system. The microsomes prepared from such recombinant insect cells were very useful to perform drug conversions. While hFMOs in insect microsomal fractions are commercially available, in-house preparation of Baculovirus membranes reduces costs and such preparations yield expression of the enzyme in the range of nanograms per milligram of material (Haining *et al.*, 1997). However, it is still an expensive approach

due to laborious procedures, low yield, and costly materials (media components and fermenters). Therefore, for larger scale production of hFMO3-related metabolites, Baculovirus expression of the membrane-associated enzyme is not a convenient solution.

Altogether, producing hFMO3 in an efficient manner still remains challenging. While eukaryotic expression has been shown to be successful in producing the enzyme, the amounts and stability of the generated enzyme samples are far from ideal. In recent years, attempts of using bacterial expression for generating easy-to-use hFMO3 or other hFMOs have been reported. Ideally, these approaches result in the production of a soluble enzyme, free from surfactants, which allows for flexibility in buffer composition and opens new avenues for more advanced applications. Based on the observation that hFMO3 and its isoforms have a highly hydrophobic C-terminus, it has been suggested that expression of soluble hFMO3 requires truncation of this part of the protein. Alternatively, fusion constructs with highly soluble fusion protein partners have been explored (Brunelle *et al.*, 1997; Hanlon *et al.*, 2012). Yet, these approaches would benefit from insight into the structural features of hFMO3: what part of the protein determines its membrane association behaviour? This chapter provides a thorough analysis of the hFMO3 sequence and reports on our attempts on expressing functional hFMO3 in *E. coli*.

1. Bioinformatic analysis of hFMO3

Sequence homology

hFMO3 is highly preserved among mammals reaching 80-95% of sequence identity. At the same time, the sequence similarity with the other four human FMO isoforms is significantly lower (Table 1). Currently, no crystal structure is available for any hFMO or mammalian FMO. The closest FMO homologue for which the crystal structure has been elucidated shares only 29% of sequence identity with hFMO3 and comes from a marine bacterium: *Methylophaga sp*. (Table 2) (Alfieri *et al.*, 2008; Orru *et al.*, 2010). This enzyme has been shown to exhibit similar oxygenating activities when compared with hFMOs. It is capable of performing S- and N-oxygenations, and was found to be able to produce indigo blue from indole (Rioz-martínez *et al.*, 2011). Also, other sequence-related microbial flavoprotein monooxygenases have been shown to exhibit similar oxygenation activities. Recently, we have shown that such enzymes can be used as hFMO mimics for the generation of FMO-generated drug metabolites (Gul *et al.*, 2016). An overview of some flavoprotein monooxygenases with similar activity to hFMO3 is presented in Table 2. Such microbial FMOs can be attractive alternative biocatalysts to mimic hFMOs as they are often easy to be produced recombinantly, and for several of these monooxygenases the crystal structure has been elucidated. The latter would enable enzyme engineering approaches to tune the respective FMO. Yet, the microbial enzymes are clearly different from the mammalian FMOs. Except for a moderate to poor sequence similarity, they exhibit

different catalytic efficiencies and substrate specificities. Therefore, an effective recombinant hFMO3 production strategy is still highly desired.

Table 1. *Sequence homology and recombinant expression of hFMO3 and some other mammalian FMOs.*

FMO	Organism	Uniprot entry	Seq. id. with hFMO3 [%]	Remarks: 1. Expression as fusion protein 2. Reported truncations
hFMO1	*Homo sapiens*	Q01740	54	No data
hFMO2	*Homo sapiens*	Q99518	58	2a. Truncation of 64 aa at the C-terminus results in inactive protein (Dolphin *et al.*, 1992, 1998) 2b. Truncation up to 45 residues did not result in cytosolic expression, but activity was retained (Geier *et al.*, 2015)
hFMO3	*Homo sapiens*	P31513	100	1. hFMO3 with N-terminal MBP purified using Triton-X100 (Brunelle *et al.*, 1997; Lattard *et al.*, 2003; Cashman and Lomri, 2004) 2a. 17 aa truncated hFMO3 was reported to give the same cellular localization as the wild type and resulted in inactive enzyme (Yamazaki *et al.*, 2007; Shimizu, Kobayashi and Yamazaki, 2012) 2b. P510Stop truncation yielded inactive enzyme (Yamazaki *et al.*, 2007; Shimizu, Kobayashi and Yamazaki, 2012) 2c. His tags at C- and N-terminus with C-terminal 17 aa truncation was reported to be expressed as cytosolic protein (Catucci *et al.*, 2012) 2d. Truncation of 17 aa at C-terminus retained enzyme activity in whole cells, but did not relocate protein into soluble fraction. Fusing PTDH to the N-terminus gives the same result (this thesis)
hFMO4	*Homo sapiens*	P31512	52	No data
hFMO5	*Homo sapiens*	P49326	54	1a. Expression with His-SUMO tag at N-terminus: the enzyme could be purified using Triton X-100, and the tag could be removed (Fiorentini *et al.*, 2016) 1b. Active hFMO5 was obtained using *E. coli* JM 109 (White and Atta-asafo-adjei, 2011)
FMO2	*Oryctolagus cuniculus*	P17635	58	2a. Truncation of 26 aa at C-terminus did not result expression of soluble protein in Baculovirus, but increased cytosolic fraction upon addition of high salt (Krueger *et al.*, 2006) 2b. Truncation of 26 aa at C-terminus did not change the subcellular localization (Lawton and Philpot, 1993)
FMO2	*Rhesus macaque*	Q28505	57	2. 64 aa truncation did not change subcellular distribution (Krueger *et al.*, 2001)

***Table 2**. Some microbial flavin-containing monooxygenases and their similarity with hFMO3.*

Mono-oxygenase	Organism	PDB entry	Identity with hFMO3 [%]	Activity	Literature
PAMO	*Thermobifida fusca*	1W4X	15	Baeyer-Villiger oxidations, N-and S-oxygenations	de Gonzalo et al. 2005
FMO	*Schizosaccharo-myces pombe*	1VQW	25	N-oxygenations	Eswaramoorthy et al. 2006
FMO	*Methylophaga* sp.	2VQ7	29	N-oxygenations	Orru et al. 2010
CHMO	*Acinetobacter sp.*	-	17	N-oxygenation of nicotine, S-oxygen-ation of albendazole	Gul et al. 2016
$BVMO_{Mt1}$	*Myceliophthora thermophila*	-	14	N-oxygenation of lidocaine, enantio-selective S-oxygen-ation of albendazole	Gul et al. 2016
$BVMO_{Rj24}$	*Rhodococcus jostii*	-	16	N-oxygenation of lidocaine	Gul et al. 2016
FMO	*Saccharomyces cerevisiae*	-	27	S-oxygenations	Zhang and Robertus 2002
FMO	*Pseudomonas stutzeri*	-	22	Enantioselective S-oxygenations	Jensen et al. 2014

SEQUENCE MOTIFS

Although no protein structure is available for hFMOs, a thorough sequence analysis may provide clues concerning the structural organisation of these enzymes. For our analysis, we focused on the hFMO3 protein sequence (Uniprot entry P31513) which entails 532 amino acids. The predicted protein mass is 60,033 Da (without its FAD cofactor bound) and the predicted pI is 7.9. For mammalian FMOs, multiple sites of phosphorylation have been suggested. In fact, the PhosNet server, which detects possible phosphorylation sites in eukaryotic proteins, suggests around 80 of them in hFMO3 (www.phosphosite.org). Nevertheless, for hFMO3 only a few sites have been experimentally confirmed. The strongest evidence for a phosphorylation site is at Tyr90. Also Ser159 and the C-terminal Thr532 have been found to be phosphorylated. The NetNGlyc server predicts only one putative glycosylation site for hFMO3: Asn61 (www.cbs.dtu.dk/services/NetNGlyc). This residue was found to be highly conserved within eukaryotic FMOs and is crucial for catalysis (Koukouritaki *et al.*, 2007). Based on studies on enzymes mutated at this position and inspection of the structures of related monooxygenases, one can conclude that Asn61 is part of the active site of hFMOs and is not a candidate for glycosylation. In fact, posttranslational modifications do not seem to be required for hFMO3 enzyme activity. One piece of evidence comes from our own work and work by other groups (Geier et al. 2015; Hanlon et al. 2012b) showing that active hFMO3 can be produced in *E. coli* (vide

infra). Additionally, when expressed in Baculovirus, glycosylation of hFMO3 was excluded based on mass spectroscopy analysis of the recombinant protein (Haining *et al.*, 1997).

Table 3. *Sequence features of hFMO3 – occurrence of conserved residues, motifs and regions. The PRINTS database was used for identification of the majority of the motifs(Attwood et al. 2012). The occurrence of sequence motifs in FMOs has also been reviewed by Krueger and Williams (2005).*

Residues	**Sequence characteristic**	**Comments**	**Source**
1-20	Highly hydrophobic, sometimes suggested to contain a signal sequence	Highly conserved in all species, gives negative result using the tested signal peptide recognition tools	www.csbio.sjtu.edu.cn www.cbs.dtu.dk/services/SignalP-4.1
9-14	GXGXXG Rossmann fold sequence motif	Part or the FAD binding domain	(Krueger and Williams, 2005)
60 (Ser)	Conserved residue	Conserved in FMOs, predicted to be part of the active site	(White and Atta-asafo-adjei, 2011)
61 (Asn)	Conserved residue	Conserved in FMOs, predicted to have a catalytic role, point mutations cause loss of activity for all substrates	(Lomri, Gu and Cashman, 1995)
66-78	Low complexity	Highly conserved, mutation of M66 leads to loss of FAD	pfam.xfam.org (Treacy *et al.*, 1998)
150-157	VMVSGHH	Highly conserved in mammalian FMOs, predicted to be linking NADPH and FAD binding domains	(Lomri, Gu and Cashman, 1995)
165-171	FXGXXXHXXXYK	Preserved in FMOs and described as contributing to the NADPH binding A very similar motif is present in BVMOs	(Fraaije *et al.*, 2002; Krueger and Williams, 2005)
191 - 196	GXGXXG Rossman fold sequence motif	Part or the NADPH binding domain	(Lomri, Gu and Cashman, 1995)
327 - 331	FATGY	Part of the NADPH binding domain	(Fraaije *et al.*, 2002; Krueger and Williams, 2005)
364 - 373	(A/F)**a**(I/V)Gxx**b**; a – hydrophobic residue b – polar residue	Conserved within all mammalian and bacterial FMOs. Potentially involved in interactions with both cofactors	Vide infra

Table 3 shows an overview of sequence motifs that can be found in the hFMO3 sequence. Their specific locations are also marked in the sequence alignment (Figure 1). Several canonical flavoenzyme sequence motifs, like Rossmann fold sequence motifs, are fully preserved in hFMO3. Besides that, some FMO-specific motifs could be identified. For example, the FxGxxxHxxxYK motif is also present. This motif is highly specific for FMOs, and can be used for identification of FMO sequences in predicted proteomes and discrimination of FMOs from other sequence-related

flavoprotein monooxygenases (Riebel, de Gonzalo and Fraaije, 2013). When inspecting the multiple sequence alignment we also observed strong conservation for all FMOs in the 360-380 region of hFMO3. Interestingly, the conservation in this region is not present in BVMOs. The highest conservation concentrates on a few residues, based on which a motif can be defined as (A/F)**a**(I/V)Gxx**b**, where **a** represents a hydrophobic residue, and **b** is a polar residue. From the sequence alone it is impossible to deduce the molecular basis for the observed conservation. The motif was not noticed before, and to verify its role, it would be interesting to study the effect of mutating one or more of the conserved residues. In the next paragraph the possible structural role of the motif is discussed.

As mentioned before, no crystal structure is available neither for hFMO3 nor any other mammalian FMO. When looking for proteins homologous to hFMO3 in the PDB database, the best hit is a bacterial FMO. This protein shares 29% identity with hFMO3 and comes from the marine bacterium *Methylophaga sp*. The respective bacterium was isolated from sea and the FMO is supposed to facilitate catabolism of amines. Several crystal structures of this enzyme complexed with both cofactors, FAD and $NADP^+$, have been elucidated (*i.e.* PDB entry 2XLP (Orru *et al.*, 2010)). These structures provide insight into the architecture of this specific enzyme but also of the sequence-related mammalian FMOs, including hFMO3. For example, many hFMO3 mutations known to cause trimethylaminuria can now be located in the bacterial FMO structure (Orru *et al.*, 2010). The roles of some of these residues in catalysis and/or structural integrity could be inferred from the structure. For example, it provided clear evidence for an important role in catalysis for Asn61 as it is located next to the reactive part of the flavin cofactor and the bound $NADP^+$ cofactor. Apart from that, the newly identified motif (A/F)**a**(I/V)Gxx**b** is present in the bacterial FMO as FYIGxxD and is part of the binding pocket around the pyrophosphate moiety of the FAD cofactor while the aspartate (Asp322) is close to the bound $NADP^+$ cofactor (Figure 2). In fact, it is within H-bond distance from the 3-OH of the ribose moiety of the bound $NADP^+$. This is a strong indication that it is involved in proper binding of NADPH, and assures efficient reduction of the FAD cofactor. A multiple sequence alignment of bacterial and mammalian FMOs (116 sequences, data not shown) revealed that this specific residues is highly conserved, and mostly an Asp or Gln. Both amino acids can form hydrogen bounds suggesting a conserved role. Interestingly, in mammalian FMOs a dependency between the type of residue **b** and substrate specificity is observed. Asp and Gln are present in most hFMOs (hFMO2, hFMO3, and hFMO5) which are active on various amines. At the same time hFMO1, with Lys as residue **b**, oxidises primarily tertiary amines (Cashman, 2000) and for hFMO4, with a Gly as **b,** no clear substrate have been identified (Krueger and Williams, 2005). It would be interesting to verify whether this correlation is true by enzyme engineering studies. Very recently, a similar suggestion regarding an important role of this residue in a newly described bacterial FMO marine was suggested, based on its elucidated crystal structure (Li *et al.*, 2017). Again, the corresponding aspartate in the crystal structure

of this FMO from *Roseovarius nubinhibens* interacts with the bound $NADP^+$. The latter enzyme shares 65% sequence identity with the FMO from *Methylophaga* and 20% with hFMO3. Overall, the newly discovered motif [(A/F)a(I/V)Gxxb] reflects an important structural element of FMOs from both, bacteria and animals.

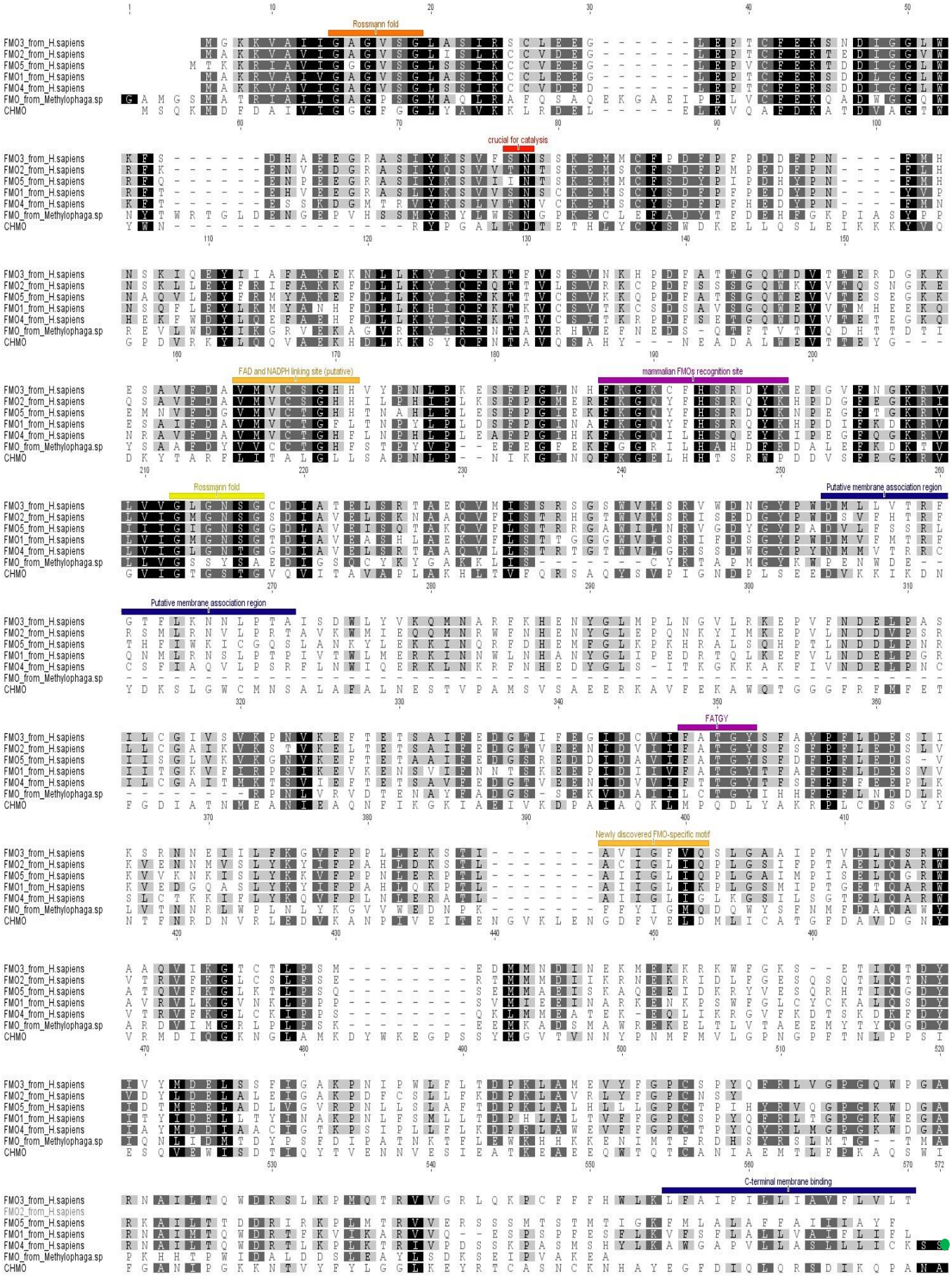
Rossmann fold
crucial for catalysis
FAD and NADPH linking site (putative)
mammalian FMOs recognition site
Rossmann fold
Putative membrane association region
Putative membrane association region
FATGY
Newly discovered FMO-specific motif
C-terminal membrane binding
FMO3_from_H.sapiens
FMO2_from_H.sapiens
FMO5_from_H.sapiens
FMO1_from_H.sapiens
FMO4_from_H.sapiens
FMO_from_Methylophaga.sp
CHMO

***Figure 1**. Multiple sequence alignment of all hFMOs, FMO form Methylophaga sp. and a Baeyer-Villiger monooxygenase (cyclohexanone monooxygenase from Acinetobacter sp., CHMO). Conserved residues and motifs are indicated in color. The putative membrane-association regions are also marked (dark blue). The catalytic residues S60 and N61 are highlighted in red. The green dot behind the hFMO4 sequence indicates removal of 24 amino acids form the alignment.*

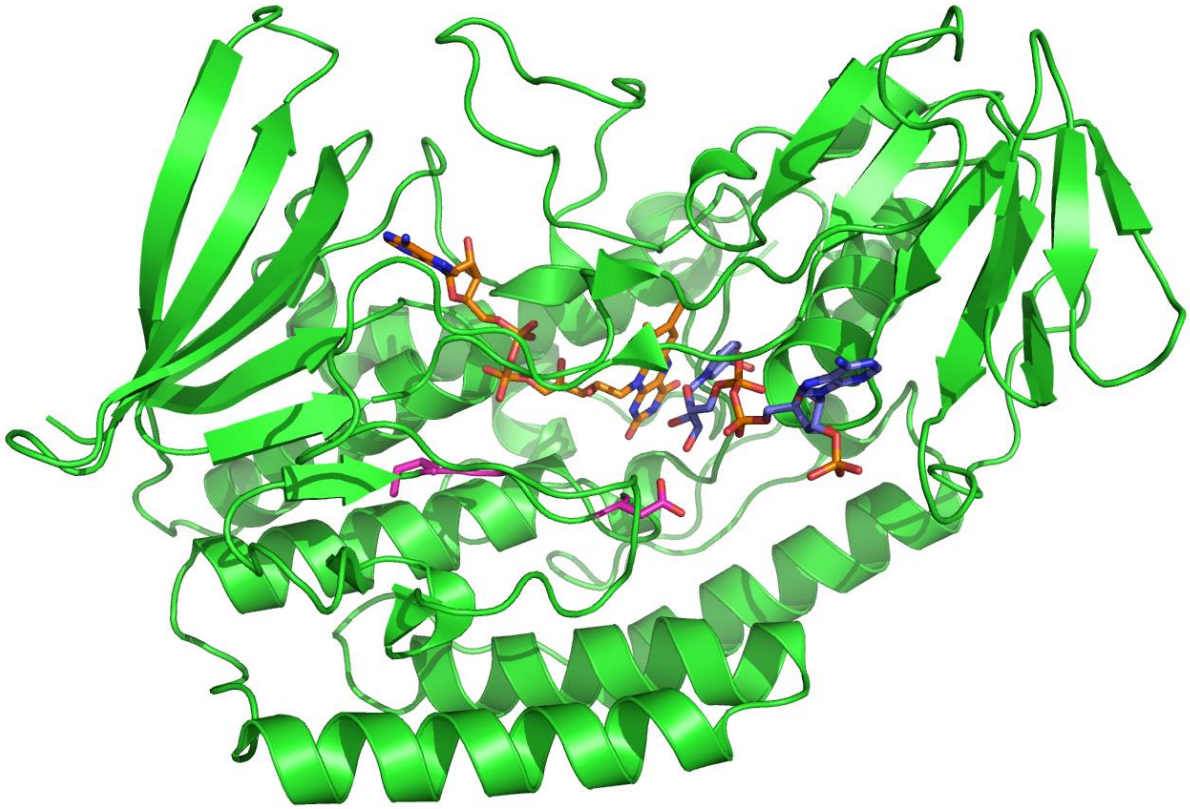

***Figure 2.** Crystal structure of the bacterial FMO from Methylophaga (PDB:2XLP). The cofactors are in sticks: FAD on the left and NADP$^+$ on the right. The conserved residues in the new (A/F)a(I/V)Gxxb motif are highlighted in magenta (IG on the left, D on the right).*

PREDICTING MEMBRANE ASSOCIATION REGIONS

hFMO3 is as microsomal, membrane-associated enzyme. However, the exact molecular basis for the interaction with the lipid bilayer it is not completely clear till now. The C-terminus of hFMOs typically contain a relatively large number of hydrophobic amino acids and is often described as a membrane anchoring domain (Krueger *et al.*, 2006). However, while highly identical to hFMO3, hFMO2 is shorter and lacks a hydrophobic C terminus while it is membrane associated (Geier *et al.*, 2015). It has also been demonstrated that the C-terminus may not be the only membrane association segment in mammalian FMOs (Cashman and Lomri, 2004; Krueger *et al.*, 2006). For rabbit FMO2, membrane association has been found to be based on more complex interactions (Krueger et al. 2006).

Table 4. *Membrane binding regions in hFMO3 predicted by computational tools. The TOPCONS server combines the outcome of several tools (indicated in grey) to generate a consensus prediction.*

Algorithm	**Putative membrane associated regions**	**Source**
TMHMM v2.0	509-531 (E)	www.cbs.dtu.dk/services/TMHMM
HMMTOP	321-338 (C); 365-382 (D); 524-531 (E)	www.enzim.hu/hmmtop (Tusnády and Simon, 2001)
MPex software	232-250 (B); 325-343 (C); 362-370 (D); 510-530 (E)	blanco.biomol.uci.edu/mpex
OCTOPUS	315-335 (C); 360-380 (D); 511-531 (E)	topcons.cbr.su.se (Viklund and Elofsson, 2008)
SCAMPI	2-22 (A); 364-384 (D); 510-530 (E)	topcons.cbr.su.se (Bernsel *et al.*, 2008)
Philius	1-21 (A) signal peptide 510-531 (E)	topcons.cbr.su.se (Reynolds *et al.*, 2008)
Polyphobious	1-21 (A) signal peptide 513-531 (E)	topcons.cbr.su.se (Käll, Krogh and Sonnhammer, 2005)
SPOCTOPUS	1-17 (A) signal peptide 360-380 (D); 511-531 (E)	topcons.cbr.su.se (Viklund et al. 2008)
TOPCONS	1-22 (A) signal peptide 360-380 (D); 511-531 (E)	topcons.cbr.su.se (Tsirigos et al. 2015)

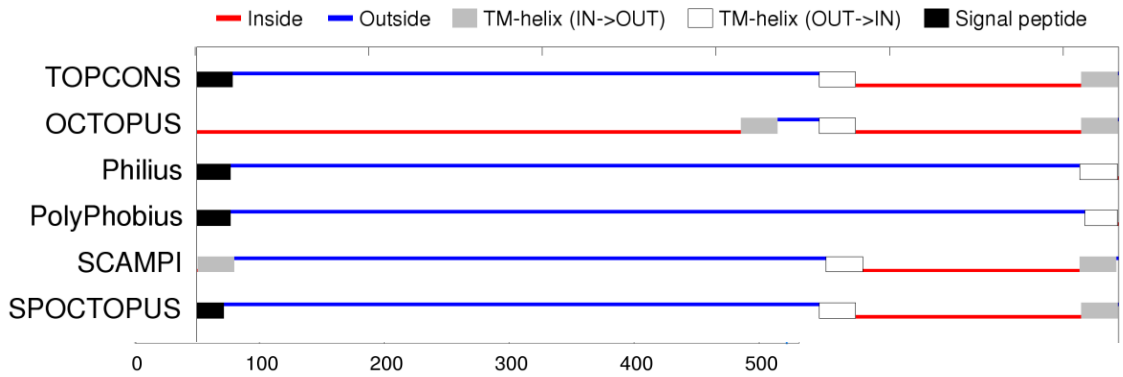

Figure 3*. Output of the TOPCONS server when analyzing hFMO3.*

Using computational tools, we analysed which parts of the hFMO3 sequence are predicted to anchor the enzyme in the membrane. Computational predictions concerning the topology of hFMO3 are shown in Table 4 and Figure 3. In total, 5 regions are indicated as potential transmembrane or signal sequences (Table 4). The suggested function of the 20 N-terminal amino acids as signal peptide can be dismissed because this part of the sequence contains the typifying Rossmann fold sequence motif (GxGxxG) which is always preceded by a short stretch of hydrophobic residues. While this sequence segment displays characteristics of being a signal peptide (hydrophobic residues followed by some small residues), it is clearly part of the FAD binding domain and cannot make extensive interactions with a membrane. Except for the consistent prediction of a C-terminal transmembrane segment, none

of the other predicted transmembrane segments are predicted by all computational protocol. Only one tool (MPex) suggests region 232-250 to represent a transmembrane segment. By inspection of sequence alignments we have found that this part of the sequence is lacking in the sequence of the soluble bacterial and yeast FMOs (alignment not shown). The crystal structures of the bacterial FMOs suggests that this segment can form an excursion from the NADPH-binding domain. Therefore, this part of hFMO3 may indeed interact with a membrane. The segments 321-338 and 365-382 are suggested as candidates for transmembrane segments by some of the computational tools. However, both sequence regions overlap with sequence motifs that were also in Table 3. Based on the analysis of the structures of the bacterial FMOs, it appears that these segments are integral parts of the NADPH binding domain and are unlikely to play a role in the interaction with the membrane. The C-terminal segment 511-531 is consistently predicted to represent a transmembrane segment. This suggests that hFMO3, and most other mammalian FMOs, are anchored to the membrane via their C-terminus.

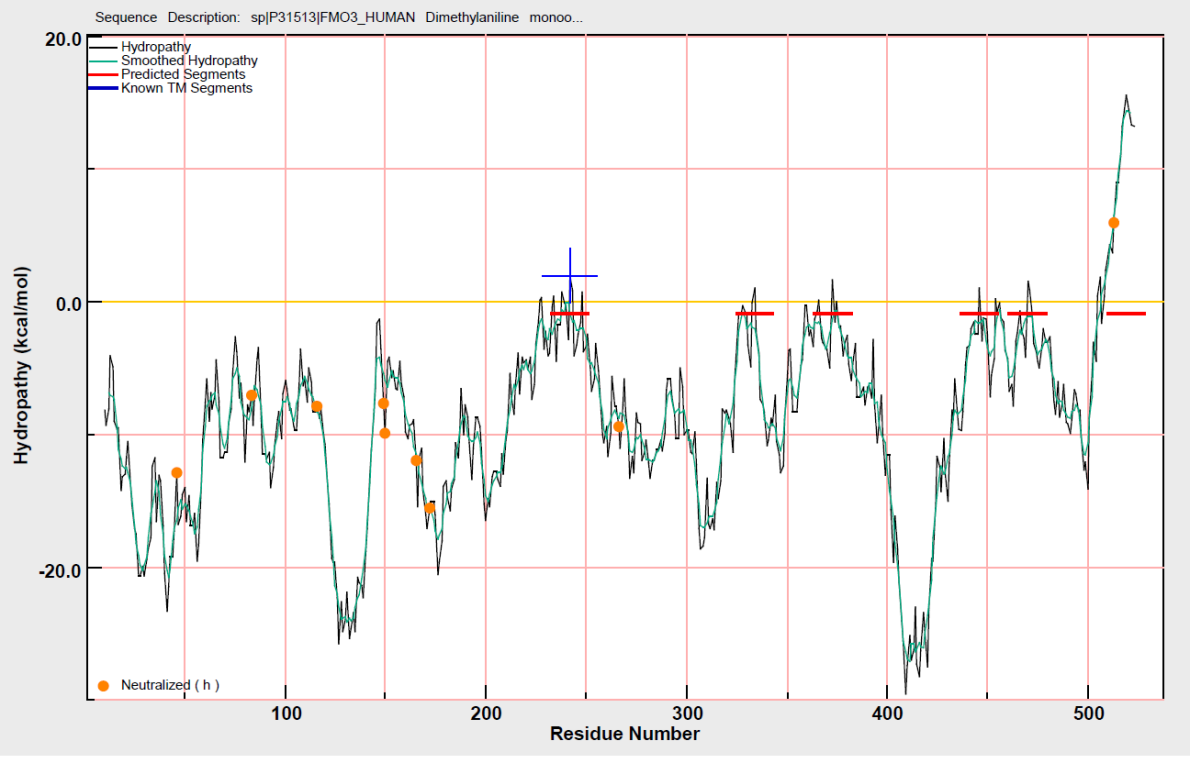

Figure 4. *Hydropathy plot generated by the Membrane Protein Explorer tool using default parameters (Jayasinghe, Hristova and White, 2001). Red lines indicate predicted membrane association segments while the blue cross indicates a segment of interest as discussed in the text (residues 232-250).*

An additional approach to identify sequence segments that may play a role in membrane association, a hydropathy analysis was performed (Figure 4). This approach identified most of the regions mentioned in Table 4. The C-terminus stands out in the hydropathy plot, and, interestingly, also the 232-250

region is again identified as potential membrane association segment. Importantly, the membrane binding part does not need to be based only on hydrophobic regions. A protein might also interact with the membrane through electrostatic attractions. Such interactions were observed for rabbit FMO2 (Krueger *et al.*, 2006). It was shown that a significant solubility increase of rabbit FMO2 can be achieved by using high final salt concentrations.

Concluding, there are strong indications that the C-terminus of hFMO3 plays an important role in the membrane association of the enzyme. Yet, also other parts of the enzyme may play a role in its affinity towards the membrane. The lack of more detailed structural information, for example a crystal structure of a more closely related FMO, hampers accurate predictions on which residues of hFMO3 participate in membrane interactions. We could identify a region (residues 232-250) that may responsible for such interactions. Future mutagenesis studies would reveal whether this part of hFMO3 is indeed involved in the membrane anchoring. Clearly, elucidation of the structure of hFMO3 would solve the above issues.

2. Toward recombinant expression of soluble hFMO3

Previous work

For a better understanding of the enzyme properties of hFMO3 and its use as biocatalyst, it is essential to be able to isolate this enzyme. As isolation from human tissue is cumbersome and inefficient, it is highly attractive to develop a recombinant expression system. The first trials for FMO expression in microbial hosts were reported in the early 90s. Already at that time, the issue of membrane association was addressed by attempts to express a C-terminally truncated mutant (Lawton and Philpot, 1993). Table 1 provides an overview of the reports on hFMO3 expression trials. Various attempts which aimed at producing C-terminally truncated variants failed in obtaining soluble enzyme. It is worth mentioning that Krueger *et al* (Krueger *et al.*, 2006) were able to increase the amount of soluble cytosolic enzyme by a combination of producing a truncated mutant and employing high salt concentration, while using Baculovirus as expression host. A similar experiment resulted in no subcellular relocalization, even when a high salt concentration was used, when yeast or *E. coli* JM 109 was used as expression host (Lawton and Philpot, 1993). This suggests that the successful expression of a significant part of the enzyme as soluble protein may be due to the use of the specific Baculovirus expression system. In 1993 Lomri et al published on the successful cloning of cDNA from human liver in the expression vector pTrc for enzyme production in *E. coli* NM522. This study described that the monooxygenase could be obtained in a soluble fraction when using detergents (Triton X-100 and phosphatidylcholine). Remarkably, activity of the purified enzyme was found to be limited to tertiary amines and no S-oxygenation activity was detected (Lomri, Yang and Cashman, 1993). Recently, another research group reported on the expression of hFMO3 as a cytosolic and active enzyme in *E.*

coli JM109 using the pJL2 vector (Catucci *et al.*, 2012). For this expression construct, the gene had been truncated in such a way that 17 C-terminal amino acids were not part of the recombinant protein. Furthermore, the truncated hFMO3 was decorated with poly-histidine tags at both termini. Interestingly, similar hFMO3 expression experiments reported before failed to result in expression of soluble enzyme. In 2006, cDNA from Japanese patients was used for creating pTrc99A vector-based expression constructs for producing truncated hFMO3 (truncated by 7 or 33 C-terminal amino acids). Using *E. coli* JM109, the recombinant hFMO3 was still membrane associated or insoluble and displayed no more than 10% of the expected activity. In addition, over two decades ago the same host in combination with another expression vector (pKKHC) was employed for the expression of a 26 amino acid C-terminally truncated FMO2 from rabbit (Lawton and Philpot, 1993). This experiment revealed that the engineered monooxygenase also remains attached to the membrane.

The findings discussed above and the data summarized in Table 1 suggest that recombinant production of soluble and active hFMO3 is feasible with the use of detergents. Yet, several studies contradict such conclusion. In fact, in the studies that report on soluble and active (truncated) hFMO3, often the isolated amount or measured monooxygenase activity is rather low or not reported (Catucci *et al.*, 2012). From the latter report, it is also difficult to retrieve all required experimental details for reproducing the expression and purification. For example, the paper of Catucci *et al* (2012) contains a rather cryptic section describing the experimental procedures and lacks vital details regarding centrifugation steps, used temperature and buffers. Besides that, remarkably, the presented UV-Vis spectra of the wild type and truncated hFMO3 appear fully identical, which is rather unexpected (see Figs. 2C and 2D in Catucci et al, 2012). Also, a quartz crystal microbalance experiment to test the membrane association of the truncated enzyme purified from the cytosolic fraction and the wild type enzyme obtained from the membrane fraction lacks a negative control. This makes it difficult to judge whether remaining membrane particles could have resulted in a false positive result for the wild type enzyme sample. Interestingly, Shimizu et al (2012), in a letter to the editor, put forward their findings that in their hands an identically truncated hFMO3, while expressed in the same *E. coli* strain, did not end up on the soluble fraction (Shimizu, Kobayashi and Yamazaki, 2012). The response of the Gilardi group to this letter (Enna, 2012) does not convincingly take away worries concerning the potential flaws. Additionally, the group has shown reluctance to share the expression vector with others which makes it impossible to reproduce the reported results.

Several studies have demonstrated that the recombinant expression of hFMO3 fused to a protein partner can be successful. Maltose binding protein (MBP) has been a popular fusion protein and is typically fused to the N-terminus of hFMO3 (Brunelle *et al.*, 1997; Lattard *et al.*, 2003; Reddy *et al.*, 2010). For this fusion, a rather peculiar linker with a repeat of ten asparagines has been used. This approach was also successfully applied for another FMO isoforms (Table 1). The purification of MBP fusion proteins is relatively simple because affinity chromatography can be used, exploiting the

affinity of MBP towards amylose column material. Purification of MBP-hFMO3 yields around 2-5 mg of protein per 1 L of bacterial culture (Reddy *et al.*, 2010). Though MBP often improves the solubility of the fusion partner protein, the created MBP-hFMO3 fusion still required surfactants in the purification procedure. Typically, 0.5 % Triton X-100 is used (Motika *et al.*, 2009; Reddy *et al.*, 2010). It has been reported that the MBP-hFMO3 fusion displays a slower turnover rate compared to native hFMO3 (Reddy *et al.*, 2010). Probably the interaction between MBP and the monooxygenase influences the accessibility and/or architecture of the active site of hFMO3. The effect of detergents on activity are similar for the fusion and the non-fused enzyme (Reddy *et al.*, 2010). Interestingly, it has been observed that fusing hFMO3 to MBP increases its thermostability and resistance towards proteolysis (Brunelle *et al.*, 1997).

All in all, active MBP-hFMO3 fusions can be expressed in *E. coli* and the recombinant enzyme can be purified and used for *in vitro* research on human metabolism (Reddy *et al.*, 2010). The fact that, using detergents, the fusion enzyme can be obtained as active enzyme demonstrates that membrane binding is not required for hFMO3 activity. Encouraged by this, we set out to develop a new recombinant expression vector to produce hFMO3 that could be easily isolated and used.

A NEW APPROACH: EXPRESSION OF (TRUNCATED) HFMO3 FUSED TO PHOSPHITE DEHYDROGENASE

In 2008 it was shown that various Baeyer-Villiger monooxygenases (BVMOs) can be overexpressed in *E. coli* when fused to phosphite dehydrogenase (PTDH) (Pazmino et al. 2008). Such fusion enzymes have been described as self-sufficient BVMOs as they can regenerate NADPH at the expense of (cheap) phosphite. The approach of fusing PTDH was also successfully shown for various other flavoprotein monooxygenases and a P450 monooxygenase (Torres Pazmiño *et al.*, 2009; Beyer *et al.*, 2016). For expression of these latter fusion proteins a dedicated pBAD-based expression vector (pCRE) containing a codon-optimized gene encoding for an engineered PTDH that is thermostable, solvent tolerant His-tagged, and active with both NAD^+ and $NADP^+$, was developed (Torres Pazmiño *et al.*, 2009). Except for optimizing the PTDH-encoding gene, also the linker that fused the two enzymes was optimized (Riebel et al. 2009). By equipping the target enzyme with an effective coenzyme recycling activity, which facilitates the use of these enzyme in a cost-effective manner, the fusion with PTDH was also found to promote higher expression of soluble protein. This effect has previously been described when using maltose-binding protein (MBP) or the so-called Small Ubiquitin-like Modifier protein (SUMO) as fusion tags. Because FMOs are sequence related to BVMOs, we decided to use the pCRE expression vector to express hFMO3 fused to His-tagged PTDH (as N-terminal tag). Except for expressing a fusion protein, we also generated pBAD-based expression plasmids for the expression of N-terminally His-tagged hFMO3, C-terminally truncated hFMO3, and C-terminally truncated hFMO3 with a C-terminal His-tag (see Table 7).

Upon testing different culture conditions and subsequent SDS-PAGE analysis, it was found that none of the non-fused hFMO3 expression plasmids resulted in soluble or solubilized hFMO3. Irrespective of the used temperature or arabinose concentration, for the N-terminally His-tagged hFMO3 no significant overexpression was observed in the prepared crude cell extracts. Overexpression of C-terminally truncated hFMO3 was observed at all tested growth temperatures as evidenced by a clear protein band at around 63 kDa upon SDS-PAGE analysis. Yet, the overexpressed protein always was found to be insoluble. A similar result was found for the His-tagged version of the truncated hFMO3. Importantly, analysis of the crude cell extract of cells containing the expression plasmid for expression of the PTDH-fused hFMO3 revealed clear overexpression of a protein with molecular mass of around 100 kDa (predicted mass is 103 kDa) (Figure 5). By subcellular fractionation, it became clear that in this case the recombinant protein is in the membrane fraction after the first mild fractionation step (Figure 6). Unfortunately, the protein could not be solubilized with the tested detergents. This suggests that the fusion protein is membrane associated and that solubilisation from the membrane is difficult or that the protein tends to aggregate during the fractionation procedure.

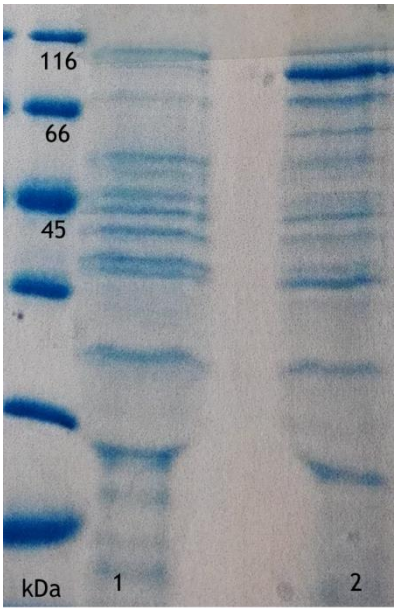

Figure 5. SDS-PAGE analysis of the expressed His-PTDH-hFMO3T. The gel shows good overexpression in the crude cell extract (growth and induction at 17 °C (lane 2). Lane 1: negative control, cell extract of cells devoid of any plasmid.

Using Ni-Sepharose affinity chromatography, it was attempted to isolate the recombinant PTDH-hFMO3 from crude cell extracts. Unfortunately, SDS-PAGE analysis revealed that none of the tested elution buffers contained a protein with the expected molecular mass. In fact, it was found that the fusion protein eluted in the flow-through fraction. The fusion protein could also not be purified from a detergent-enriched crude extract. There are many plausible reasons for the resilience towards purification. It could be that the used detergent did not result in solubilisation or did induce aggregation of the protein. Another possible reason can be a shielded His-tag (possible covered by the fused hFMO3), not accessible to bind to the Ni-Sepharose.

Motivated by the observation that the PTDH-fused hFMO3 is expressed differently when compared with the other hFMO3 expression constructs, we set out to use recombinant cells for testing a hFMO3-catalyzed oxidation reaction. Cells were grown for expressing all four different recombinant proteins using conditions for which expression of the protein had been confirmed (Table 5). As test reaction, the sulfoxidation of albendazole was analysed. The highest sulfoxidation activity was observed for the cells that had expressed PTDH-hFMO3. These cells displayed 2-3 fold higher activity when compared with cells containing no plasmid or another hFMO3 expression plasmid. The observed hFMO3 activity is line with the expression of the PTDH-hFMO3 as membrane-associated protein in *E. coli*. It is also another confirmation that hFMO3 can be functionally expressed in a bacterial expression host.

Table 5. *Expression conditions and activity of recombinant E. coli cells expressing all different hFMO3 variants.*

construct	expression conditions		albendazole sulfoxide formation [%][a]
	temperature [°C]	arabinose concentration [%]	
His-PTDH-hFMO3T	24	0.002	238
His-hFMO3	30	0.02	152
hFMO3T	24	0.02	142
hFMO3T-His	24	0.02	123
no plasmid	24	0	100

4. CONCLUSIONS

Human FMO3 plays a crucial role in the oxidative metabolism. So far, no crystal structure has been solved for this membrane-associated flavoenzyme and the molecular basis for its interactions with the membrane remain mysterious. It appears that the C-terminus acts as membrane anchor, but at the same time it does not seem to be the only membrane-binding protein segment. In this chapter, based on a bioinformatics analysis, a candidate region (residues 232-250) residue has been identified that may play a role in membrane-binding. Future experimental work may confirm such a structural role. It may help to engineer a hFMO3 variant which can be expressed as a soluble and functional monooxygenase. Besides the finding described above, inspection of a multiple sequence alignments revealed a new FMO-specific sequence motif: (A/F)**a**(I/V)Gxx**b**, where **a** is a hydrophobic and **b** is a polar amino acid. Upon analysis of related flavoprotein structures, it can be concluded that the conserved (I/V)G residues are part of a structural motif that allows proper FAD cofactor - protein interactions. The

conservation of the polar residue seems to be involved in an interaction with the NADPH cofactor. This shows that the motif is at the core of the protein structure, involved in interactions with both FMO cofactors. It would be interesting to experimentally verify whether the type of amino acid at position **b** directly affects enzyme activity.

In the experimental part of this chapter, we tested expression of several engineered hFMO3 variants in *E. coli*. For that, we prepared expression plasmids for producing hFMO3 with or without PTDH as fusion partner (Torres Pazmiño *et al.*, 2009), with or without a C-terminal truncation, and with or without a His-tag. Unfortunately, none of the constructs resulted in expression of hFMO3 that could be purified as soluble or solubilized protein. Gratifyingly, the expression of the PTDH-hFMO3 fusion revealed significant monooxygenase activity when using whole cells. This is in line with the observation that this was the only recombinant protein that did end up in the membrane fraction. All other constructs led to no expression or expression as insoluble protein. The successful expression of PTDH-hFMO3 may provide a lead to develop an effective expression system that can be used to perform hFMO3 metabolite synthesis and analysis. The fusion partner may help in efficient regeneration of NADPH that is needed for hFMO3 activity.

MATERIALS AND METHODS

Bioinformatics - The multiple sequence alignment (using ClustalW) and visualization was performed using Geneious 8.0.5. Visualisation and inspection of enzyme structures has been performed using the PyMOL software. All other employed bioinformatics tools are indicated in the text.

Materials - All chemicals were obtained from ACROS Organics, Sigma-Aldrich, PROMEGA, Qiagen, Roche Applied Sciences, New England or ThermoScience and used without further purification. Oligonucleotide primers for PCR reactions were obtained from Sigma and DNA sequencing was done at the GATC. Amplifications of inserts and vectors were performed with the Expand Long Range dNTPack kit from Roche. Digestion and ligation buffers, if not indicated, were purchased from the New England. Three vectors were used: pBAD/myc-HisA, pCRE (Torres Pazmiño *et al.*, 2009; Mascotti *et al.*, 2013) and pPTDH (a pBAD vector with a gene encoding a 18x PTDH mutant, see(Dudek *et al.*, 2013). The *E. coli* codon-optimized gene for hFMO3 expression (UniProt entry P13531) was purchased from GenScript (the sequence is shown in the supplementary material).

Cloning - The Sequence and Ligation Independent Cloning approach (SLIC) was taken to generate the desired expression plasmids. For this, the general procedure reported before (Li and Elledge, 2012) was slightly modified. For the amplification of the insert, primers of 26 base pairs with an additional 15 base pairs complementary to the vector overhangs were used. Primers for vector amplification had a similar length and blunt ends. PCRs conditions are described in Table 6, and all the used primers are

listed in **Error! Reference source not found.**7. In 10 µL water supplemented with 1 µL of buffer 4, 50 ng of amplified vector was incubated for 22 min at 22 °C with 0.025 U of polymerase T4. The reaction was stopped by the addition of 1 mM dCTP. Subsequent ligation was performed in PROMEGA ligation buffer for 30 min at 37 °C. For the ligation, 1:2 insert to vector molar ratio was used.

***Table 6**. PCR conditions for amplification for SLIC.*

	Temp [°C]		Time [min : sec]
	94		0:29
34 cycles	94		0:10
	Touch up	50-64 for pCRE 54-67 for pBAD and pPTDH 50-67 for hFMO3	0:15
	68		4:10 (for vector) 3:00 (for insert)
	68		10:00
	8		∞

***Table 7.** Primers used for vector and insert amplifications. For the two last constructs the stop codon was introduced already in the primer and an extra QuickChange reaction was not needed. The position of "His" in the names indicates whether a His-tag is present as N- or C-terminal tag. The "T" in the names indicates a C-terminal truncation.*

Name	Truncation at C-terminus	Vector	Vector amplification primers	Insert amplification primers
			If used: primers for extra QuickChange for addition or removal of the STOP codon	
hFMO3T-His	16	pBAD	FW: ATGTAATTCCTCCTGTTAGCCCAAAAAAC RW: CTGCAGCTGGTACCATATCGGAATTC	FW:CAGGAGGAATTACATCATATGGGTAAGAAAGTTGCTATCATTGGTGCTG RW:TGGTACCAGCTGCAGTTTCAGCCAATGAAAGAAAAAGCACGG
			FW: GCATCGGTTTCAGATAGCGATCCCACTGGGT RW: ACCCAGTGGGATCGCTATCTGAAACCGATGC	
His-hFMO3	-	pPTDH	FW:GGGCCCGAACAAAAACTCATCTCAGAAGAGGATC RW: GCTGCCGCGCGGCACCAG	FW:GCCGCGCGGCAGCCATATGGGTAAGAAAGTTGCTATCATTGG RW:GTTTTTGTTCGGGCCCCTTTTAGGTCAGCACCAGGAAGAC
hFMO3T	17	pPTDH	FW: ATGTAATTCCTCCTGTTAGCCCAAAAAAC RW: TTGGGCCCGAACAAAAACTCATC	FW:CTAACAGGAGGAATTACATATGGGTAAGAAAGTTGCTATCATTGGTGC RW:GGTACCATATCGGAATTCGAAGCTTGGGCCCGAACAAAAACTCATCTC
			FW: CTTTCATTGGCTGTAACTGTTCGCCATCCCG RW: CGGGATGGCGAACAGTTACAGCCAATGAAAG	
His-PTDH-hFMO3T	17	pCRE	FW: ACCAGCTGCAGATCTCGAGTCAG RW: TTGGGCCCGAACAAAAACTCATC	FW:GATCTGCAGCTGGTCATATGGGTAAGAAAGTTGCTATCATTGCTATC RW:TTTGTTCGGGCCCAAGGCGAACAGTTTACAGCCAATGAAAGAAAAAG

The DNA was transformed into chemically competent *E. coli* TOP10 cells and the sequences of the obtained plasmids were verified by DNA sequencing. Some constructs required a QuickChange reaction for introducing or removing a STOP codon (for creating a C-terminal His-tag). By this approach, the hFMO3 gene was inserted into the pCRE vector, while in case of pPTDH, the PTDH gene was replaced with hFMO3. The QuickChange reactions were performed using the MasterMix kit

from Thermo Scientific using the conditions recommended by the manufacturer. The final constructs were named as indicated in Table 7.

Enzyme expression optimization and subcellular localization

E. coli TOP10 cells were transformed with the prepared plasmids and grown overnight at 37 °C in 5 mL of Luria–Bertani medium (LB) supplemented with 50 µg/mL ampicillin. The next day, 5 mL of LB with the same concentration of ampicillin and 0.02% or 0.002 % (w/v) L-arabinose were inoculated 1:100 v/v with the cultures from the previous day. Subsequently, the cells were grown for 48 h at 37, 30, 24 °C or 72 h at 17 °C. Cells were harvested by centrifugation and analysed for expression and subcellular localisation of the recombinant protein according to the scheme shown in Figure 6. The collected fractions were analysed with SDS-PAGE.

His-tag purification of recombinant His-PTDH-hFMO3

Using different culture temperatures (24, 30, and 37 °C) and 0.002 % arabinose, several 100 mL cultures were grown. All the following steps were performed at 4 °C. Cells of each culture were harvested and resuspended in 10 mL 50 mM Tris/HCl (pH 8) containing 100 µM FAD, 0.5 % Triton X-100 and EDTA-free protease inhibitor mix from Thermo Scientific. The cell suspension was sonicated and the obtained cell lysate was fractionated according to the scheme in Figure 6. The fractions with soluble or solubilized proteins were used for protein purification. For this, each fraction was incubated with Ni-Sepharose in 50 mM Tris/HCl (pH 8). The bound protein was eluted using three different elution buffers: 5, 200, and 500 mM imidazole in 50 mM Tris/HCl, 5 % glycerol (pH 8). The buffers were applied one after another. The eluted fractions were analysed by SDS-PAGE.

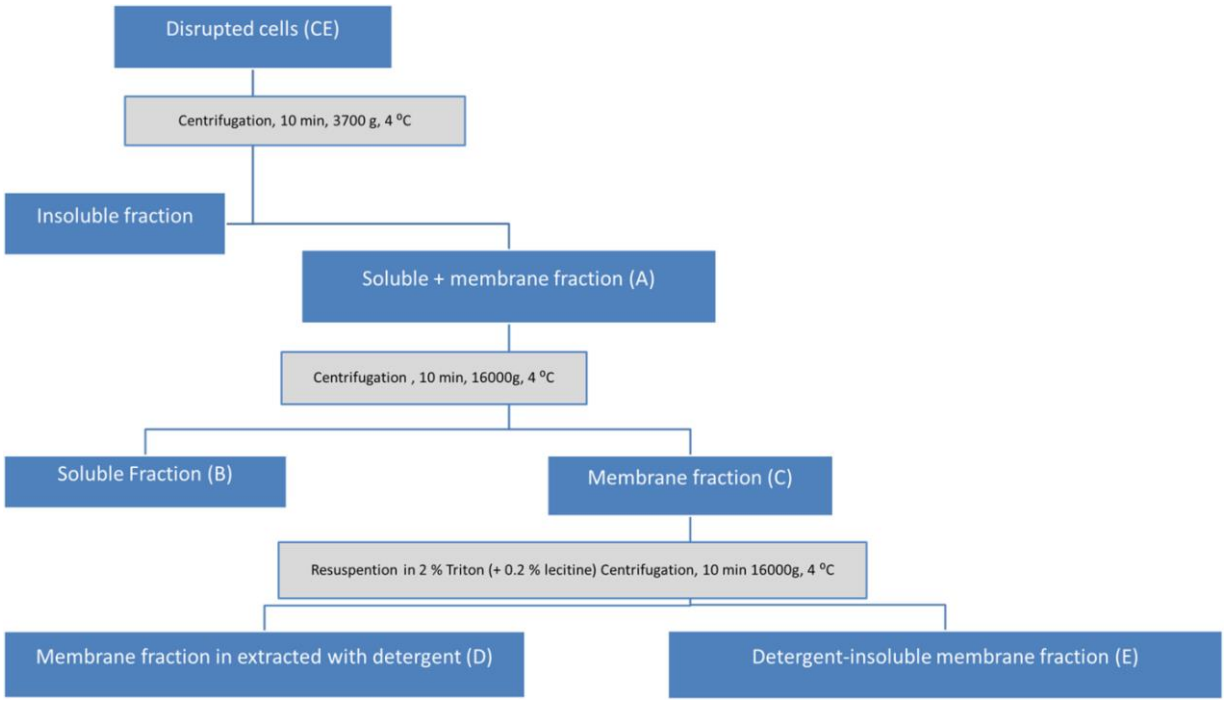

***Figure 6**. Scheme showing the protocol for preparation of cellular fractions for determining the subcellular localisation of expressed protein.*

WHOLE CELL CONVERSIONS OF ALBENDAZOLE

For activity screening upon expression using different conditions, an enzyme activity assay was used based on the assay published before (Prasad, Girisham and Reddy, 2010). For that, sterile test tubes containing 1 mL of LB supplemented with 50 mg/L ampicillin, 4 mM β-cyclodextrin and 100 mg/L of albendazole (1% final concentration of DMSO) were inoculated 1:100 (v/v) with overnight grown cultures. To analyse the formation of the albendazole sulfoxide, cells were spun down and the supernatant was diluted with acetonitrile (ACN) 1:1 (v/v) and centrifuged at 8000 g for 4 min. The resulting supernatant was diluted with ACN containing 0.2 % formic acid and again centrifuged at 8000 g for 4 min. The resulting supernatant was supplemented with an internal standard (IS), acetaminophen and subsequently analysed by LC-MS. The apparatus (Thermo Scientific HPLC) was equipped with a C18 reversed-phase column (GraceSmart RP 18 5 μm, 2.1×150 mm; Grace Davison, Lokeren, Belgium). Solvent A (H_2O with 0.1 % formic acid) and solvent B (ACN with 0.1 % formic acid) were used for elution using the following program: 5 to 50 % B over 10 min, increase to 95 % B in 2 min, and 1 min hold.

The flow rate was 250 μL/min. The LC was coupled to the ESI mass spectrometer equipped with a triple quadrupole analyser from Thermo Finnigan. Analysis was performed in the positive mode (settings: spray voltage 4000 V, skimmer offset -0 V, sheath gas pressure 30, auxiliary gas pressure 15, tube lens offset 89 V, capillary temperature 300 ºC, scan range *m/z* 50-400). For selected reaction monitoring (SRM), the following transitions were analysed: albendazole (266/234), albendazole sulfoxide (282/240), albendazole sulfone (298/266) and the IS (152/110). For each sample, the results were normalized for the internal standard and corrected for the formation of albendazole sulfoxide by the negative control sample (*E. coli* without a hFMO3-expression plasmid).

REFERENCES

Alfieri, A. et al., 2008. Revealing the moonlighting role of NADP in the structure of a flavin-containing monooxygenase. Proc Natl Acad Sci U S A, 105(18), pp.6572–6577.

Attwood, T.K. et al., 2012. The PRINTS database: A fine-grained protein sequence annotation and analysis resource-its status in 2012. Database, 2012.

Ballard, J.E., Prueksaritanont, T. & Tang, C., 2007. Hepatic metabolism of MK-0457, a potent Aurora kinase inhibitor: Interspecies comparison and role of human cytochrome P450 and flavin-containing monooxygenase. Drug Metabolism and Disposition, 35(9), pp.1447–1451.

Bernsel, A. et al., 2008. Prediction of membrane-protein topology from first principles. Proceedings of the National Academy of Sciences of the United States of America, 105(20), pp.7177–7181.

Beyer, N. et al., 2016. P450BM3 fused to phosphite dehydrogenase allows phosphite-driven selective oxidations. Applied Microbiology and Biotechnology, 101(6), pp.2319-2331.

Brunelle, A. et al., 1997. Characterization of two human flavin-containing monooxygenase (form 3) enzymes expressed in *Escherichia coli* as maltose binding protein fusions. Drug Metabolism and Disposition, 25(8), pp.1001–1007.

Cashman, J.R., 2000. Human flavin-containing monooxygenase: substrate specificity and role in drug metabolism. Current Drug Metabolism, 1(2), pp.181–191.

Cashman, J.R. et al., 1995. Role of hepatic flavin-containing monooxygenase 3 in drug and chemical metabolism in adult humans. Chemico-Biological Interactions, 96(1), pp.33–46.

Cashman, J.R. & Lomri, N., 2004. DNA sequence encoding flavin-containing monooxygenase.

Cashman, J.R. & Zhang, J., 2006. Human flavin-containing monooxygenases. Annual review of pharmacology and toxicology, 46, pp.65–100.

Catucci, G. et al., 2012. In vitro drug metabolism by C-terminally truncated human flavin-containing monooxygenase 3. Biochemical Pharmacology, 83(4), pp.551–558.

Dolphin, C.T. et al., 1992. Cloning, primary sequence and chromosomal localization of human FMO2, a new member of the flavin-containing mono-oxygenase family. The Biochemical journal, 287, pp.261–7.

Dolphin, C.T. et al., 1998. The flavin-containing monooxygenase 2 gene (FMO2) of humans, but not of other primates, encodes a truncated, nonfunctional protein. Journal of Biological Chemistry, 273(46), pp.30599–30607.

Dudek, H.M. et al., 2013. A generic, whole-cell-based screening method for Baeyer-Villiger monooxygenases. Journal of biomolecular screening, 18(6), pp.678–87.

Enna, S.J., 2012. Note to readers. Biochemical Pharmacology, 84(3), p.411.

Eswaramoorthy, S. et al., 2006. Mechanism of action of a flavin-containing monooxygenase. Proceedings of the National Academy of Sciences, 103(26), pp.9832–9837.

Fiorentini, F. et al., 2016. Biocatalytic characterization of human FMO5: unearthing Baeyer–Villiger reactions in humans. ACS Chemical Biology, 11(4), pp.1039-1048.

Fraaije, M.W. et al., 2002. Identification of a Baeyer-Villiger monooxygenase sequence motif. FEBS Letters, 518(1–3), pp.43–47.

Geier, M. et al., 2015. Human FMO2-based microbial whole-cell catalysts for drug metabolite synthesis. Microbial Cell Factories, 14(1), p.82.

de Gonzalo, G. et al., 2005. Oxidations catalyzed by phenylacetone monooxygenase from *Thermobifida fusca*. Tetrahedron: Asymmetry, 16(18), pp.3077–3083.

Gul, T. et al., 2016. Microbial flavoprotein monooxygenases as mimics of mammalian flavin-containing monooxygenases for the enantioselective preparation of drug metabolites. Drug Metabolism and Disposition, 44(8), pp.1270-1276.

Haining, R.L. et al., 1997. Baculovirus-mediated expression and purification of human FMO3: Catalytic, immunochemical, and structural characterization. Drug Metabolism and Disposition, 25(7), pp.790–797.

Hanlon, S.P. et al., 2012. Expression of recombinant human flavin monooxygenase and moclobemide-N-oxide synthesis on multi-mg scale. Chemical communications, pp.6001–6003.

Jayasinghe, S., Hristova, K. & White, S.H., 2001. Energetics, stability, and prediction of transmembrane helices. Journal of Molecular Biology, 312, pp.927–934.

Jensen, C.N. et al., 2014. Exploring nicotinamide cofactor promiscuity in NAD(P)H-dependent flavin containing monooxygenases (FMOs) using natural variation within the phosphate binding loop. Structure and activity of FMOs from *Cellvibrio* sp. BR and *Pseudomonas stutzeri* NF13. Journal of Molecular Catalysis B: Enzymatic, 109, pp.191–198.

Käll, L., Krogh, A. & Sonnhammer, E.L.L., 2005. An HMM posterior decoder for sequence feature prediction that includes homology information. Bioinformatics, 21(SUPPL. 1), pp.251–257.

Koukouritaki, S.B. et al., 2007. Identification and functional analysis of common human flavin-containing monooxygenase 3 genetic variants. Journal of Pharmacology and Experimental Therapeutics, 320, pp.226–273.

Krueger, S.K. et al., 2006. C-terminal truncation of rabbit flavin-containing monooxygenase isoform 2 enhances solubility. Archives of Biochemistry and Biophysics, 450(2), pp.149–156.

Krueger, S.K. et al., 2001. Characterization of expressed full-length and truncated FMO2 from rhesus monkey. Drug Metabolism and Disposition, 29(5), pp.693–700.

Krueger, S.K. & Williams, D.E., 2005. Mammalian flavin-containing monooxygenases: structure/function, genetic polymorphisms and role in drug metabolism. Pharmacology & Therapeutics, 106(3), pp.357–387.

Lattard, V. et al., 2003. Two new polymorphisms of the FMO3 gene in Caucasian and African-American populations: Comparative genetic and functional studies. Drug Metabolism and Disposition, 31(7), pp.854–860.

Lawton, M.P. & Philpot, R.M., 1993. Functional characterization of flavin-containing monooxygenase 1B1 expressed in *Saccharomyces cerevisiae* and *Escherichia coli* and analysis of proposed FAD- and membrane-binding domains. Journal of Biological Chemistry, 268(8), pp.5728–5734.

Li, C. et al., 2017. Structural mechanism for bacterial oxidation of oceanic trimethylamine into trimethylamine N-oxide. Molecular Biology, pp.1365–2958.

Li, M.Z. & Elledge, S.J., 2012. SLIC: A method for sequence- and ligation-independent cloning. Methods in Molecular Biology, 852, pp.51–59.

Lomri, N., Gu, Q. & Cashman, J.R., 1995. Molecular cloning of the flavin-containing monooxygenase (form II) cDNA from adult human liver. Proceedings of the National Academy of Sciences of the United States of America, 92(21), p.9910.

Lomri, N., Yang, Z. & Cashman, J.R., 1993. Expression in *Escherichia coli* of the flavin-containing monooxygenase d (form 11) from adult human liver: determination of a distinct tertiary amine substrate specificity. Chemical Research in Toxicology, 6(11), pp.425–429.

Mascotti, M.L. et al., 2013. Cloning, overexpression and biocatalytic exploration of a novel Baeyer-Villiger monooxygenase from *Aspergillus fumigatus* Af293. AMB Express, 3(1), p.33.

Motika, M.S. et al., 2009. Novel variants of the human flavin-containing monooxygenase 3 (FMO3) gene associated with trimethylaminuria. Molecular genetics and metabolism, 97(2), pp.128–135.

Orru, R. et al., 2010. Joint functions of protein residues and NADP(H) in oxygen activation by flavin-containing monooxygenase. Journal of Biological Chemistry, 285(45), pp.35021–35028.

Prasad, G.S., Girisham, S. & Reddy, S.M., 2010. Microbial transformation of albendazole. Indian Journal of Experimental Biology, 48(4), pp.415–420.

Prost, F., Caslavska, J. & Thormann, W., 2002. Chiral analysis of albendazole sulfoxide enantiomers in human plasma and saliva using capillary electrophoresis with on-column absorption and fluorescence detection site:sciencedirect.com. Journal of Separation Science, (25), pp.1043–1054.

Reddy, R.R. et al., 2010. Characterization of human flavin-containing monooxygenase (FMO) 3 and FMO5 expressed as maltose-binding protein fusions. Drug Metabolism and Disposition, 38(12), pp.2239–2245.

Reynolds, S.M. et al., 2008. Transmembrane topology and signal peptide prediction using dynamic Bayesian networks. PLoS Computational Biology, 4(11).

Riebel, A., de Gonzalo, G. & Fraaije, M.W., 2013. Expanding the biocatalytic toolbox of flavoprotein monooxygenases from *Rhodococcus jostii* RHA1. Journal of Molecular Catalysis B: Enzymatic, 88, pp.20–25.

Rioz-martínez, A. et al., 2011. Exploring the biocatalytic scope of a bacterial flavin-containing monooxygenase. Org. Biomol. Chem., 9(5), pp.1337-1341.

Shimizu, M., Kobayashi, Y. & Yamazaki, H., 2012. RE: “In vitro drug metabolism by C-terminally truncated human flavin-containing monooxygenase 3” by Catucci et al. [Letter to editor]. Biochemical Pharmacology, 84, p.411.

Störmer, E., Roots, I. & Brockmöller, J., 2000. Benzydamine N-oxidation as an index reaction reflecting FMO activity in human liver microsomes and impact of FMO3 polymorphisms on enzyme activity. British Journal of Clinical Pharmacology, 50(6), pp.553–561.

Torres Pazmiño, D.E. et al., 2009. Efficient biooxidations catalyzed by a new generation of self-sufficient Baeyer-Villiger monooxygenases. ChemBioChem, 10(16), pp.2595–2598.

Treacy, E.P. et al., 1998. Mutations of the flavin-containing monooxygenase gene (FMO3) cause trimethylaminuria, a defect in detoxication. Human Molecular Genetics, 7(5), pp.839–845.

Tusnády, G.E. & Simon, I., 2001. The HMMTOP transmembrane topology prediction server. Bioinformatics, 17(9), pp.849–50.

Viklund, H. & Elofsson, A., 2008. OCTOPUS: Improving topology prediction by two-track ANN-based preference scores and an extended topological grammar. Bioinformatics, 24(15), pp.1662–1668.

White, E. & Atta-Asafo-Adjei, E., 2011. Multi site-directed mutagenesis of human flavin-containing monooxygenase 5 (FMO5) produces a mutant with 20-fold higher affinity for methimazole : evidence that Ile61 is crucial for catalytic activity. Atlas Journal of Chemistry & Biochemistry, 1(1), pp.14–22.

Yamazaki, H. et al., 2007. Stop codon mutations in the flavin-containing monooxygenase 3 (FMO3) gene responsible for trimethylaminuria in a Japanese population. Molecular Genetics and Metabolism Reports, 90, pp.58–63.

Zhang, M. & Robertus, J.D., 2002. Molecular cloning and characterization of a full-length flavin-dependent monooxygenase from yeast. Archives of Biochemistry and Biophysics, 403(2), pp.277–283.

SUPPLEMENTARY DATA

DNA sequence of codon-optimised hFMO3 purchased from the GenScript

CATATGGGTAAGAAAGTTGCTATCATTGGTGCTGGTGTCAGTGGCCTGGCATCGATTCGCAGTTGTCT
GGAAGAAGGTCTGGAACCGACCTGCTTCGAAAAATCTAATGATATCGGCGGTCTGTGGAAATTTTCAG
ACCATGCAGAAGAAGGCCGTGCTTCGATTTATAAATCAGTTTTCTCGAACAGCTCTAAAGAAATGATG
TGTTTTCCGGATTTCCCGTTTCCGGATGACTTCCCGAACTTCATGCATAACAGCAAAATCCAGGAATA
CATTATCGCGTTTGCCAAAGAGAAAAACCTGCTGAAATACATCCAATTCAAAACCTTCGTCAGTTCCG
TGAACAAACACCCGGATTTTGCGACCACGGGCCAGTGGGATGTCACCACGGAACGCGACGGCAAGAAA
GAAAGTGCGGTGTTCGACGCCGTTATGGTCTGCTCCGGTCATCACGTTTATCCGAATCTGCCGAAAGA
ATCTTTTCCGGGCCTGAACCATTTCAAGGGTAAATGTTTTCACTCTCGTGATTACAAAGAACCGGGCG
TCTTTAATGGTAAACGCGTTCTGGTGGTGGGCCTGGGTAACAGCGGCTGCGACATCGCAACCGAACTG
TCTCGTACGGCTGAACAGGTGATGATTTCATCGCGTAGTGGCTCCTGGGTTATGAGTCGCGTCTGGGA
TAATGGTTATCCGTGGGACATGCTGCTGGTTACCCGCTTCGGCACGTTTCTGAAAAACAATCTGCCGA
CCGCGATCTCCGATTGGCTGTATGTCAAACAAATGAACGCCCGTTTCAAACACGAAAATTACGGCCTG
ATGCCGCTGAACGGTGTTCTGCGCAAAGAACCGGTCTTTAATGACGAACTGCCGGCAAGTATTCTGTG
CGGCATCGTGTCCGTTAAACCGAACGTTAAAGAATTCACCGAAACGTCAGCCATTTTCGAAGATGGCA
CCATTTTTGAAGGTATCGACTGTGTGATTTTTGCGACGGGCTATTCGTTCGCCTACCCGTTTCTGGAT
GAAAGCATCATCAAATCTCGTAACAACGAAATCATCCTGTTCAAAGGTGTTTTCCCGCCGCTGCTGGA
AAAATCAACCATTGCCGTGATCGGCTTTGTTCAGTCGCTGGGTGCAGCAATCCCGACCGTGGATCTGC
AGAGTCGTTGGGCAGCTCAAGTTATTAAAGGTACCTGTACGCTGCCGTCCATGGAAGATATGATGAAC
GACATCAACGAAAAAATGGAGAAAAAACGTAAATGGTTTGGCAAAAGCGAAACCATCCAGACGGATTA
TATTGTGTACATGGACGAACTGAGCTCTTTCATCGGTGCAAAACCGAATATTCCGTGGCTGTTTCTGA
CCGATCCGAAACTGGCTATGGAAGTCTATTTCGGCCCGTGCAGCCCGTACCAGTTTCGCCTGGTGGGC
CCGGGTCAATGGCCGGGTGCACGTAACGCTATTCTGACCCAGTGGGATCGCTCTCTGAAACCGATGCA
GACGCGTGTCGTGGGCCGCCTGCAAAAACCGTGCTTTTTCTTTCATTGGCTGAAACTGTTCGCCATCC
CGATTCTGCTGATTGCTGTCTTCCTGGTGCTGACCTAAAAGCTT

CHAPTER 5

MICROBIAL FLAVOPROTEIN MONOOXYGENASES AS MIMICS OF MAMMALIAN FLAVIN-CONTAINING MONOOXYGENASES FOR THE ENANTIOSELECTIVE PREPARATION OF DRUG METABOLITES

Turan Gul [a1], Marzena Krzek[b1], Hjalmar P. Permentier [a], Marco W. Fraaije[b] and Rainer Bischoff [a]

[a] University of Groningen, Department of Pharmacy, Analytical Biochemistry, Antonius-Deusinglaan 1, 9713 AV Groningen, The Netherlands

[b] Molecular Enzymology Group, University of Groningen, Nijenborgh 4, 9747 AG Groningen, The Netherlands

[1] Autors contributed equally to this work

Published in Drug Metabolism and Disposition August 2016, 44 (8) 1270-1276;
DOI: https://doi.org/10.1124/dmd.115.069104

ABSTRACT

Mammalian flavin-containing monooxygenases, which are difficult to obtain and study, play a major role in detoxifying various xenobiotics. To provide alternative biocatalytic tools to generate flavin-containing monooxygenases (FMO)–derived drug metabolites, a collection of microbial flavoprotein monooxygenases, sequence-related to human FMOs, was tested for their ability to oxidize a set of xenobiotic compounds. For all tested xenobiotics [nicotine, lidocaine, 3-(methylthio)aniline, albendazole, and fenbendazole], one or more monooxygenases were identified capable of converting the target compound. Chiral liquid chromatography with tandem mass spectrometry analyses of the conversions of 3-(methylthio)aniline, albendazole, and fenbendazole revealed that the respective sulfoxides are formed in good to excellent enantiomeric excess (*e.e.*) by several of the tested monooxygenases. Intriguingly, depending on the chosen microbial monooxygenase, either the (*R*)- or (*S*)-sulfoxide was formed. For example, when using a monooxygenase from Rhodococcus jostii the (*S*)-sulfoxide of albendazole (ricobendazole) was obtained with a 95% *e.e.* whereas a fungal monooxygenase yielded the respective (*R*)-sulfoxide in 57% *e.e.* For nicotine and lidocaine, monooxygenases could be identified that convert the amines into their respective *N*-oxides. This study shows that recombinantly expressed microbial monooxygenases represent a valuable toolbox of mammalian FMO mimics that can be exploited for the production of FMO-associated xenobiotic metabolites.

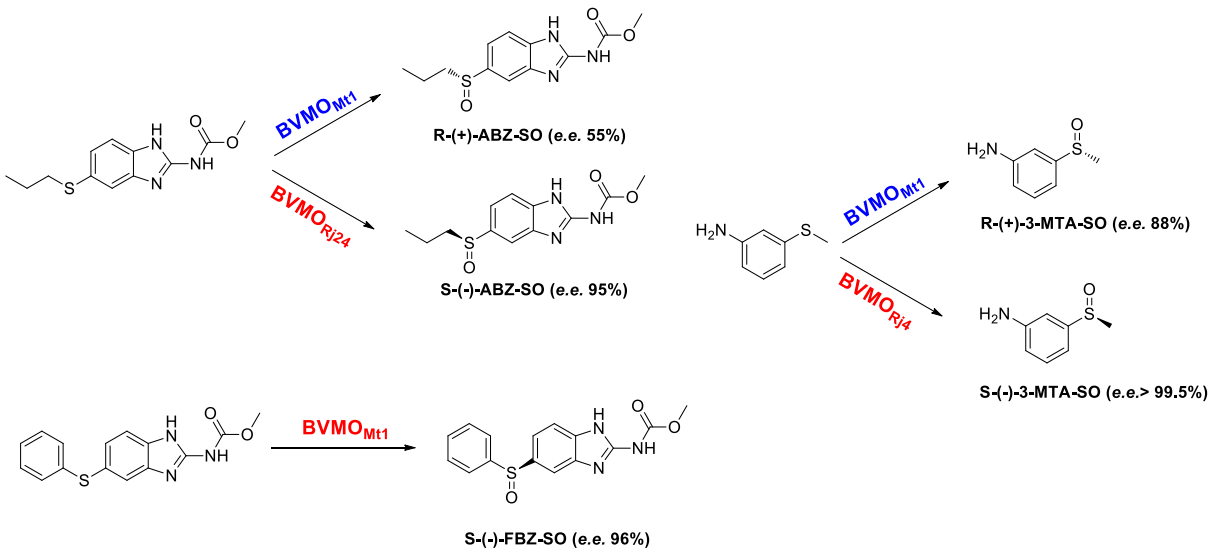

Abbreviations: BVMO, Baeyer-Villiger monooxygenase; CD, circular dichroism; CHMO, cyclohexanone monooxygenase; CYP450, cytochrome P450; e.e., enantiomeric excess; FAD, flavin adenine dinucleotide; FMO, flavin-containing monooxygenase; HILIC, hydrophilic interaction chromatography; IPTG, isopropyl β-D-thiogalactopyranoside; LB medium, lysogeny broth medium; LC, liquid chromatography; MS/MS, tandem mass spectrometry; NADPH, reduced nicotinamide adenine dinucleotide phosphate; OD, optical density; PAMO, phenylacetone monooxygenase; SDS-PAGE**,** sodium dodecyl sulfate polyacrylamide gel electrophoresis; SPE, solid phase extraction; SRM, selected reaction monitoring

1. INTRODUCTION

Metabolism of xenobiotics in humans and other mammals often starts with oxidation of the target molecule. Most of the Phase I metabolism reactions are catalyzed by cytochrome P450 mono-oxygenases (CYP450s) (Cashman et al., 2005). However, apart from CYP450s, recent studies have shown that the so-called flavin-containing monooxygenases (FMOs) also play a crucial role in the biotransformation of a large variety of xenobiotics, including pharmaceuticals and natural products. Mammals typically employ several FMO isoforms. The human proteome contains 5 isoforms, FMO1-FMO5, all of which have their typical tissue-dependent expression patterns and roles in metabolism. FMOs have been shown to be involved in the oxygenation of heteroatom-containing compounds, such as amines and sulfides (Cashman and Zhang, 2006; Cashman et al., 2004; Krueger and Williams, 2005). Different from CYP450s, which contain a heme cofactor, FMOs utilize a flavin cofactor for oxidations which also translates into a different oxidative mechanism. Furthermore, to discriminate between metabolism by human FMOs or CYP50s, often differences in stability and specific inhibitors can be used (Taniguchi-Takizawa et al., 2015). The reduced flavin subsequently reacts with molecular oxygen resulting in the formation of a reactive 4a-hydroperoxyflavin. This reactive flavin intermediate is able to perform a variety of oxygenation reactions, for example sulfoxidations and N-hydroxylations (see (Cashman et al., 2005; Cashman and Zhang, 2006; Krueger and Williams, 2005; van Berkel et al., 2006; Ziegler et al., 1993; Malito et al., 2004; Ziegler et al., 1990) for mechanistic details).

While it has been established that human FMOs are essential in oxidizing a variety of xenobiotics, biochemical and metabolic studies on these enzymes are hampered by their poor availability. Human FMOs (hFMOs) and their mammalian orthologs are typically membrane associated and often thermo-lable which appear to be the major reasons for their problematic isolation from tissue (Cashman et al., 1995; Wu et al., 2004) and inefficient recombinant production. Although human FMOs can be studied using microsomal preparations and some human FMOs were expressed as functional enzymes in heterologous hosts(Motika et al., 2009; Balke et al., 2012; Geier et al., 2015; Shimizu et al., 2015), these enzyme preparations involve costly and cumbersome isolation procedures, and often suffer from low activity and stability (Cashman and Zhang, 2006; Cashman et al., 1992). Sequence comparison studies have revealed that FMOs are part of a large family of monooxygenases, the so-called Class B flavoprotein monooxygenases (Reddy *et al.*, 2010). Intriguingly, many bacteria and fungi contain sequence-related Class B flavin-containing monooxygenases (Mascotti, Lapadula and Juri Ayub, 2015) that are typically involved in catalyzing Baeyer-Villiger oxidations forming a subfamily of Baeyer-Villiger monooxygenases (BVMOs). Biocatalytic studies on these microbial monooxygenases confirmed that they employ the same catalytic mechanism as FMOs (Torres Pazmiño *et al.*, 2008) and, interestingly, are also able to catalyze oxygenations of heteroatom containing compounds. In contrast

to hFMOs, many microbial BVMOs are soluble enzymes and can be easily produced in recombinant form (de Gonzalo, Mihovilovic and Fraaije, 2010).

Inspired by the observation that microbial BVMOs are sequence-related to human FMOs and exhibit similar activities, we set out to explore their use as mammalian FMO mimics. By testing a panel of xenobiotic compounds, including drug molecules, with a collection of microbial BVMOs, we discovered that these biocatalysts may serve as tools to prepare metabolites. By choosing the proper monooxygenase, all tested xenobiotics (nicotine, lidocaine, 3-(methylthio)aniline, albendazole, and fenbendazole, see Figure 1) could be converted. Chiral LC-MS/MS analysis showed that sulfides were converted to the corresponding sulfoxides with excellent and complementary enantioselectivities. This study reveals that recombinant microbial BVMOs, which are relatively easy to produce and robust as biocatalysts, represent attractive alternatives to mammalian FMOs for the preparation of FMO-related metabolites.

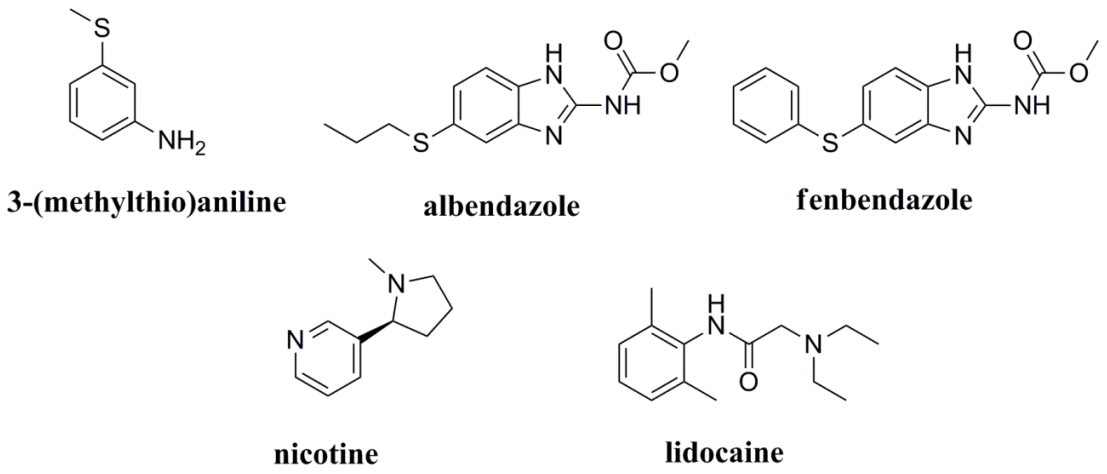

Figure 7: *Substrates used in microbial monooxygenase-catalyzed conversions.*

2. MATERIALS AND METHODS

2..1 MATERIALS

3-(Methylthio)aniline, albendazole, ricobendazole (racemic albendazole sulfoxide), fenbendazole, lidocaine, nicotine, 1,4-dioxane and Tris were purchased from Sigma-Aldrich (Zwijndrecht, The Netherlands). Acetaminophen was purchased from Fluka, ultra-pure HPLC grade acetonitrile and HPLC grade methanol were purchased from Biosolve (Valkenswaard, The Netherlands). Catalase was purchased from Fluka while phosphite dehydrogenase was prepared using an established protocol (Dudek *et al.*, 2011). Ultrapure water was obtained from a Milli-Q Advantage A10 Water Purification system (Millipore Corp., Billerica, MA, USA). Oasis HLB 30 mg solid phase extraction (SPE) cartridges were purchased from Waters (Manchester, UK).

2.2 Recombinant expression of BVMOs and preparation of cell extracts

The enzymes were overexpressed in *Escherichia coli* using previously established conditions and protocols. $CHMO_{Ac}$, $PAMO_{M446G}$ and $BVMO_{Rj24}$ were expressed using the pCRE2 expression vector (Pazmiño et al., 2009), yielding the enzyme fused to His-tagged phosphite dehydrogenase which facilitates cofactor regeneration. His-tagged PAMO and Strep-tagged FMO_{RjE} were expressed as described previously (Fraaije *et al.*, 2005) while for expressing $BVMO_{Mt1}$, a pET_SUMO vector was used. Precultures were grown overnight at 37 °C with shaking (180 rpm) in Lysogeny Broth (LB) medium containing ampicillin (50 μg/mL). The exception was $BVMO_{Mt1}$ for which cells were grown in the presence of kanamycin (100 μg/mL). Flasks containing 200 mL TB medium with the respective antibiotic were inoculated 1:100 (v/v) using the preculture and grown for another 4 h at 30 °C. After that, each flask was supplemented with inducer: 1.0 mM isopropyl β-D-thiogalactopyranoside (IPTG) for $BVMO_{Mt1}$, and 0.02% arabinose for PAMO, $PAMO_{M446G}$, and $CHMO_{Ac}$, and 0.002 % arabinose for the remaining enzymes. After 48 h of growth at 24 °C with shaking (130 rpm) cells were harvested by centrifugation at 4 °C, 17,000 g and resuspended in 50 mM Tris buffer pH 8. Cells were diluted to an OD_{600} of 212 for TB samples and an OD_{600} of 98 for LB samples. Subsequently, the cells were disrupted by sonication for 90 s using 2 s sonication pulses and 2 s breaks, while on ice. The prepared cell extracts were supplemented with glycerol (15%), aliquoted (100 μL in Eppendorf tubes), frozen in liquid nitrogen, and stored at -80 °C. As negative control *E. coli* cells were grown without expression plasmid and used for the preparation of cell extract as described above. Overexpression of the enzymes was confirmed with SDS-PAGE by analyzing OD-normalized samples from bacterial cultures.

2.3 Monooxygenase-catalyzed conversions

For conversions, cell extracts (100 μL) were supplemented with 1.0 mM substrates (except for 3-(methylthio)aniline: 3.0 mM was used) using 1,4-dioxane as a cosolvent (1% v/v for all substrates except for 3-(methylthio)aniline (0.6% v/v)), 100 μM NADPH, 20 mM phosphite, 5.0 μM phosphite dehydrogenase, 20 mU catalase and 50 mM Tris-HCl (pH 8.5) in a total volume of 300 μL. In order to increase the solubility of albendazole and fenbendazole, 9.6 mM β-cyclodextrine was added. Negative control experiments were performed by incubating substrates with cell extracts that did not contain any expressed monooxygenase. All the conversions were performed in duplicate. After 135 min of incubation at room temperature, a 100 μL sample was taken and proteins were precipitated by adding 300 μL acetonitrile containing 0.2 % formic acid. Samples were vortexed for 30 s and centrifuged at 13000 rpm for 6.5 min. After centrifugation, 200 μL of the supernatants was evaporated to dryness under nitrogen prior to solid phase extraction (SPE). SPE was performed on Oasis HLB 30 mg

cartridges that were wetted with acetonitrile and equilibrated with H_2O/acetonitrile (95:5). Dried samples were dissolved in 200 μL water and loaded onto the cartridge. Water (3 x 250 μL) was used to wash the cartridges and the final elution was performed with acetonitrile (4 x 250 μL). For the LC-MS/MS analysis, samples were 10x diluted in water containing 10 μM acetaminophen, as an internal standard for LC-MS/MS signal normalization.

2.4 Chiral LC-MS/MS in the Selected Reaction Monitoring (SRM) mode

LC-MS/MS analyses in the SRM mode were carried out on an HPLC system with an Accela Autosampler and a Surveyor Pump coupled to a TSQ Quantum AM triple quadrupole mass spectrometer (Thermo Finnigan, San José, CA) with an ESI interface in the positive mode (see Tables S1 and S2 supplemental data for details). 3-(Methylthio)aniline, albendazole, fenbendazole and their chiral sulfoxide products were separated with an amylose tris(3-chlorophenylcarbamate)-based chiral column (Chiralpak ID, 5 μm particle size, 2.1×150 mm; Chiral Technologies Europe, Illkirch, France) at a flow rate of either 100 or 200 μL/min. The LC separation of lidocaine and its products was performed with a C_{18} reversed-phase column (GraceSmart RP 18, 5 μm particle size, 2.1×150 mm; Grace Davison, Lokeren, Belgium) at a flow rate of 250 μL/min. The LC separation of nicotine and its products was performed with a hydrophilic interaction (HILIC) column (Xbridge amide, 3.5 μm particle size, 2.1x150 mm; Waters, Milford, MA, USA) at a flow a rate of 250 μL/min. The following set of solvents was used for the separations: solvent A (H_2O with 0.1% formic acid), solvent B (acetonitrile with 0.1% formic acid), solvent C (H_2O with 20 mM ammonium bicarbonate (pH 9, adjusted with NH_3)), solvent D (acetonitrile) and solvent E (H_2O with 10 mM ammonium formate, pH 5.5). Separation of the two 3-(methylthio)aniline sulfoxide enantiomers was performed isocratically at 100 μL/min (20 min) with 90% solvent C / 10% solvent D. The albendazole sulfoxide enantiomers were separated isocratically with 50% solvent C / 50% solvent D at 200 μL/min (20 min) and fenbendazole sulfoxides were separated with 40% solvent C / 60% solvent D at 200 μL/min (15 min), using the Chiralpak column. The LC-MS/MS analysis of lidocaine and its N-oxide was performed by reversed-phase LC applying a linear gradient starting from 5% to 95% solvent B in solvent A over 11 min which was held for 1 min. Solvent B was decreased rapidly to 5% in 20 s and the column re-equilibrated at 5% solvent B for 4 min. The LC-MS/MS analysis of nicotine and its N-oxide was performed by HILIC applying a linear gradient starting from 10% to 90% solvent E in solvent D (acetonitrile) over 8 min which was held for 2 min. Solvent E was decreased rapidly to 10% in 20 s and finally the column re-equilibrated at 10% solvent E for 3 min. Acetaminophen was used as internal standard to normalize the peak areas across LC-MS/MS runs.

2.5 Circular Dichroism (CD)

In order to assign the absolute configuration of the products, samples were analyzed by CD spectroscopy. Samples were purified with SPE, dried by evaporation of acetonitrile, and dissolved in methanol to a nominal concentration of 0.75 mM. For CD analysis samples were further diluted 4 times in methanol. CD spectra were recorded on a J-810 spectropolarimeter (JASCO, Tokyo, Japan) using a 1 mm quartz cell cuvette and scanning from 200 to 350 nm at 25 °C; methanol was used as a blank.

3. RESULTS

3.1 CONVERSION OF THE SULFIDE 3-(METHYLTHIO)ANILINE

We selected seven microbial flavoprotein monooxygenases originating from three different microorganisms. Besides, three well-studied BVMOs, phenylacetone monooxygenase (PAMO) from *Thermobifida fusca* (Fraaije *et al.*, 2005), the Met446Gly PAMO mutant ($PAMO_{M446G}$) (de Gonzalo *et al.*, 2012) and cyclohexanone monooxygenase from *Acinetobacter calcoaceticus* ($CHMO_{Ac}$) (Pazmiño et al., 2009), two recently discovered BVMOs from *Rhodoccocus jostii* ($BVMO_{Rj4}$ and $BVMO_{Rj24}$) (Riebel, de Gonzalo and Fraaije, 2013) and a BVMO from the fungus *Myceliophthora thermophila* ($BVMO_{Mt1}$) were included in this study. Furthermore, we also included a representative of a newly discovered distinct subfamily of microbial monooxygenases, the so-called Type II FMOs, that share characteristics of both BVMOs and FMOs: FMO_{RjE} from *R. jostii* (Riebel, de Gonzalo and Fraaije, 2013). All studied monooxygenases belong to the Class B flavoprotein monooxygenases and, hence, are distantly related to mammalian FMOs as evidenced by significant sequence identities (20-40 %) and highly conserved sequence motifs (Krueger and Williams, 2005). Also the obtained crystal structures of a bacterial FMO and several BVMOs have confirmed that Class B flavoprotein monooxygenases share structural and mechanistic features (Malito et al., 2004; Alfieri et al., 2008). $CHMO_{Ac}$ and PAMO display complementary and broad substrate acceptance profiles (Pazmino & Fraaije, 2008), while the other monooxygenases have been hardly explored for their substrate scope. Therefore, we anticipated that by studying such a large panel of different microbial monooxygenases, several targeted compounds could be converted by one or more monooxygenases.

All monooxygenases were produced in *E. coli* as expression host. SDS-PAGE gel analysis confirmed high and quantitatively comparable overexpression in soluble form of all investigated enzymes. In all cell extracts, the expressed monooxygenase was the most prominent protein band on the SDS PAGE gel. Because *E. coli* does not contain any endogenous enzymes with similar activity, BVMO- or FMO-type monooxygenases, no enzyme purification step was required and the cell extracts were used for performing the conversions. As a first test substrate, 3-(methylthio)aniline was used. PAMO and PAMO mutants have been shown to be able to efficiently convert aromatic sulfides (de Gonzalo *et al.*, 2005). Human FMOs are also known for their ability to perform sulfoxidations of aromatic sulfides or

thioureas (Cashman and Zhang, 2006; Motika et al., 2007). Depending on the type of sulfide and FMO isoform, various enantioselectivities by mammalian FMOs have been described (Hai et al., 2009; Virkel et al., 2004; Moroni et al., 1995). Conversion of this relatively simple aromatic thioether was probed with all 7 studied monooxygenases. For the conversions, 3.0 mM 3-(methylthio)aniline was incubated with cell extracts supplemented with phosphite, NADPH and phosphite dehydrogenase to regenerate the reduced coenzyme. After 135 min incubation, product analysis was performed by chiral LC-MS/MS in the SRM mode. The absolute configuration of the observed sulfoxides was determined by CD spectroscopy of the isolated enantiomers. Control reactions also resulted in formation of low amounts of sulfoxides due to spontaneous reaction with molecular oxygen. These reactions are not enantioselective, and the observed amounts in the enzymatic conversions were corrected for the background oxidation level. All tested monooxygenases produced significant amounts of sulfoxides but with markedly different enantioselectivity (Figure 2). CD analysis of the 3-(methylthio)aniline sulfoxides formed in the $BVMO_{Rj4}$ and $BVMO_{Mt1}$ samples gave $[a]_D^{25}$ values of +20.8 and -16.0, respectively (Figure S1 supplemental data). Based on comparison with literature data for (*R*)-3-(methylthio)aniline we assign the first eluting enantiomer (at 8.4 min) to (+)-(*R*)-3-(methylthio)aniline sulfoxide and the second eluting enantiomer (at 11.2 min) to (-)-(*S*)-3-(methylthio)aniline sulfoxide (Slack et al., 2012; Folli et al., 1973).

Most monooxygenases have a preference for forming the (+)-(*R*)-3-(methylthio)aniline sulfoxide (*e.e.* values 66-88%). However, $BVMO_{Rj4}$ produced the (-)-(*S*)-3-(methylthio)aniline sulfoxide with an *e.e.* of > 99.5% showing that this set of monooxygenases allows the synthesis of both sulfoxide enantiomers in very good to excellent enantiomeric excess. Only $BVMO_{Rj4}$ and $BVMO_{Mt1}$ produced an additional sulfone product at less than 2% of the amount of the sulfoxide. The standard addition method was used to quantify the conversion of 3-(methylthio)aniline after 135 min incubation. The conversion reached 72% for $BVMO_{Rj24}$ and 97% for $BVMO_{Mt1}$ (Figures S2-S4 supplemental data). This indicates that with the current approach 4-5 mg of enantiopure sulfoxide metabolite is produced in 1 h using a cell extract from a 1 L culture.

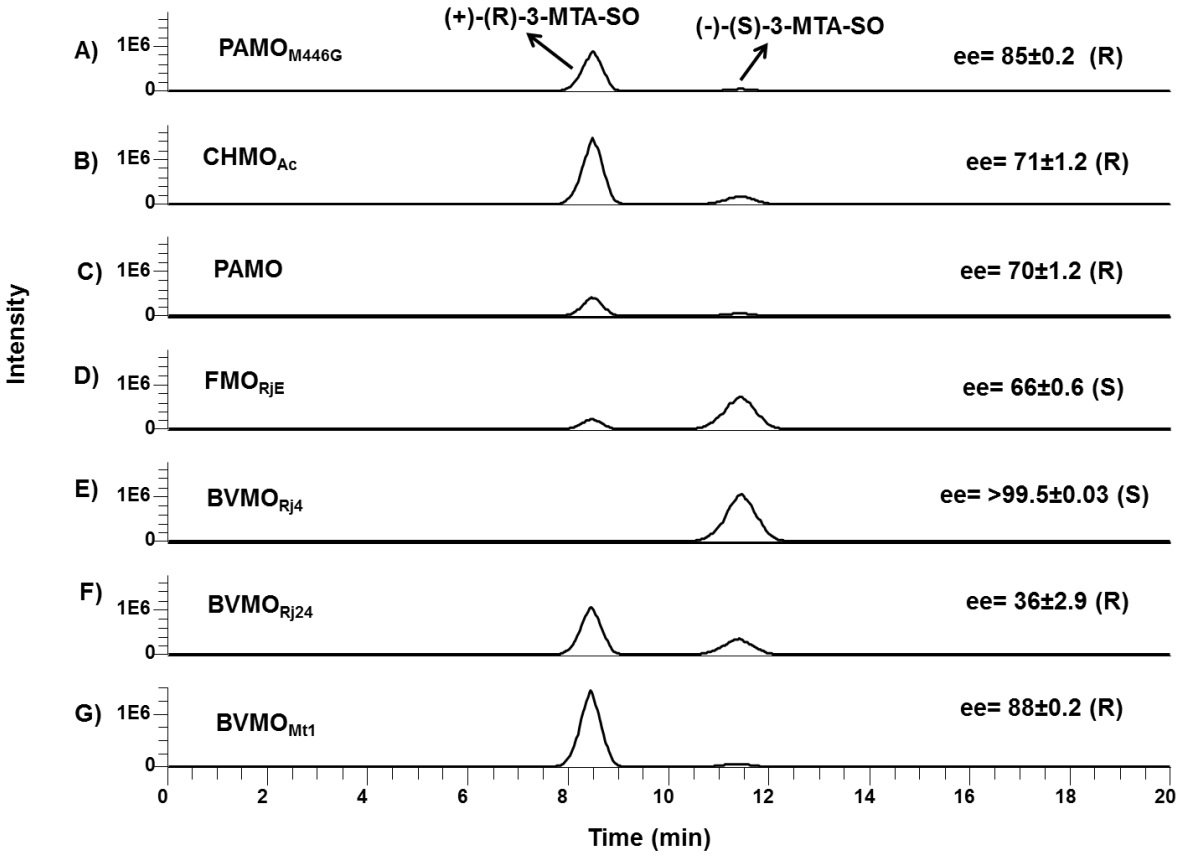

Figure 2: *Chiral LC-MS/MS in the SRM mode of 3-(methylthio)aniline sulfoxide (3-MTA-SO) (SRM transition: 156/93). 3-(methylthio)aniline was incubated for 135 min in the presence of the following microbial monooxygenases: a) PAMOM446G, b) CHMOAc, c) PAMO, d) FMORjE, e) BVMORj4, f) BVMORj24 and g) BVMOMt1. Based on CD analysis and data reported in the literature, the first eluting enantiomer at 8.4 min was assigned to (R)-3-methylthioaniline sulfoxide and the second eluting enantiomer at 11.5 min to (S)-3-methylthioaniline sulfoxide (Slack et al., 2012). The enantiomeric excess is given as e.e..*

3.2 Conversion of the thioether drugs, albendazole and fenbendazole

Two drugs that are commonly used to treat worm infestations in mammals, albendazole and fenbendazole, are known to be converted in an enantioselective manner into their sulfoxides by mammalian FMOs (Moroni et al., 1995; Virkel et al., 2004). Testing the panel of microbial monooxygenases revealed that three monooxygenases (CHMO$_{Ac}$, BVMO$_{Rj24}$ and BVMO$_{Mt1}$) converted albendazole, yielding sulfoxides in significant enantiomeric excess (Figure 3). Only BVMO$_{Mt1}$ was able to catalyze the sulfoxidation of fenbendazole. Determination of the $[\alpha]_D^{25}$values by CD analysis could not be performed, because the yields of the albendazole and fenbendazole sulfoxides were too low. However, the sulfoxide enantiomers of albendazole and fenbendazole have been characterized using the same chiral column and a similar solvent system by Materazzo et al. (2014), allowing us to assign the first eluting enantiomers to (*R*)-albendazole sulfoxide (3.1 min) and (*R*)-fenbendazole sulfoxide (3.5 min), respectively, and the second eluting enantiomers to (*S*)-albendazole sulfoxide (5.5 min) and (*S*)-fenbendazole sulfoxide (7.1 min), respectively. Chiral LC-MS/MS in the SRM mode

showed that $CHMO_{Ac}$ and $BVMO_{Mt1}$ formed the same product as mammalian FMOs, (*R*)-albendazole sulfoxide (32 and 55% *e.e.*, respectively), whereas $BVMO_{Rj24}$ enzyme produced (*S*)-albendazole sulfoxide with an enantiomeric excess of 95%. The yields of albendazole sulfoxide were determined with standard addition and reached 55% for $BVMO_{Rj24}$ and 25% for $BVMO_{Mt1}$ (Figures S5-S7 supplemental data). This corresponds to 1-2 mg/h and per L of bacterial culture. Less than 1% of the sulfone product was formed by $BVMO_{Rj24,}$ $BVMO_{Mt1}$ and $CHMO_{Ac}$ upon conversion. No other side products were detected. Chiral LC-MS/MS in the SRM mode showed that conversion of fenbendazole by $BVMO_{Mt1}$ yields (*S*)-fenbendazole sulfoxide in 96% *e.e.* (Figure 4).

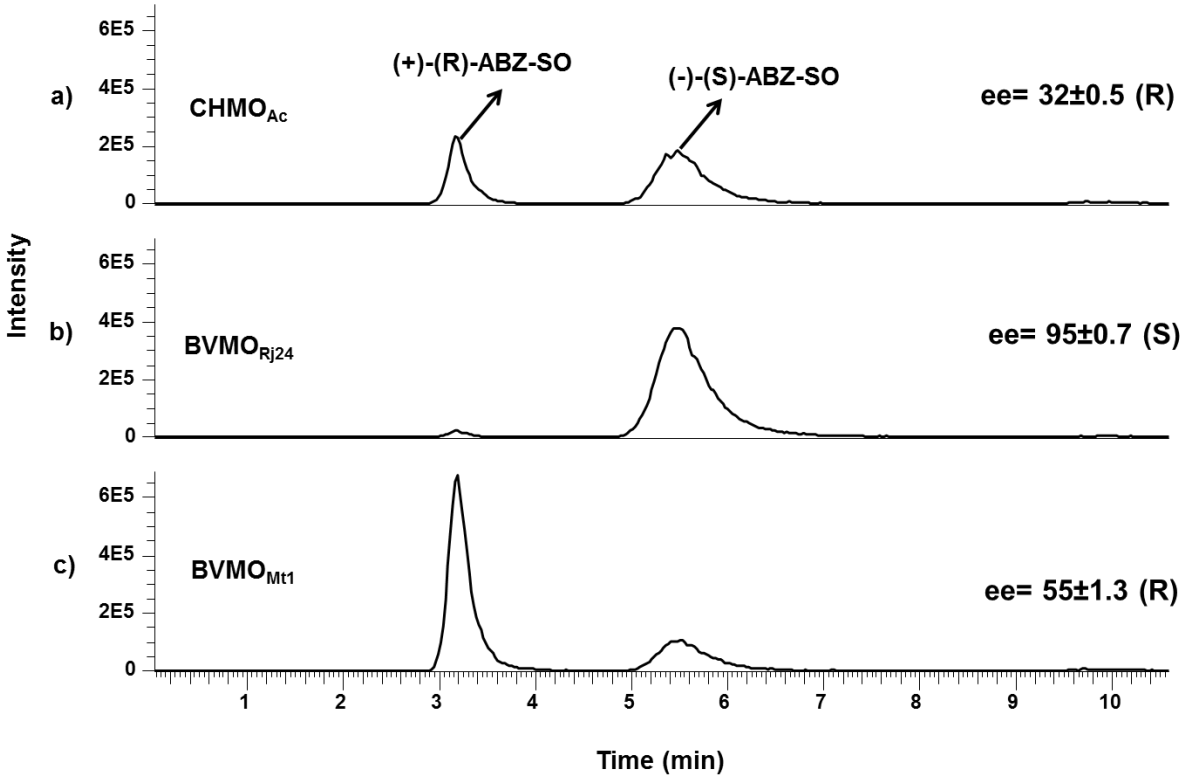

Figure 3: *Chiral LC-MS/MS in the SRM mode of albendazole sulfoxide (ABZ-SO) (SRM transition: 282/240). Albendazole was incubated for 135 min in the presence of the following monooxygenases: a) $CHMO_{Ac}$, b) $BVMO_{Rj24}$, c) $BVMO_{Mt1}$. The first eluting enantiomer at 3.1 min was assigned to (R)-albendazole sulfoxide and the second eluting enantiomer at 5.5 min to (S)-albendazole sulfoxide based on literature data (Materazzo et al., 2014).*

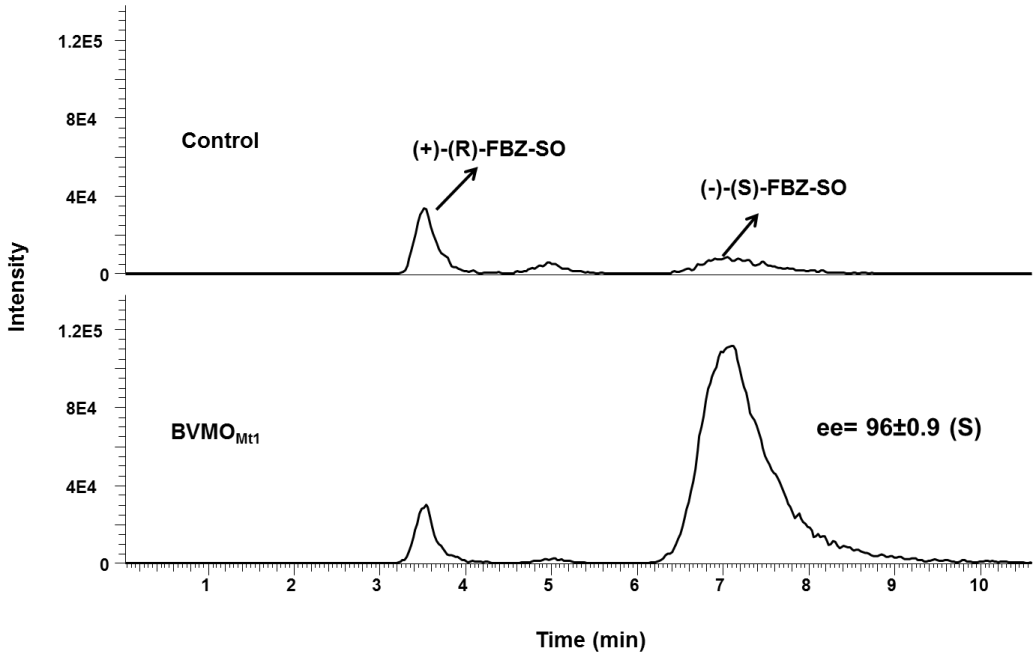

Figure 4: *Chiral LC-MS/MS in the SRM mode of fenbendazole sulfoxide (FBZ-SO) (SRM transition: 316/284). Fenbendazole was incubated for 135 min in the presence of the studied monooxygenases of which only $BVMO_{Mt1}$ showed activity. The first eluting enantiomer at 3.5 min was assigned to (R)-fenbendazole sulfoxide and the second eluting enantiomer at 7.1 min to (S)-fenbendazole sulfoxide based on literature data (Materazzo et al., 2014).*

3.3 CONVERSION OF THE AMINES, LIDOCAINE AND NICOTINE

Lidocaine and nicotine contain a regular and a cyclic tertiary amine group, respectively. Lidocaine is a widely-used local anesthetic while nicotine is a plant alkaloid which acts as a stimulant. Both drugs are known to be oxidized by mammalian FMOs into their corresponding N-oxides. LC-MS/MS analysis showed that significant conversion of lidocaine into the N-oxide is performed by $BVMO_{Rj24}$, while nicotine is converted by $CHMO_{Ac}$ (Figure 5). With the applied conditions, the degree of conversion for both substrates was rather low, below 10%.

For lidocaine no other products (specifically the cytochrome P450-catalyzed N-dealkylation or aromatic hydroxylation products) were observed in significant amounts. The N-oxide of lidocaine can be distinguished from other monooxygenation products by its specific SRM transition (*m/z* 251/130). Additionally, its retention time was confirmed using a chemically oxidized lidocaine N-oxide standard.

LC-MS/MS analysis of the nicotine conversion samples showed two N-oxidation products which could be assigned on the basis of their fragmentation patterns; the SRM transition of *m/z* 179/117 is unique for nicotine-1`-N-oxide (oxidation of nitrogen on the pyrrolidine ring) and the *m/z* 179/148 transition is unique for nicotine-1-N-oxide (oxidation of nitrogen on the pyridine ring) (Piller et al., 2014; Smyth et al., 2007). The nicotine-1`-N-oxide product was the major N-oxide formed by $CHMO_{Ac}$. The low amount of nicotine-1-N-oxide was similar to the amount formed in the control reaction.

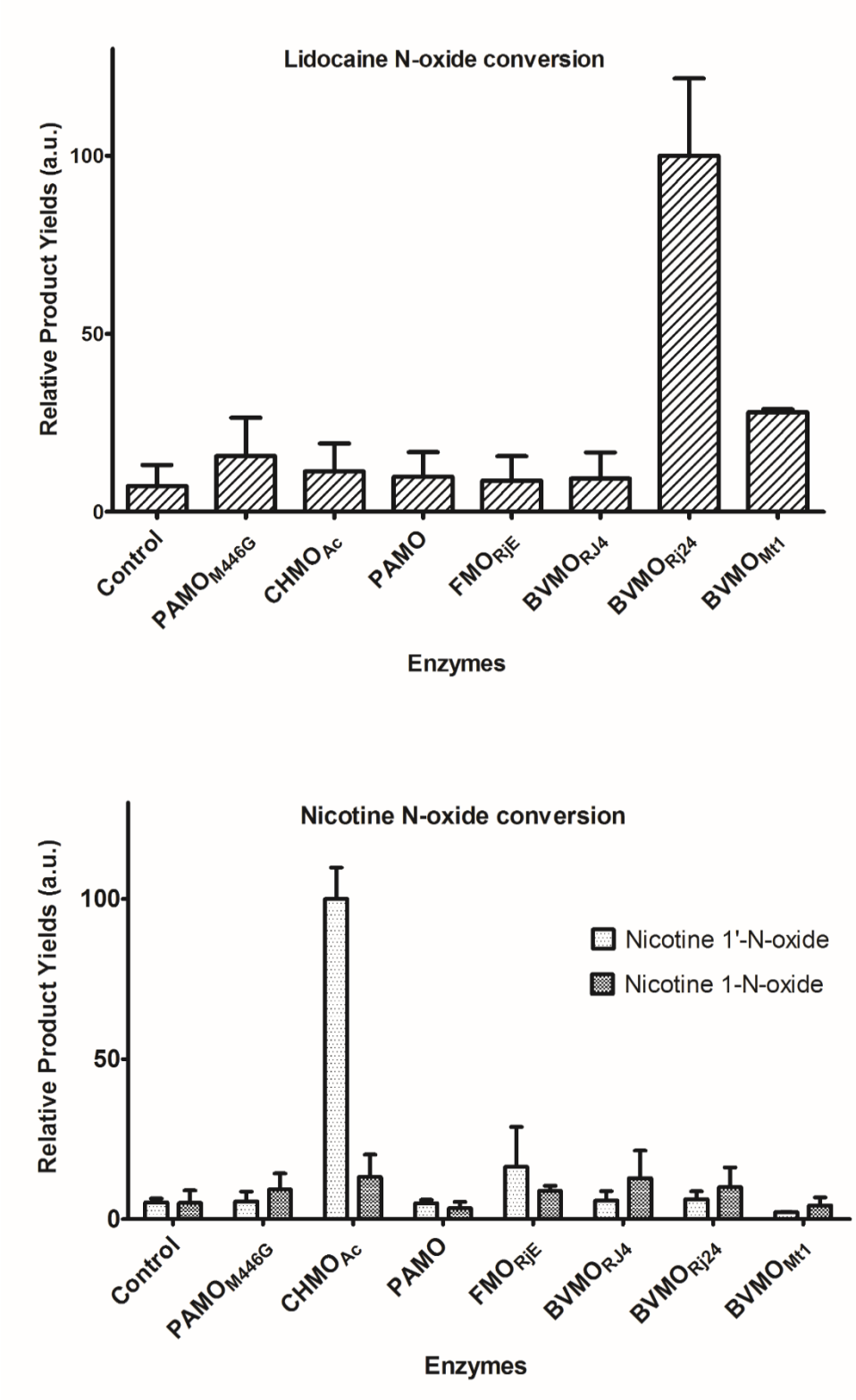

***Figure 5**: Relative yields of the N-oxide products of lidocaine (top) and nicotine (bottom) in the presence of different bacterial monooxygenases as determined by LC-MS/MS in the SRM mode. Experiments were performed in duplicate.*

4. DISCUSSION

Human FMOs and other mammalian FMOs play a crucial role in degrading a wide range of xenobiotics, including many drugs. While they are known for their chemo- and enantioselective oxidations, mammalian FMOs are notoriously difficult to obtain or to use as isolated biocatalysts. To provide an alternative for the biocatalytic production of FMO-derived metabolites, we explored the use of the microbial Class B flavoprotein monooxygenases which are all sequence-related to FMOs.

Besides sequence similarities, members of the Class B flavoprotein monooxygenases all share a similar structural fold. They are composed of FAD-binding domain with a tightly bound FAD as a prosthetic group and a NADPH binding domain which binds NADPH as coenzyme during catalysis (Krueger and Williams, 2005). In addition, kinetic and mechanistic studies on FMOs and BVMOs have revealed that these flavoprotein monooxygenases also share a common catalytic mechanism.

This is also reflected in the type of oxygenations reactions that are catalyzed by members of both monooxygenase groups: they overlap and include N-oxygenations, sulfoxidations and Baeyer-Villiger oxidations (Fiorentini et al., 2016). The catalytic cycle starts with binding of the reduced coenzyme NADPH which results in reduction of the flavin cofactor. Through a subsequent fast reaction with molecular oxygen, the peroxyflavin intermediate is formed that is key to catalyze substrate oxygenation (Beaty and Ballou, 1981; Pazmiño et al., 2008). The reactive peroxyflavin is stabilized through interactions with active site residues and awaits entry of a suitable substrate in the active pocket. The accessibility, character and size of the active site pocket determines the substrate specificity and the enantio- and regioselectivity of each monooxygenase. As a consequence and different from many other flavoprotein monooxygenases and CYP450, formation of the reactive oxygenating enzyme intermediate is not dependent on binding of a substrate. Many Class B monooxygenases, including human FMOs, have been shown to display a relaxed substrate acceptance profile. This triggered our study to explore the catalytic potential of microbial flavoprotein monooxygenases, that are sequence related to mammalian FMOs, for the conversion of FMO substrates. One of the advantages of using such enzymes for *in vitro* conversion of FMO-targeted xenobiotics is the ease of production of the microbial enzymes at high levels and in soluble form in *E. coli*. Upon growth of the recombinant bacteria, the cell extracts could be immediately used for conversion of the targeted xenobiotics. Another advantage of this approach is the fact that in the last decade a large number of recombinant microbial flavoprotein monooxygenases have become available. For example, we have generated an in-house library of >30 different microbial flavoprotein monooxygenases (Fraaije et al., 2005; Riebel et al., 2013). For our study we decided to explore a set of seven monooxygenases that are known to display dissimilar substrate acceptance and oxygenation selectivity profiles.

Five different xenobiotics (3-(methylthio)aniline, albendazole, fenbendazole, lidocaine and nicotine) were chosen to examine enantio-, region- and chemoselective oxygenation by using a panel of seven

different recombinant microbial flavoprotein monooxygenases. Chiral LC-MS/MS in the SRM mode was instrumental in establishing activity and selectivity of each enzyme towards each test compound. The enzymes that were found to be able to convert albendazole and fenbendazole formed the corresponding sulfoxides with very good enantiomeric excess. Both enantiomers of albendazole sulfoxide were produced in enantiomeric excess ($CHMO_{Ac}$ and $BVMO_{Mt1}$ for the (*R*)-sulfoxide and $BVMO_{Rj24}$ for the (*S*)-sulfoxide). Previously, it has been shown that mammalian FMOs have a preference for forming (*R*)-albendazole sulfoxide from albendazole (Virkel et al., 2004; Moroni et al., 1995). For fenbendazole, only one active enzyme ($BVMO_{Mt1}$) was identified which preferentially forms the (*S*)-sulfoxide. Fenbendazole has been shown to be converted into the (*R*)-sulfoxide by mammalian FMOs with significant enantiomeric excess (Virkel *et al.*, 2004). The observation that only one out of seven enzymes was active on fenbendazole may reflect the fact that fenbendazole differs from albendazole in having a phenyl moiety replacing a propyl moiety making it more bulky, sterically hindering oxidation of the thioether. It is worth mentioning that, except for the formation of low amounts of sulfones, no other oxidation products were formed upon conversion of the tested thioethers which demonstrates that the monooxygenases are chemo-, regio- and enantioselective. Monooxygenases that form the N-oxides of nicotine ($CHMO_{Ac}$) and lidocaine ($BVMO_{Rj24}$) were also identified. In the literature it was reported that human FMO3 is responsible for selective formation of nicotine-1`-N-oxide (Cashman *et al.*, 1992), which was also the major N-oxide formed by $CHMO_{Ac}$. This shows that the microbial monooxygenases can also be used for chemo- and regioselective N-oxidations of xenobiotics.

Our study illustrates that sequence-related microbial monooxygenases can be used for the production of FMO-related metabolites. As for mammalian FMOs (Wu et al., 2004; Cashman et al., 1992), each tested oxidation was very specific and no side products were formed in considerable amounts. This makes them interesting biocatalysts for the production of pharmaceutically relevant drug metabolites.

ACKNOWLEDGEMENTS

We thank Assunta Green (Chiral Technologies Europe) for screening chiral columns and Prof. Wesley Browne and PhD Yigit Altay (University of Groningen, Stratingh Institute for Chemistry) for CD analysis.

FOOTNOTES

The authors acknowledge funding from the Dutch Technology Foundation (STW) [Grant 11957]; and the Dutch Foundation for Scientific Research (NWO, ECHO) [Grant 711.012.006].

REFERENCES

Balke, K. et al., 2012. Discovery, application and protein engineering of Baeyer–Villiger monooxygenases for organic synthesis. Organic & Biomolecular Chemistry, 10(31), pp.6249–6265.

van Berkel, W.J.H., Kamerbeek, N.M. & Fraaije, M.W., 2006. Flavoprotein monooxygenases, a diverse class of oxidative biocatalysts. Journal of Biotechnology, 124(4), pp.670–689.

Cashman, J.R. et al., 1992. Metabolism of nicotine by human liver microsomes: stereoselective formation of trans-nicotine N'-oxide. Chemical research in toxicology, 5(5), pp.639–646.

Cashman, J.R. et al., 1995. Role of hepatic flavin-containing monooxygenase 3 in drug and chemical metabolism in adult humans. Chemico-Biological Interactions, 96(1), pp.33–46.

Cashman, J.R., 2005. Some distinctions between flavin-containing and cytochrome P450 monooxygenases. Biochemical and biophysical research communications, 338(1), pp.599–604.

Cashman, J.R., 2004. The implications of polymorphisms in mammalian flavin-containing monooxygenases in drug discovery and development. Drug Discovery Today, 9(13), pp.574–581.

Cashman, J.R. & Zhang, J., 2006. Human flavin-containing monooxygenases. Annual review of pharmacology and toxicology, 46, pp.65–100.

Dudek, H.M. et al., 2011. Mapping the substrate binding site of phenylacetone monooxygenase from thermobifida fusca by mutational analysis. Applied and Environmental Microbiology, 77(16), pp.5730–5738.

Folli, U., Iarossi, D. & Taddei, F., 1973. Intramolecular hydrogen bonds in aromatic sulphoxides: 1H nuclear magnetic resonance and acidity constant measurements. Journal of the Chemical Society, Perkin Transactions 2, (6), p.848.

Fraaije, M.W. et al., 2005. Discovery of a thermostable Baeyer–Villiger monooxygenase by genome mining. Applied Microbiology and Biotechnology, 66(4), pp.393–400.

Geier, M. et al., 2015. Human FMO2-based microbial whole-cell catalysts for drug metabolite synthesis. Microbial Cell Factories, 14(1), p.82.

de Gonzalo, G. et al., 2012. Improvement of the biocatalytic properties of one phenylacetone monooxygenase mutant in hydrophilic organic solvents. Enzyme and Microbial Technology, 50(1), pp.43–49.

de Gonzalo, G. et al., 2005. Oxidations catalyzed by phenylacetone monooxygenase from *Thermobifida fusca*. Tetrahedron: Asymmetry, 16(18), pp.3077–3083.

de Gonzalo, G., Mihovilovic, M.D. & Fraaije, M.W., 2010. Recent developments in the application of Baeyer-Villiger monooxygenases as biocatalysts. ChemBioChem, 11(16), pp.2208–2231.

Hai, X. et al., 2009. Enantioselective in-line and off-line CE methods for the kinetic study on cimetidine and its chiral metabolites with reference to flavin-containing monooxygenase genetic isoforms. Electrophoresis, 30(7), pp.1248–1257.

Krueger, S.K. & Williams, D.E., 2005. Mammalian flavin-containing monooxygenases: structure/function, genetic polymorphisms and role in drug metabolism. Pharmacology & Therapeutics, 106(3), pp.357–387.

Malito, E. et al., 2004. Crystal structure of a Baeyer-Villiger monooxygenase. Proceedings of the National Academy of Sciences, 101(36), pp.13157–13162.

Mascotti, M.L., Lapadula, W.J. & Juri Ayub, M., 2015. The origin and evolution of Baeyer-Villiger monooxygenases (BVMOs): an ancestral family of flavin monooxygenases. Plos One, 10(7), p.e0132689.

Materazzo, S. et al., 2014. Effect of the water content on the retention and enantioselectivity of albendazole and fenbendazole sulfoxides using amylose-based chiral stationary phases in organic–aqueous conditions. Journal of Chromatography A, 1327, pp.73–79.

Moroni, P. et al., 1995. Chiral sulfoxidation of albendazole by the flavin adenine dinucleotide-containing and cytochrome P450-dependent monooxygenases from rat liver microsomes. Drug metabolism and disposition: the biological fate of chemicals, 23(2), pp.160–165.

Motika, M.S. et al., 2009. Novel variants of the human flavin-containing monooxygenase 3 (FMO3) gene associated with trimethylaminuria. Molecular genetics and metabolism, 97(2), pp.128–135.

Motika, M.S., Zhang, J. & Cashman, J.R., 2007. Flavin-containing monooxygenase 3 and human disease. Expert Opinion on Drug Metabolism & Toxicology, 3(6), pp.831–845.

Piller, M. et al., 2014. Simple, fast and sensitive LC–MS/MS analysis for the simultaneous quantification of nicotine and 10 of its major metabolites. Journal of Chromatography B, 951–952, pp.7–15.

Reddy, R.R. et al., 2010. Characterization of human flavin-containing monooxygenase (FMO) 3 and FMO5 expressed as maltose-binding protein fusions. Drug Metabolism and Disposition, 38(12), pp.2239–2245.

Riebel, A., de Gonzalo, G. & Fraaije, M.W., 2013. Expanding the biocatalytic toolbox of flavoprotein monooxygenases from *Rhodococcus jostii* RHA1. Journal of Molecular Catalysis B: Enzymatic, 88, pp.20–25.

Shimizu, M. et al., 2015. Analysis of six novel flavin-containing monooxygenase 3 (FMO3) gene variants found in a Japanese population suffering from trimethylaminuria. Molecular Genetics and Metabolism Reports, 5, pp.89–93.

Slack, R.D. et al., 2012. Malaria-infected mice are completely cured by one 6 mg/kg oral dose of a new monomeric trioxane sulfide combined with mefloquine. Journal of Medicinal Chemistry, 55(1), pp.291–296.

Smyth, T.J. et al., 2007. Characterisation of nicotine and related compounds using electrospray ionisation with ion trap mass spectrometry and with quadrupole time-of-flight mass spectrometry and their detection by liquid chromatography/electrospray ionisation mass spectrometry. Rapid Communications in Mass Spectrometry, 21(4), pp.557–566.

Torres Pazmiño, D.E. et al., 2009. Efficient biooxidations catalyzed by a new generation of self-sufficient Baeyer-Villiger monooxygenases. ChemBioChem, 10(16), pp.2595–2598.

Torres Pazmiño, D.E. et al., 2008. Kinetic mechanism of phenylacetone monooxygenase from *Thermobifida fusca*. Biochemistry, 47(13), pp.4082–4093.

Torres Pazmiño, D.E. & Fraaije, M.W., 2008. Discovery, redesign and applications of Baeyer-Villiger monooxygenases. In T. Mastuda, ed. Future directions in biocatalysis. Amsterdam: Elsevier, pp. 107–128.

Virkel, G. et al., 2004. Comparative hepatic and extrahepatic enantioselective sulfoxidation of albendazole and fenbendazole in sheep and cattle. Drug metabolism and disposition: the biological fate of chemicals, 32(5), pp.536–544.

Wu, R.F. et al., 2004. Porcine FAD-containing monooxygenase metabolizes lidocaine, bupivacaine and propranolol in vitro. Life Sciences, 75(8), pp.1011–1019.

Ziegler, D.M., 1990. Flavin-containing monooxygenases: enzymes adapted for multisubstrate specificity. Trends in Pharmacological Sciences, 11(8), pp.321–324.

Ziegler, D.M., 1993. Recent studies on the structure and function of multisubstrate flavin-containing monooxygenases. Annual review of pharmacology and toxicology, 33, pp.179–199.

SUPPLEMENTAL DATA

QUANTIFICATION OF PRODUCT YIELDS WITH STANDARD ADDITION METHOD

3-(METHYLTHIO)ANILINE

Since a 3-(methylthio)aniline sulfoxide standard was not available, we measured the concentration of 3-(methylthio)aniline remaining after the 135 min conversion reaction. During the conversion reaction 3 mM 3-(methylthio)aniline was used. In the extraction step, the sample was diluted 4 times (to a nominal concentration of 750 μM) and in the SPE purification step it was diluted a further 20 times. For the LC-MS/MS quantification, control (extract with no monooxygenase expressed), $BVMO_{Rj24}$ and $BVMO_{Mt1}$ samples were diluted 10 times more, and used as unknowns in the standard addition method (see Table S3). All the quantification experiments were duplicated.

The control sample was used to determine the 3-(methylthio)aniline concentration after extraction and SPE cleanup, but without conversion. Samples were analyzed with LC-MS/MS and peak areas were plotted (Figure S2). According to the standard addition curve the concentration of unknown (control) was 3.2 μM. The remaining 3-(methylthio)aniline concentrations after 135 min incubation in $BVMO_{Rj24}$ and $BVMO_{C1a}$ samples were found to be 0.9 μM and 0.1 μM (Figure S3 and S4). Based on these concentrations and that of the control, the consumption of 3-(methylthio)aniline after 135 min incubation was calculated to be roughly 72% for $BVMO_{Rj24}$ and 97% for $BVMO_{Mt1}$, without correcting for recovery or sample instability during storage.

ALBENDAZOLE SULFOXIDE

$BVMO_{Rj24}$ and $BVMO_{Mt1}$ samples, which showed the highest of albendazole sulfoxide peaks in LC-MS/MS were used for quantification. The same extraction, SPE purification and dilution steps were followed for albendazole as stated for 3-(methylthio)aniline(see Table S3).

To a control extract 1 mM of ricobendazole (racemic albendazole sulfoxide) was added and used as a control (Figure S5) to correct for the loss during the extraction and SPE purification steps. The concentration determined to be 2.0 μM. The albendazole sulfoxide product concentrations were calculated to be 1.1 μM for $BVMO_{Rj24}$ and 0.5 μM for $BVMO_{Mt1}$. The estimated product yield of albendazole sulfoxide is therefore 55% for $BVMO_{Rj24}$ and 25% for $BVMO_{Mt1}$.

Table S1 Parameters for the MS analysis of the different substrates and their conversion products. Scan time, Q1 peak width and skimmer offset were set to 1 s, 0.70 amu FWHM and 0, respectively.

MS parameters Compounds	Spray Voltage V	Sheath gas	Auxiliary gas	Capillary Temp. °C	Tube lens offset	Scan Range m/z
3-(methylthio)aniline	2750	60	30	270	74	50-300
Albendazole	3000	30	15	300	90	50-400
fenbendazole	3000	40	15	350	90	50-500
lidocaine	3500	40	20	350	90	50-300
nicotine	2500	60	15	350	80	50-250

Table S2 *SRM transitions and corresponding collision energies for the substrates and their oxidation products. All SRM measurements were performed with a dwell time of 100 ms and Q1 and Q3 peak widths of 0.70 amu FWHM. 1 mTorr collision gas pressure was used for all compounds except for nicotine and its N-oxide products (1.5 mTorr).*

Compounds	SRM Transition *m/z*	Collision Energy (V)
3-(methylthio)aniline	140/93	20
3-(methylthio)aniline sulfoxide	156/93	20
albendazole	266/234	20
albendazole sulfoxide (ricobendazole)	282/240	20
fenbendazole	300/268	20
fenbendazole sulfoxide	316/191	21
lidocaine	235/86	30
lidocaine N-oxide	251/86	30
nicotine	163/132	20
nicotine-1`N-oxide	179/117	15
nicotine-1-N-oxide	179/148	15
acetaminophen (IS)	152/110	20

Table S3 *Standard addition method used for quantification of 3-(methylthio)aniline, albendazole and albendazole sulfoxide in enzymatic conversion. All dilution series had a total volume of 1 mL.*

Unknown (µL)	Acetaminophen (IS) (µL)	Reference std (µL)	Concentration of reference std (µM)	Water (µL)
100	100	0	0	800
100	100	100 (1 µM stock)	0.1	700
100	100	200 (1 µM stock)	0.2	600
100	100	400 (1 µM stock)	0.4	400
100	100	80 (10 µM stock)	0.8	720
100	100	160 (10 µM stock)	1.6	640

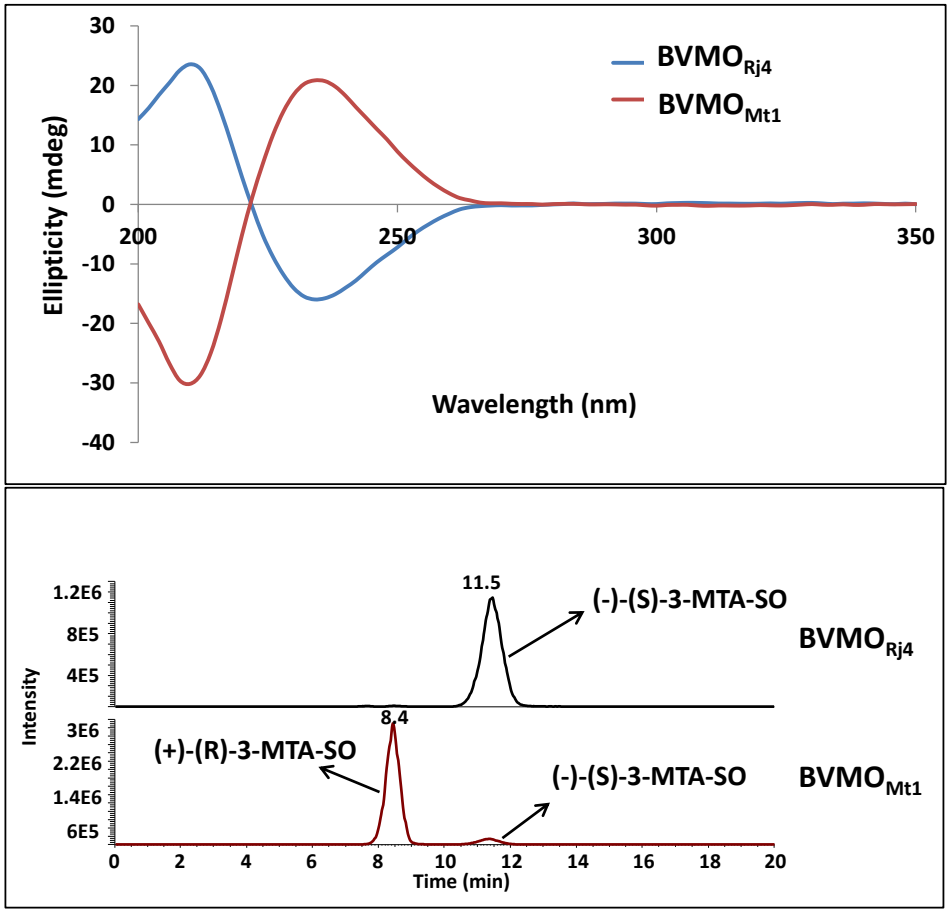

Figure S1 *Top panel: CD spectra of 3-methylthioaniline sulfoxide enantiomers. Bottom panel: assignment of the first eluting enantiomer to (+)-(R)-3-(methylthio)aniline sulfoxide and the second eluting enantiomer to (-)-(S)-3-(methylthio)aniline sulfoxide based on the CD spectra and reported* $[a]_D^{25}$ *value in literature data (Slack et al., 2012; Folli et al., 1973).*

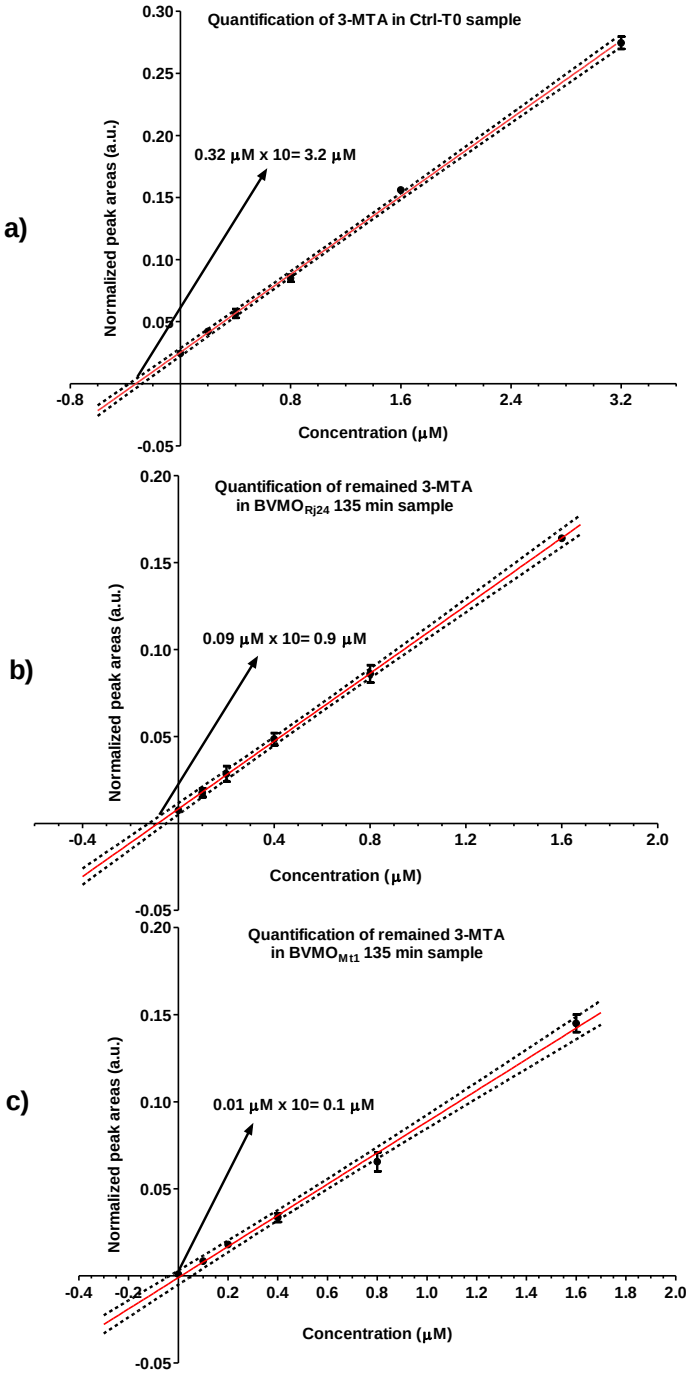

Figure S2*. Standard addition curve of 3-(methylthio)aniline. The concentration of 3-(methylthio)aniline in: a) control sample was found to be 3.2 µM, b) BVMO$_{Rj24}$ was found to be 0.9 µM, and c) BVMO$_{Mt1}$ was found to be 0.1 µM.*

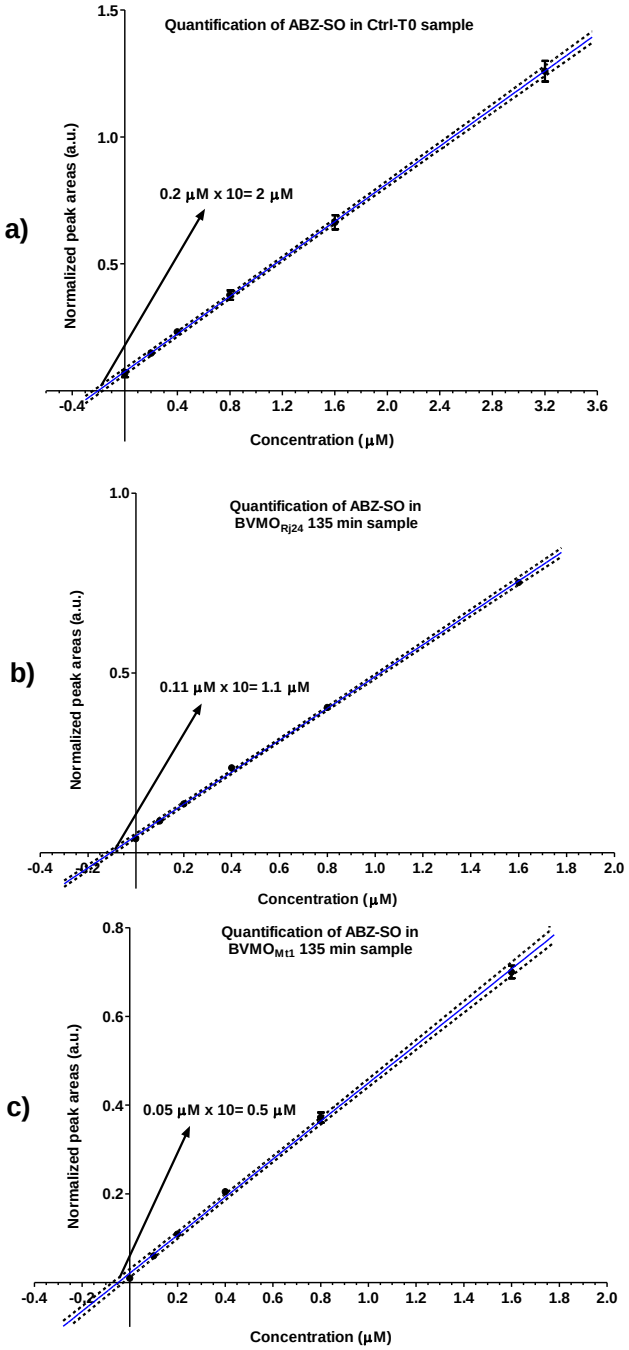

Figure S3. *Standard addition curves of albendazole sulfoxide. The concentration of albendazole sulfoxide in: a) control sample was found to be 2 µM, b) BVMO$_{Rj24}$ was found to be 1.1 µM, and c) BVMO$_{Mt1}$ was found to be 0.5 µM.*

CHAPTER 6

SUMMARY

Marzena Krzek, Marco W. Fraaije

Molecular Enzymology Group, University of Groningen, Nijenborgh 4, 9747 AG Groningen, The Netherlands

Nature harbours an enormous number of flavoproteins. Most of these proteins function as enzymes catalysing redox reactions in which the flavin cofactor plays a crucial catalytic role. Because of their catalytic properties, numerous flavoenzymes have found biotechnological applications. Especially the use of oxidative flavoenzymes can be highly attractive when enantio-, chemo- and/or regioselective oxidations need to be performed (Torres Pazmiño and Fraaije, 2008; de Gonzalo, Mihovilovic and Fraaije, 2010).

In the last decade, the toolbox of flavoenzymes has significantly expanded through the discovery of new enzymes and the redesign of existing ones (Balke *et al.*, 2012; Riebel *et al.*, 2012; Riebel, de Gonzalo and Fraaije, 2013; Mascotti, Lapadula and Juri Ayub, 2015). The work described in this thesis focused on expanding the applicability of flavoenzymes, particularly flavoprotein monooxygenases, by:

- exploring possibilities to produce and evaluate a set of flavoprotein monooxygenases, and
- developing a new method for selective immobilisation of flavoenzymes.

Chapter 2 - In this chapter a new flavin cofactor-mediated immobilization method is described. For this method, carrier material was covalently functionalised with a chemically modified FAD cofactor. The employed synthetic flavin cofactor contains a reactive group attached at the adenine N^6 moiety of the FAD cofactor. This moiety is the best position for attachment of a linker containing a reactive group as it is far from the redox-active part (isoalloxazine ring) of the cofactor. Furthermore, upon inspecting known FAD-containing flavoprotein structures, it can be concluded that the N^6 tends to be close to or even at the surface of flavoproteins, while the rest of the flavin cofactor is embedded within the protein matrix. As reactive group, a succinimidyl ester moiety was used which enabled efficient and specific covalent attachment of the synthetic flavin cofactor to a carrier decorated with primary amines. The generated FAD-coated carrier material was found to be highly stable and could be used for repetitive immobilizations of a prototype Baeyer-Villiger monooxygenase: phenylacetone monooxygenase (PAMO). Reconstitution of apo PAMO on the FAD-decorated material yielded a fully functional and reusable immobilized biocatalyst. Interestingly, the immobilized enzyme displayed enhanced thermostability versus non-immobilised enzyme. This novel method of immobilizing an enzyme via its flavin cofactor can be applied to other flavoenzymes as long as they (i) can be prepared in their apo form and (ii) bind to N^6-modified FAD. An particular attractive feature of this method is the ability to control the way an enzyme is immobilized. By altering the character and length of the linked attached to the FAD cofactor, the distance between the enzyme and the carrier and orientation of the enzyme can be fine-tuned. It allows the creation of defined monolayers of enzyme on a surface.

Chapter 3 - A downside of the procedure described in Chapter 2 is the poor availability of the required FAD derivative and lack of efficient synthetic routes towards such complex molecule. For

derivatization of the water-soluble FAD flavin cofactor, only a few chemical synthetic approaches have been published. This inspired us to develop a new synthetic approach for the preparation of N^6-modified FAD, with improved yield and time efficiency when compared with existing procedures. For that, a previously patented method served as a starting point (Krzek *et al.*, 2016). This method involves a two-step synthesis route in which alkylation at the FAD adenosine position 1 is performed first, and subsequently a Dimroth rearrangement into the N^6 derivative is performed. For an improvement of this procedure, we focused first on the design and synthesis of an alkylation agent with enhanced electrophilicity while containing a blocked primary amine, the terminal reactive group. The FAD substitution at the strongest nucleophilic atom (adenosine 1) was performed by using microwave irradiation and an optimised mixture of solvents (water/DMSO/DMF). This resulted in a relatively fast and effective alkylation. Purification of the alkylated flavin cofactor was also optimized. In the next step, the Dimroth rearrangement of the N^1–alkylated FAD into the N^6 analogue, was catalysed by using a buffered aquatic solution containing 5 % diethylamine, a non-basic nucleophile. This yielded an almost complete Dimroth rearrangement, which is a significant improvement when compared with previous reports. Within the same step, the reactive terminal amine is deprotected yielding the desired modified FAD which can be used for enzyme immobilization as described in Chapter 2. Overall this novel synthetic approach results in a better total yield and less side-products when compared with existing synthetic protocols.

Chapter 4 - Many flavoenzymes play important roles in drug metabolism in humans and other mammals. It is estimated that about ten percent of oxidative human metabolism is catalysed by the NADPH-dependent flavin-containing monooxygenase 3 (hFMO3). This microsomal enzyme converts xenobiotics containing nucleophilic heteroatoms like sulphur or nitrogen into easily secreted metabolites. It uses NADPH as natural electron donor and molecular oxygen as oxidant to perform oxygenations. Mammalian FMOs are difficult to obtain for biochemical studies. Their isolation is hampered by the fact that they are membrane associated. In addition, isolated hFMO3 displays low activity and is rather unstable. Attempts to produce hFMO3 and other FMO isoforms in a recombinant manner have met limited success. In the last decades research efforts have focused on finding efficient and cheap model systems for human metabolism. Chapter 4 presents an overview on the sequence and structural features of hFMO3. Besides that, it provides a summary of previous hFMO3 engineering and recombinant expression studies. Also our attempts to express hFMO3 fused to phosphite dehydrogenase (PTDH) in *Escherichia coli* are described. This resulted in low expression of functional hFMO3: using whole cells we could demonstrate that PTDH-hFMO3 can be produced in a bacterial host. Yet, improvement in PTDH-hFMO3 expression levels is needed to use *E. coli* as effective production system. If successful, it would generate an easy-to-use self-sufficient hFMO3 for metabolites preparation, as it can be driven with phosphite to regenerate the required NADPH.

Chapter 5 - As an alternative approach to generate drug metabolites we studied the use of microbial flavin-containing monooxygenases. By testing a panel of different flavoprotein monooxygenases, we could show that several prototype xenobiotics and drugs could be oxidized in a selective manner. With this, the formation of FMO-associated drug metabolites could be mimicked, circumventing the issues related to the in vitro use of hFMO3 and other mammalian FMOs. Enantio- and regiospecific FMO-dependent metabolites could be prepared using crude cells extracts containing recombinantly expressed flavoprotein monooxygenases. The use of the microbial monooxygenases was demonstrated for two substrate types: oxidations of sulphur-containing compounds (albendazole, fenbendazole) and nitrogen-containing compounds (nicotine, lidocaine).

In summary, this thesis presents new approaches towards applications of flavin-containing enzymes as biocatalysts. A novel method of cofactor-mediated immobilisation is described while also the use of microbial enzymes for the synthesis of drug metabolites is demonstrated. These findings will fuel future biotechnological applications in which flavin-containing enzyme can play a crucial role.

REFERENCES

Balke, K. et al., 2012. Discovery, application and protein engineering of Baeyer–Villiger monooxygenases for organic synthesis. Organic & Biomolecular Chemistry, 10(31), pp.6249–6265.

de Gonzalo, G., Mihovilovic, M.D. & Fraaije, M.W., 2010. Recent developments in the application of Baeyer-Villiger monooxygenases as biocatalysts. ChemBioChem, 11(16), pp.2208–2231.

Krzek, M. et al., 2016. Covalent immobilization of a flavoprotein monooxygenase via its flavin cofactor. Enzyme and Microbial Technology, 82, pp.138–143.

Mascotti, M.L., Lapadula, W.J. & Juri Ayub, M., 2015. The origin and evolution of Baeyer-Villiger monooxygenases (BVMOs): an ancestral family of flavin monooxygenases. Plos One, 10(7), p.e0132689.

Riebel, A. et al., 2012. Expanding the set of rhodococcal Baeyer-Villiger monooxygenases by high-throughput cloning, expression and substrate screening. Applied Microbiology and Biotechnology, 95(6), pp.1479–1489.

Riebel, A., de Gonzalo, G. & Fraaije, M.W., 2013. Expanding the biocatalytic toolbox of flavoprotein monooxygenases from *Rhodococcus jostii* RHA1. Journal of Molecular Catalysis B: Enzymatic, 88, pp.20–25.

Torres Pazmiño, D.E. & Fraaije, M.W., 2008. Discovery, redesign and applications of Baeyer-Villiger monooxygenases. In T. Mastuda, ed. Future directions in biocatalysis. Amsterdam: Elsevier, pp. 107–128.

NEDERLANDSE SAMENVATTING

Marzena Krzek, Marco W. Fraaije

Molecular Enzymology Group, University of Groningen, Nijenborgh 4, 9747 AG Groningen, The Netherlands

De natuur kent een grote verscheidenheid aan flavine-bevattende eiwitten. Een overgroot deel van deze eiwitten zijn enzymen die redox reacties katalyseren. De flavinecofactor speelt hierbij een cruciale rol. Vele flavine-bevattende enzymen worden toegepast in de biotechnologie, vooral voor oxidatieve reacties met enantio-, chemo- en regioselectiviteit (Torres Pazmiño and Fraaije, 2008; de Gonzalo, Mihovilovic and Fraaije, 2010).

Afgelopen decennium zijn veel nieuwe flavine-bevattende enzymen ontdekt. Ook zijn veel van de al bekende enzymen geoptimaliseerd door ze te modificeren (Balke *et al.*, 2012; Riebel *et al.*, 2012; Riebel, de Gonzalo and Fraaije, 2013; Mascotti, Lapadula and Juri Ayub, 2015). Het onderzoek dat beschreven wordt in dit proefschrift is gericht op het vergroten van de toepasbaarheid van deze enzymen, met de nadruk op flavine-bevattende monooxygenases, doormiddel van:

- Het onderzoeken van de mogelijkheden om een eeks flavine-bevattende monooxygenasen te produceren en te evalueren.
- Het ontwikkelen van een nieuwe methode voor de selectieve immobilisatie van deze enzymen.

Hoofdstuk 2 - In dit hoofdstuk wordt een nieuwe flavinecofactor-gemediëerde immobilisatie methode beschreven. Voor deze methode werd dragermateriaal covalent gefunctionaliseerd met een chemisch gemodificeerde flavine-adeninedinucleotide (FAD)-cofactor. De gebruikte synthetische flavinecofactor bevat een linker die via een reactieve groep aan het adenine N6-gedeelte van de FAD-cofactor is gebonden. Het N6-gedeelte is de beste positie voor het koppelen van een linker, aangezien het ver van het redoxactieve deel (isoalloxazine ring) van de cofactor ligt. Bovendien kan na het inspecteren van de eiwitstructuren van bekende FAD-bevattende eiwitten worden geconcludeerd dat de N6 zich dichtbij of zelfs op het oppervlak van deze eiwitten bevindt, terwijl de rest van de flavinecofactor zich binnen in de eiwitmatrix bevindt. Als reactieve groep werd een succinimidylestergroep gebruikt, die efficiënte en specifieke covalente binding tussen de synthetische flavinecofactor en het drager materiaal, dat gecoat is met primaire amines, mogelijk maakt. Het op deze manier gevormde dragermateriaal bleek zeer stabiel te zijn en kon worden gebruikt voor herhaaldelijk immobiliseren van een prototype Baeyer-Villiger monooxygenase: fenylacetonmonooxygenase (PAMO). Reconstitutie van apo PAMO op het verkregen dragermateriaal leverde een volledig functionele en herbruikbare geïmmobiliseerde biokatalysator op. Interessant genoeg vertoonde het geïmmobiliseerde enzym verbeterde thermostabiliteit ten opzichte van niet-geïmmobiliseerd enzym. Deze nieuwe methode voor immobilisatie van een enzym via zijn flavinecofactor kan worden toegepast op andere flavine-enzymen zolang ze (i) bereid kunnen worden in apo-vorm en (ii) binden aan N6-gemodificeerd FAD. Een bijzonder aantrekkelijk kenmerk van deze methode is het vermogen om de manier waarop een enzym geïmmobiliseerd wordt te bepalen. Door het karakter en de lengte van de linker van de synthetische FAD-cofactor te veranderen, kan de afstand tussen het enzym en de drager en de oriëntatie ten opzichte van het enzym worden verfijnd. Het laat de totstandkoming van gedefinieerde monolagen van enzym op een oppervlak toe.

Hoofdstuk 3 - Nadelen van de methode die wordt beschreven in hoofdstuk 2 zijn: de gebrekkige beschikbaarheid van het vereiste FAD-derivaat, en het ontbreken van efficiënte synthetische routes om een dergelijk complex molecuul te produceren. Voor de derivatisatie van wateroplosbaar FAD zijn slechts enkele chemische synthese routes gepubliceerd. Het gebrek hieraan heeft ons geïnspireerd om een nieuwe en verbeterde synthese route te ontwikkelen voor de productie van N6-gederivatiseerd FAD. Een synthese route met een verbeterde opbrengst- en tijdsefficiëntie in vergelijking met bestaande procedures. Een eerder gepatenteerde methode diende hiervoor als uitgangspunt (Krzek *et al.*, 2016). Deze methode omvat een synthese route die bestaat uit twee stappen. In de eerste stap wordt FAD adenosine positie 1 gealkyleerd waarna deze in een tweede stap wordt omgezet naar het N6-derivaat via een Dimroth-omlegging. Voor verbetering van deze methode richtten we ons eerst op het ontwerp en de synthese van een alkyleringsmiddel met verhoogde elektrofiliciteit, waarbij de reactieve groep, een primaire amine, is afgeschermd. De FAD substitutie van het sterkste nucleofiele atoom (adenosine 1) werd uitgevoerd met behulp van microgolfbestraling en een geoptimaliseerd mengsel van oplosmiddelen (water / DMSO / DMF). Dit resulteerde in een relatief snelle en effectieve alkylering. Zuivering van de gealkyleerde flavin cofactor werd ook geoptimaliseerd. In de volgende stap werd de Dimroth-omlegging van het N1-gealkyleerde FAD in het N6-analoog gekatalyseerd door gebruik te maken van een gebufferde waterige oplossing dat 5% diethylamine bevatte, een niet-basisch nucleofiel. Dit resulteerde in een bijna complete Dimroth-omlegging, wat een significante verbetering is in vergelijking met eerdere publicaties. In dezelfde stap wordt afscherming van de reactieve terminale amine opgeheven, waardoor de gewenste gemodificeerde FAD wordt verkregen die kan worden gebruikt voor enzym immobilisatie zoals beschreven in hoofdstuk 2. Deze nieuwe synthetische aanpak resulteerde in een betere totale opbrengst en minder bijproducten ten opzichte van bestaande synthetische protocollen.

Hoofdstuk 4 - Veel flavine-bevattende enzymen spelen een belangrijke rol in het metabolisme van mensen en andere zoogdieren om geneesmiddelen af te breken. Naar schatting wordt ongeveer 10 procent van het oxidatieve menselijke metabolisme gekatalyseerd door het NADPH-afhankelijke flavine-bevattende monooxygenase 3 (hFMO3). Dit microsomale enzym zet xenobiotica, die nucleofiele heteroatomen bevatten zoals zwavel of stikstof, om in gemakkelijk te scheiden metabolieten. NADPH wordt gebruikt als natuurlijke elektronen donor en moleculaire zuurstof als oxidator om oxygenaties te verrichten. FMO’s van zoogdieren zijn moeilijk te verkrijgen voor biochemische studies. Hun isolatie wordt belemmerd door het feit dat ze membraan geassocieerd zijn. Daarnaast heeft geïsoleerde hFMO3 een lage activiteit en is het instabiel. Pogingen om hFMO3 en andere FMO-isovormen op een recombinante manier te produceren hadden slechts beperkt succes. Onderzoek heeft zich in de afgelopen decennia gericht op het vinden van efficiënte en goedkope model systemen voor de menselijke stofwisseling. Hoofdstuk 4 geeft een overzicht van de eiwitsequentie en de structurele eigenschappen van hFMO3. Daarnaast geeft het een samenvatting van

eerdere studies naar de engineering en recombinante expressie van hFMO3. Ook worden onze pogingen tot heterologe expressie van hFMO3, gefuseerd aan fosfiet dehydrogenase (PTDH), in *Escherichia coli* beschreven. Dit resulteerde in een lage expressie van actief hFMO3. Met behulp van hele cellen konden we aantonen dat PTDH-hFMO3 in een bacteriële gastheer kon worden geproduceerd, hoewel verbetering van het expressieniveau vereist is om *E. coli* als effectief productiesysteem te gebruiken. Indien dat lukt, dan zou dit een eenvoudige zelfvoorzienende hFMO3 voor metabolietpreparatie opleveren, aangezien het systeem met fosfiet kan worden aangedreven om de vereiste NADPH te regenereren.

Hoofdstuk 5 - Als alternatieve aanpak om geneesmiddelmetabolieten te produceren, bestudeerden we het gebruik van bacteriële flavine-bevattende monooxygenasen. Door verschillende flavine-bevattende monooxygenasen te testen, konden we aantonen dat verschillende prototype xenobiotica en medicijnen op een selectieve manier geoxideerd konden worden. Hiermee zou de vorming van FMO-geassocieerde geneesmiddelmetabolieten kunnen worden nagebootst, om zo de problemen met het *in vitro* gebruik van hFMO3 en andere zoogdier-FMO's te omzeilen. Enantio- en regiospecifieke FMO-afhankelijke metabolieten kunnen worden bereid met behulp van ruwe celextracten die recombinant tot expressie gebrachte flavine-bevattende monooxygenasen bevatten. De bacteriële monooxygenasen werden toegepast voor twee soorten substraat: oxidaties van zwavelhoudende verbindingen (albendazol, fenbendazool) en stikstofbevattende verbindingen (nicotine, lidocaïne).

Samengevat presenteert dit proefschrift nieuwe benaderingen voor de toepassingen van flavine-bevattende enzymen als biokatalysatoren. Een nieuwe methode van cofactor-gemediëerde immobilisatie wordt beschreven terwijl ook het gebruik van bacteriële enzymen voor de synthese van geneesmiddelmetabolieten wordt aangetoond. Deze bevindingen zullen toekomstige biotechnologische toepassingen stimuleren waarin flavin-bevattende enzymen een cruciale rol kunnen spelen.

STRESZCZENIE

Marzena Krzek, Marco W. Fraaije

Molecular Enzymology Group, University of Groningen, Nijenborgh 4, 9747 AG Groningen, The Netherlands

Natura zaskarbia szeroką gamę flawoprotein. Większość z nich pełni funkcje enzymów, które katalizują reakcje redox, przy których kofaktor flawinowy pełni kluczową rolę. Ze względu na te właściwości wiele flawoenzymów odnalazło biotechnologiczne zastosowania. W szczególności enzymy które przeprowadzają procesy utleniania są atrakcyjne ze względu na ich enancjo-, chemo- i/oraz region-selektywność (Torres Pazmiño and Fraaije, 2008; de Gonzalo, Mihovilovic and Fraaije, 2010). W ostatniej dekadzie zasób poznanych i dostępnych flawoenzymów znacznie się poszerzył dzięki owocnym odkryciom (enzyme discovery) pośród mniej lub bardziej egzotycznych organizmów. Obecnie enzyme discovery skupia się głównie na mikroorganizmach ze względu na łatwiejsze klonowanie do zastosowalnych na skalę przemysłową systemów ekspresyjnych (*E. coli*) i późniejszą inżynierię. Sama inżynieria białkowa pozwoliła na ulepszenie między innymi (termo)-stabilności obecnie poznanych enzymów co również ułatwia ich potencjalne zastosowania przemysłowe (Balke *et al.*, 2012; Riebel *et al.*, 2012; Riebel, de Gonzalo and Fraaije, 2013; Mascotti, Lapadula and Juri Ayub, 2015). Ta rozprawa doktorska skupia sie na poszerzeniu spoektrum zastowań flavoenzymów poprzez:

- Ocenę możliwości wydajnej heterogenicznej produkcji
- Rozwój metodologii selektywnej immobilizacji flawoenzymów

Rozdział 2 – W tym rozdziale opisana została nowa technika kowalencyjnej immobilizacji flawoenzymów poprzez ich cofaktor - dinukleotyd flawinoadeninowy (FAD). Pierszym krokiem do rozwinięcia takiego systemu jest synteza pochodnej FAD prowadząca do ubogacenia tej cząsteczki w aktywną chemicznie grupę zdolną utworzyć kowalencyje wiązanie do złoża. Najbardziej odpowienim atomem do którego warto przywiązać grupę aktywną jest N^6 na części adeninowej, gdyż 1) azot ten znajduje się daleko od centurm red-ox FAD, które jest lokalizowane na pierścieniu izoalloksazynowym (nie zmieni to właściwości katalitycznych czasteczki) oraz 2) w większości flawoenzymów azot ten jest wyeksponowany blisko powierzchni białka, co ułatwi stworzenie wiązania kowalencyjnego bez naruszenia struktury białowej. [Ciekawostka:Pozostała, nieadeninowa część kofaktora FAD we flawoenzymach lokuje się w głębszych partiach proteiny. Fakt ten jest spowodowany sekwencją białkową oksydoreduktywnych flavoprotein – w większości tego rodzaju białek motyw Rossmana odpowiedzialny (skwencja białkowa umożliwiająca wiądanie adeniny, w tym kokretnym przypadku adeniny z FAD) znaduje się blisko N-końca]

W opisanych tutaj badanich jako reakwynę grupę wprowadzaoną do FAD zastosowano malenoid, który tworzy stabilne chemiczne wiązania z aminami. Do immobilizacji zastosowano komercyjną Sepharozę z terminalnymi grupami aminowymi. Po sprzęgnięciu pochodnej FAD zawierającej malenoid do tego złoża otrzymano materiał który posłużył do immobilizacji apo-flaoenzymów (flawoenzymów pozbawionych flawinowego kofaktra, czyli FAD). Materiał ten mógł być wielokrotnie wykorzystany. Tetsy przeprowadzono na modelowym enzymie Monooxygenazie

Fenyloacetonowej (PAMO), [który katalizuje rekacje Baeyer-Villigera, czyli wprowadzenia atomu tlenu w pozycję alfa do ketonów i aldehydów]. Zanotowano zrekonstułowanie apo enzymu na tak przygotowanym materiale do w pełni funkcjonalnego holoenzymu, który mógł być wielkrotnie użyty do katalizy. Ważnym faktem jest, że flawoenzym zimmobilizowany poprzez kofaktor flawinowy zyksał na (termo)-stabiliności. Ta nowa technika immobilizacji może znaleźć szerokie zastosowanie dla innych flawoenzymów nie mniej jednak ma to swoje obwarowania. Po pierwsze (i) dla danego białka przegotowanie apoenzmu powinno być łatwo osiągalne. Po drugie (ii) apoenzym ten powiniem efektywnie wiazac chemicznie zmodyfikowany kofaktor FAD i w efekcie tego zdarzenia odzyskać funkcjonalną holoformę.

Szczególne atrakcyjną cechą tej metody immobilizacji jest możliwość kontroli dystrybucji enzyme na powierzchni nośnika – nie tylko jeśli chodzi o jego zagęszczenie - poprzez zastosowanie złoża z odpowiednim zagęszczeniem grup przeznaczonych do funcjonalizacji, ale także odległość enzymu od złoża - poprzez wprowadzenie pożądanego spacera pomiędzy grupą aktywą i FAD. Pozwala to na zorganizowanie cząseczek enzymu na złożu w postaci monowarstwy, co tez jest często porządane w przypadku np. zastosowań elektorchemicznych.

Rozdział 3 – Procedura opisana w Rozdziale 2 może być wykonana tylko przy zastosowaniu odpowiedniej pochodnej FAD. Synteza tego rodzaju molekuł w chwili obecnej nie należy do najbardziej wydajnych i wymaga optymizacji. FAD jest złożoną cząsteczką, która zawiera wiele grup funkcyjnych, jest rozpuszcalania niemal tylko w środowisku wodnym a także jest niestabilna w wysokiej temperaturze skrajnym pH oraz podczas ekspozycji na światło. Fakty te wpłynęły motywująco do podjęcia optymalizacji syntezy tej istotnej to kowalnecyjnej immobilizacji enzymów molekuły: FAD modyfikają na atomie N^6adeniny. Jako punkt początkowy przyjęto publikacje opartą na wczesniejszym patencie (Bückmann, Wray and Stocker, 1997). Opisana tam synteza jako substrat używa FAD I jest dwuetaopa: pierwszy krok to alkilacja azotu N^1 w części adeninowej poprez atak elektrofilowy. Następny etap to reogranizacja zakliwowanej molekuły z pozycji N^1 do N^6 na drodze mechanizmu Dimrotha (Dimroth rearrangement). Opisana w tej rozprawie doktorkiej synteza ma podwyzszoną wydajność oraz skrócony czas syntezy w porównaniu do wpomnianej wcześniej literatury. W pierwszej kolejności skupiliśmy się na zaprojektowaniu i syntezie optymalnego czynnika alkilującego, którego chatakteryzuje silna elektrofilowość (koniec doprzęgający do FAD) oraz obecnością zablkowanej aminy (przeciwległy koniec który pozsłuży do późniejszej kowalencyjnej imobilizacji na złożu).

Pierwszy step alkilacji cząsteczki FAD na atomie adeniny N^1 został przeprowadzony w mieszaninie rozpuszczalników zoptymizowanej pod kątem rozpuszczalności flawiny oraz jak największej zawartości rozpuszczalnika organicznego (aby móc rozpuścić czynnik alkilujący); mianowicie DMSO/DMF/woda w proporcji objętościowej 2:1:2. Ponadto, do tego etapu zastosowano podwyżoną temperaturę wywołaną ekspozyją na mikrofale. Ta taktyka zaowocowała przyspieszoną i wydajną

alkilacją. Oczyszczenie produktu z mieszaniny reakcyjnej zostało ograniczne jedynie do ekstrakcji gdyż pochodna FAD podtawiona w pozycji N^1 jest nietrwała. W następnym etapie process reorganizacji Dimrotha został wywołany 5% dietylaminą którą klasyfikuje się jako niezasadowy nukleofil. Podejście to pozwoliło na praktycznie ilościową reorganizację przy zachowaniu struktury FAD. Te same warunki pozwoliły na odblokowanie grupy aminowej w tym samym etapie (5% dietylamina). Finalny produkt: FAD z pierwszorzędową grupą aminową podstawioną przy pozycji N^6 został otrzymany z wyższą niż opublikowane do tej pory wydajnością oraz znacznie mniejszą ilością produktów ubocznych. Po oczyszczeniu z diethylaminy (etap ten nie jest w pełni wydajny), która konkuruje z aktynością aminy pierwszorzędowej produkt jest gotowy do chemoselektywnego dołączenia do złoża.

Rozdział 4 – Rodzina flawoenzymów należąca do grupy Monooxygenaz pełni istotną rolę podczas metabolizmu leków u ssaków (znawa dalem enzymami FMO). Szacuje się że u człowieka około 10% oksydatywnego metabolizmu jest katalizowane przez wpomniane flawoenzymy, które wykazują zalżność od donora elektronowego - NADPH. U ludzi najistotniejszym ze względu na procentowość przeprowadzanego metabolizmu jest monooxygenaza 3 (hFMO3). Ten mikrosomalny enzym metabolizuje cząsteczki ksenobiotyków, które posiadają atomy nuklefilowe (takie jak azot czy siarka) do produktów o obniżonej toksyczności i podwyżonej ekstraktowalności ludzkiego ciała dzięki zwiększeniu lokanego ładunku w molekule. Dlategoteż FMO mają orgomny potencjał (rynkowy) do badań nad metabolizmem potenjalnych/nowych leków oraz produkcji ludzkich meabolitów. Stanowią one bardzo dobry model dla tych procesów.

Ssacze enzymy FMO są bardzo trudne do wyizolowania nie tylko ze względu na wiązanie do błony mikrosomalnej lecz take ze względu na ich niską stabilność (nawet w 37 stopniach). Ponadto detekcja ich aktywności jest trudna ze względo na ich bardzo ich bardzo małą wydajność katalityczną (rzędu minut). Do chwili obecnej podjęte próby nad heterogeniczną ekspresją i wyizolowaniem hFMO3 zarówno jak i pozostałych FMO napotkały wiele - między innymi wpsomnianych wcześniej - ograniczeń i zakonczyły się tylko częściowym sukcesem.

W Rozdziale 4 przedstawione zostały: podsumownaie podjętych dotąd badań nad hFMO3 a także podsumowanie infomacji o strukturze tego białka, które nigdy nie zostało skrystalizowane. Opisane zostały także wcześniejsze próby inżynierii hFMO3. Inoformacje te zostały uzupełnione o wyniki badań przeprowadzonych podczas tego dotoratu, gdzie: z sukcesem skonowano hFMO3 do *E. coli* i wyekspresjonowano aktywny enzym. Ponadto uzyskano w pełni funcjonalną fuzję z enzymem dehydrogenazą fosfatową (PTDH), która pozwala na przeprowadzenie katalizy bez dodtaku bardzo drogiego NADPH. [Jest to nazywane samowystarczalą monooksygenazą (self-sufficient monooxygenase), gdyż ta grupa enzymów w nature zawsze wymaga dostarcznia elektronów przez NADPH. Inaczej mówiąc w nature monooxygenazy są NAPDH-zależne]. Dodatkowo, fuzja z PTDH zwiększyła poziom ekspresji aktywnego białka w komórkach *E. coli*. Jest to istotne z punktu widznia

efektownej produkcji enzymów, która przy przekroczeniu progu komercyjnych wymogów może zaowocować zastosowaniem ludzkiego ezymu do modelowych procesów ludzkiego metabolizmu.

Rozdział 5 – Jako alternatwnę do produkcji ludzkich metabolitów zastosowaliśmy termostabiline i rozpuszczalne FMO pochodznia mikrooragnizmalnego. Ich przewagę nad ludzkim hFMO3 stanowi wyższa aktywność kataliczna i podwyższona stabilność w temeraturach nawet wyższych niż ludzkiego ciała (szybsza późniejsza bio-synteza) a także łatwość w potencjalnym wyizolowaniu z bakterii. Po przetestowaniu panelu odkrywych niedawno termostabilinych i niebłonowych FMO odnaleźliśmy enzymy o aktywności zbliżonej do ludzkiego hFMO3. Metabolizm tego białka można podzielić na dwie główne kategorie – utlenianie ksenobiotyków zaiwerających azot (nikotyna, lidokaina) do nie-enancjoselektywnych produktów, oraz ksenobiotyków zawierających siarkę (n.p. albendazole, fenanbendazol) do enancjoselektywnych produktów. Oba typy ludzkich metabolitów mogły być przygotowane używając termostabilincyh enzymów heterologiczne wyekspresjonowanych w *E. Coli*. Do tej biosyntezy użyto zagęszczonego homogenizatu bakteryjengo.

Podsumowując, nowe metodologie nakierowane na zwiększenie aplikowalności flawoenzymów jako biokatalizatorów do zastosowań farmaceutycznych i przemysłowych zostały opisane w tej pracy doktorskiej. Między innymi immobilizacja poprzez kofaktor flawinowy a także wykorzystanie enzymów pochodzenia mikroognamiznalnego do produckji ludzkich metabolitów zostały zademonstrowane. Odkrycia te umożliwią wydajniejsze biotechnologiczne zastosowanie flawoenzymów w przyszłości.

ACKNOWLEDGMENTS

My PhD research has taken 4 years and 3 months of my life. Over this time I have interacted with multiple interesting, (mostly) very helpful and diligent people. I dedicate this chapter to all, who contributed to my PhD in both, a direct and non-direct manner.

First of all, I would like to express my gratefulness to prof. Marco Fraaije for giving me the opportunity to complete my PhD thesis in the multicultural, vibrant city of Groningen among (excellent) researchers. Tank you prof. R. Bischoff for being my second supervisor and together with dr. H. Permentier for the collaboration and publishing.
My acknowledgments I would like to direct to the reading committee: prof. Dick Janssen, prof. Willem van Berkel and prof. Giovanni Maglia for the review of my Thesis.

I would like to thank all the experts with whom I collaborated:

First, I would like to express my appreciation towards all who helped me with the organic part of my thesis. Thank to prof. Adriaan Minnaard for hosting me in his laboratory during the synthesis of a FAD cofactor derivative. Jeffrey – it was interesting to do some (working!) chemistry. Thank you for the broad introduction, sharing your expertise and lots of discussions. It was nice to work for few months in the Chemical Biology group. Besides, I direct my acknowledgments to Peter van der Meulen for substantial help with my NMR experiments and Theodora for HR-MS. Eric, Hugo – thank you for the patient answers to all my questions!

I want to thank to all, with whom I did shorter projects. Dear prof Willem van Berkel, I was honored to conduct some research at the Wageningen University with you and Adri. Our conversation/discussions during scientific gatherings were for me valuable and memorable; I also want to thank Dr. Dirk Holtman for allowing me to conduct QCM at the DECHEMA. In addition, I want to express my gratefulness to Dr. Dirk Heering for sharing his broad electro-enzymological expertise with me and very valuable discussions. Dirk, I am looking forward to see publications of your more recent, interesting findings and your fresh view on the (published) data. It has a great added value to the development of the narrow electroenzymology field.
I would like to thank Filippo from Structural Biology group at the University of Pavia for very lengthy and unfruitful discussions about the still mysterious hFMO3 enzyme, and together with Valentina for the nice time at the scientific meetings.

My acknowledgments for all the committee users of the STW OTP program "Electrochemistry - Mass Spectrometry (EC-MS) for Proteomics and Drug Metabolism" for stimulating multidisciplinary meetings; inter alia for Dr. Wouter Olthuis, Dr. Mathieu Odijk, and Floris who are my current colleges. Larry, Tao, Turan – thank you also for the ECHO meetings; Dear Turan, thank you for our work and publishing.

Additionally, I would like to express my gratitude to Dr. Frank Hollman and Dr Linda Otten for the remarks which I received from them at the very beginning stage of my PhD. They were of a great value for me, regardless the fact that they strongly questioned doabilty of my project. From my own investigation I do still classify this challenge as possible while using stable enzymes, highly conductive environment and strictly controlled/measurable oxygen saturation… hopefully this issue will be solved in the future. Dear Frank, thank you also for very interesting lectures.

Importantly, I would like to acknowledge colleagues from my "home" Molecular Enzymology group and chemists from the second floor who were delocalized around.

Hania – thanks for valuable advices and discussions, as well as for your always critical view at scientific and life situations. Hugo! Great you are fine, and thanks for the substantial introduction to the lab, giving (rather often) crucial hints and asking lots of questions related to everything I have been doing. Without you two my biological part of the Thesis would not have go so smoothly!

Dear Maxymilian Joseph Ludwig Johannes Fürst and Hanna Maria Dudek, please take my gratitude for your paranimphing :)

I would like to express my appreciation to all the group members who contributed to building up nice, helpful and stimulating atmosphere.

Maxi, Cora, Ely– without you my sensation of the group would not be the same.. thanks for making the lab, corridors and Groningen city center the comfy zone, and … being there! Lanfranchi – how is your tomorrow today? ;) Thanks for all☺!; Cora – it's been always valuable time while with you. Misun and Cintita – it was my pleasure.. to laugh and talk with you! Dear Alex – we had nice trip to Thailand, success with your future plans!, Mr Thai –It has been my honour! - also it was interesting to see Asia from your perspective. Nina – may the light be with you, thank you together with Antonia and Peter for creating a friendly atmosphere in the office. Willlem –always proper and creatively cheering. Kaja –thanks for the cover! Nicola – thank you for all your embarrassing jokes ;P. Christian, you did not only make the days easier but also put some good light at them. Dana and Friso – you were calming down when it was needed! Kaja – thanks for the cover, Friso, Dana, Casper – thanks for strugglings with my dutch (summary :P). Hemant, Elvira, Gosia, Hannah, Robert, Piet, Hugo, Pati Nutella, Mohamed, Antonia, Ana, Ivana, Matt, Arne, , Robert, Ana, Filippo, Anette and all of you that were there too!

Besides a tension and everyday- lab-stress, there were both- crazy and chilling moments, Also, thank you all guys for making our Fridays never-ending.

I cannot omit all the people who were there for every-day

Dear my housemates, I will not exaggerate when saying: it was blessing to live with you during (some tough) PhD times :D. Plutofamily, thank you for international dinners and cultural exchange saturated with lots of fun. Jadestraat house! it was joy- and delight-full: La cucaracha, orange balloons flooding my room and interesting travels we did together (we need to expand distances). Thank you also for always offering me chocolate cakes/ice-creams;). Thank you Vania – for the priceless: undefinable magic and being there; our talks and berakfasts! .. for whales, dolphins.. Mamut Chiquitito… PS. I will never forget you being sorry for my MS fragmentation pattern ;D. Thank you Mr Paultje for the enormous supply of dutch: in pills which we dosed regularly, "classy" mutual singing and opening doors each time I forgot my keys :D. Gerard, thanks for being there too!

My dear Andrea, thank you for being the Sunday housemate, making me close to die at all the amusements parks we visited and for the priceless talks.

My deep gratitude for mutual flowing with the classical music upon the ground and jumping over more and less complex accords for: GICA choir – it has been quite some absorbing projects together; and for the Bragi choir - which I joined only for my few last months in Groningen. The rehearsals allowed me to fully disconnect.

Besides, also great thanks to my friends from Kraków for being always wonderful: Karuś, Gasek, Gosia, Ania, Bieniu, Monia, Graża: dzieki! ☺ Ninek! Uściski! ☺

Last but not least,

I would also like to acknowledge Coincidence and Fake for their generous and frequent presence during my research, which forced me to develop evaluation, decision-making and operational thinking skills.

I need to mention someone who lives from, - and quite often in the Space... for triggering plenty sparkles towards inter alia. my PhD completion. It has been quite nice to travel to your cactuses-free Desert.

Besides, I would like to express an appreciation to my family for the effort taken to understand my research. Dziekuje mamo, tato, ciociu, wujku za troske. Dziekuje takze za Wasze zainteresowanie moimi badaniami.

Thank you! you all shaped my "PhD (life)"

Marzena Krzek

2017, Enschede

CONTENTS